A HEURISTIC OPTIMAL APPROACH FOR COORDINATED VOLT/VAR CONTROL IN DISTRIBUTION NETWORKS

by

Lesiba Mokgonyana

Submitted in partial fulfillment of the requirements for the degree

Master of Engineering (Electrical Engineering)

in the

Department of Electrical, Electronic and Computer Engineering
Faculty of Engineering, Built Environment and Information Technology
UNIVERSITY OF PRETORIA

NOVEMBER 2014

SUMMARY

A HEURISTIC OPTIMAL APPROACH FOR COORDINATED VOLT/VAR CONTROL IN DISTRIBUTION NETWORKS

by

Lesiba Mokgonyana

Supervisor(s):	Prof. X. Xia and Mr. L. Zhang
Department:	Electrical, Electronic and Computer Engineering
University:	University of Pretoria
Degree:	Master of Engineering (Electrical Engineering)
Keywords:	Capacitor, distribution network, losses, on-load tap changer, particle swarm optimization, reactive power control, voltage control

This dissertation focuses on daily volt/var control in distribution networks with feeder capacitors, substation capacitors and transformers equipped with on-load tap changers. A hybrid approach is proposed to solve the daily volt/var control problem. To reduce the computational requirements of the problem, this approach combines two methods, namely heuristic and optimal scheduling for the substation and feeder sub-problems respectively.

The feeder capacitor dispatch schedule is determined based on a heuristic reactive power set-point method. At this stage the objective is to minimize the reactive power flow through the substation bus in every time-interval. And as such, mathematical modeling of the distribution network components is adapted to suit time-varying conditions. Furthermore, an optimization model to determine a proper dispatch schedule of the substation devices is formulated. The objective of this model is to minimize the daily total energy loss and voltage deviations. Additionally, the reference voltage of the substation secondary bus and the transformer tap position limits are modified to adapt to given load profiles. The optimization model is solved with a discrete particle swarm optimization algorithm, which incorporates Newton's method to determine the power-flow solution.

The proposed method is applied to a time-varying distribution system and evaluated under different operational scenarios. It is also compared to on-line volt/var control with various settings.

Simulation results show that the proposed approach minimizes both the voltage deviations and the total energy loss, while on-line control prioritizes one objective over the other depending on the specified settings.

OPSOMMING

'N HEURISTIESE OPTIMALE BENADERING TOT DIE GEKOÖRDINEERDE VOLT/VAR-BEHEER IN DISTRIBUSIENETTE

deur

Lesiba Mokgonyana

Studieleier(s):	Prof. X. Xia en Mnr. L. Zhang
Departement:	Elektriese, Elektroniese en Rekenaar-Ingenieurswese
Universiteit:	Universiteit van Pretoria
Graad:	Magister in Ingenieurswese (Elektriese Ingenieurswese)
Sleutelwoorde:	Kapasitor, distribusienet, verliese, onderlastapwisselaar, partikelswerm-optimalisering, reaktiewe kragbeheer, spanningsbeheer

Die verhandeling fokus op die daaglikse volt/var-beheer in distribusienette wat komponente soos voerderkapasitors, substasiekapasitors en transformators met onderlastapwisselaars bevat. Om die aantal berekenings te verminder wat vereis word om die daaglike volt/var-beheerprobleem op te los, word 'n hibriede benadering voorgestel. Die twee metodes wat in die benadering gekombineer word, is die heuristiese en optimale skedulering van die substasie en voerder onderskeidelik.

Die versendingskedule van die voerderkapasitor word gebaseer op 'n heuristiese reaktiewekragstelpuntmetode. Die doelwit is om die reaktiewe kragvloei deur die substasiestam per tydinterval te verminder. Die wiskundige modellering van die distribusienetkomponente word dan aangepas by die tydveranderlike nettoestande. 'n Optimaliseringsmodel word geformuleer om die mees gepaste versendingskedule vir die substasietoerusting te bepaal. Die doel van die model is om die daaglikse totale energieverlies en spanningsafwykings te minimeer. Die verwysingspanning van die substasiesekondêrestam en die posisielimiete van die transformatortapwisselaar word aangepas vir sekere lasprofiele. Die optimaliseringsmodel word opgelos deur 'n diskrete partikelswerm-optimaliseringsalgoritme wat die Netwon-metode bevat om die kragvloeiprobleem op te los.

Die voorgestelde metode word toegepas met verwysing na 'n tydafhanklike distribusienet en word ge-evalueer onder verskillende operasionele toestande. Dit word ook vergelyk met aanlyn volt/var-beheer met verskeie instellings.

Die resultate van die simulasie toon dat die voorgestelde benadering beide die spanning-safwykings en die totale energieverlies minimeer, terwyl aanlynkontrole, afhangende van die spesifieke instellings, die een doelstellling bevoordeel ten koste van die ander een.

ACKNOWLEDGEMENTS

I would like to express my deepest gratitude to the following people for their involvement throughout the writing of this dissertation.

- Prof. X. Xia, for his insights and for serving as my supervisor for this dissertation.
- Prof. J. Zhang, my early supervisor, for his inspiring guidance and also for cultivating the ideas presented in this research.
- Mr L. Zhang, for providing valuable suggestions that helped refine this dissertation.
- My family and especially my fiancée Zintle, for their constant support and encouragement even when I had to work late on many nights and over weekends.
- My friends and colleagues, particularly Ndabeni Stenane and Esrom Malatji, for serving as a sounding board for my initial research ideas.

LIST OF ABBREVIATIONS

AVR	Automatic Voltage Regulation
FVC	Feeder Var Control
HV	High Voltage
LV	Low Voltage
LDC	Line Drop Compensation
MV	Medium Voltage
MINLP	Mixed Integer Non-Linear Programming
OLTC	On-Load Tap Changer
OSC	Optimal Substation Control
PF	Power Factor
PSO	Particle Swarm Optimization
VDI	Voltage Deviation Index
VVC	Volt/Var Control

TABLE OF CONTENTS

CHAPTER 1

INTRODUCTION

1.1 PROBLEM STATEMENT

1.1.1 Context of the Problem

Distribution networks are parts of electric circuits that receive and deliver power from transmission systems to electricity end users [1]. These networks are expected to supply good-quality electricity to the end users [2]. Poor power supply quality, more specifically poor voltage regulation, holds the implication of complaints and the possibility of claims from customers due to equipment failures and halted activities. In such cases it would be failure on the part of the distributor to align their activities with guidelines as set out by regulators [3].

Simultaneously, it would be beneficial for distributors to explore strategies to improve energy efficiency. Such strategies would form part of considerations for the design and operation of distribution networks. Ultimately, initiatives to reduce energy losses are known to yield cost savings for distributors [4].

One way to manage voltage quality and losses is to install voltage and reactive power resources in distribution networks. Typically, these resources are transformers with on-load tap changers (OLTC) and capacitors [1]. The control of these resources is referred to as volt/var control (VVC).

Many VVC approaches already exist; some control resources manually and others automatically. These strategies are implemented off-line, based on load predictions, or on-line, using

real-time measurements. Usually, the objective of both approaches is to minimize voltage deviations or to reduce energy losses. In some cases both objectives are dealt with. On-line control can respond to real-time constraints such as the requirement to keep voltage below permissible limits. On the other hand, off-line control is usually formulated as an optimization problem that focuses on the daily dispatch of VVC devices. Unlike on-line control, off-line control cannot respond to unexpected changes in real-time but it can satisfy constraints on the daily control effort of the VVC devices.

1.1.2 Research Gap

Traditionally, distributors use manual control or automatic control methods based on fixed settings that rely on local conditions at the controlled location for the VVC problem. The focus of this study is on off-line VVC.

Several approaches have been proposed to solve the daily VVC problem. The ones that coordinate all the distribution control resources using optimization models are computationally demanding [5]. On the other hand, there are approaches that simplify the problem [6], while others suggest reducing the size of the solution space [7]. These methods generally exclude some aspects of the problem before control actions are determined. Decoupling the problem to focus on groups of control devices is another alternative [8]. However, the subproblem involving the OLTC solely considers the controlled bus instead of all network buses. Furthermore, the performance of these approaches in relation to more conventional methods is not well documented.

1.2 RESEARCH OBJECTIVE AND QUESTIONS

The main objective is to develop a hybrid VVC approach with reduced computational requirements. The proposed approach should meet the following requirements:

- Minimize voltage deviations and energy losses in distribution networks over a scheduling period of 24 hours;
- Produce bus voltages that are within permissible levels at every time interval during the scheduling period;

- Coordinate the operation of an OLTC and capacitors with limited daily switching capability.

The proposed VVC formulation is guided by the following research questions:

- Can hybrid VVC yield feasible and optimal solutions when applied to distribution networks employing capacitors and OLTCs in a constrained environment?
- How does hybrid VVC perform in comparison with conventional control in distribution networks?
- What is the impact of load and network model changes on hybrid VVC?

1.3 HYPOTHESES

The hypotheses that are formulated for this study are stated as follows:

- Total daily distribution network loss and voltage deviation can be minimized by coordinated substation control and feeder reactive power control.
- The dimensions of VVC in distribution networks can be reduced with a hybrid VVC method, while maintaining the advantage of loss and voltage deviation reduction over conventional control methods.
- The dispatch schedule of the substation capacitor and OLTC can be determined using discrete PSO.
- The hybrid VVC system can perform satisfactorily even under tighter control device constraints.
- The hybrid VVC system can perform satisfactorily in the presence of load and model disturbances.

1.4 RESEARCH GOALS

The goal of this thesis is to develop a novel coordination strategy to improve the performance of distribution systems. The algorithm proposed in this thesis focuses on proactive coordination of OLTCs and capacitors according to the network model and day-ahead forecasts of the load demand. The output of the algorithm is the switching sequences of the control devices for the next 24 hours. The coordination scheme is implemented as an optimization problem integrated with a preliminary heuristic switching plan. This approach schedules operation of the control devices with respect to the voltage limits and the equipment switching limitations imposed by the operator. Concurrently, the substation bus reference voltage and transformer tap position range both adapt to the load profile observed by the algorithm.

1.5 RESEARCH CONTRIBUTION

In this research a two-stage approach to VVC is presented but the devices are controlled in a manner different from the methods presented in literature. First, a strategy to determine the feeder capacitor dispatch schedule is developed using reactive power set-points. Then, with the feeder capacitor schedule used as input, coordination of the substation capacitor and OLTC is formulated as an optimization problem. The advantage of this approach is that the voltage deviations can be reduced further by adjusting the transformer tap ratio, together with the capacitor on/off statuses. The reason is that transformers present smaller discrete steps than capacitors, therefore the application of this control can achieve better results. Voltage magnitudes at all load buses are primarily controlled at the substation, with the statuses of feeder capacitors taken as input. Since the voltage constraint at each load bus is handled at the substation, the feeder capacitor control problem focuses solely on loss reduction.

A comprehensive power-flow model is developed, which makes it possible to obtain accurate bus voltages and power-flows for the whole distribution network. This formulation facilitates the adoption of a technique relying only on reactive power-flows at the substation to determine the statuses of feeder capacitors. The feeder capacitor control sub-problem minimizes the reactive power-flow through the distribution feeders at the substation bus, while the OLTC and substation capacitor sub-problem minimizes both the total loss and the voltage deviations

at all distribution network buses.

The feeder capacitor control problem is solved with a heuristic method, while the OLTC and substation capacitor control problem is solved by the particle swarm optimization (PSO) method. The problem is classified as a mixed integer non-linear programming problem (MINLP). Hence, a discrete variant of PSO is used to compute values of the discrete variables. On the other hand, a numerical power flow approach is adopted for the continuous variables to fulfil a non-linear objective and satisfy problem constraints, some of which are non-linear. The performance of the proposed approach is compared to conventional strategies under various settings and loading conditions. Unlike conventional approaches, the proposed method states the objectives and constraints mathematically, which allows for easy adjustments of the model depending on operating conditions. Simulation results show that the proposed approach minimizes both the voltage deviations and the total energy loss, while on-line control falls short of this aim by compromising one to minimize the other depending on the specified settings.

1.6 OVERVIEW OF STUDY

Chapter 1 is an introduction to the work undertaken in this dissertation.

Chapter 2 provides an introduction to conventional VVC resources and methods. An evaluation of more advanced VVC methods is presented and the proposed method is aligned with the existing approaches. Finally the research focus of this work is discussed.

Chapter 3 presents distribution network modeling and formulates the mathematical model of the proposed control strategy, which consists of two parts, i.e. feeder capacitor control and substation control (which are referred to as 'feeder var control and optimal substation control' - FVC-OSC). The formulation is preceded by a description of the conventional and optimum settings approach to VVC.

The algorithm for solving the proposed FVC-OSC model is developed in Chapter 4. For the optimization model, discrete particle swarm optimization (PSO) is applied. Also, the details of the distribution system case study are specified.

Chapter 5 is dedicated to the simulations of VVC. The simulation scenarios include compar-

ison of conventional control, the optimum settings approach and FVC-OSC as well as the impact of disturbances on conventional control and FVC-OSC.

Chapter 6 provides a summary of findings, concludes the study and provides recommendations for future work.

CHAPTER 2

VOLT/VAR CONTROL IN DISTRIBUTION NETWORKS

2.1 CHAPTER OBJECTIVES

In Chapter 2 the devices that are typically used for VVC and the control methods thereof are described. Also discussed are the more advanced VVC approaches which are evaluated with the focus on daily VVC. It is shown that existing approaches do not address all daily VVC control possibilities. Finally, the specific focus as well as the research method, boundaries, and assumptions of this study are presented.

2.2 EVALUATION OF TRADITIONAL VOLT/VAR EQUIPMENT

Distribution systems commonly make use of OLTCs and capacitors to control voltage and reactive power. The impact of the VVC devices is described in terms of voltage, current and power expressions.

2.2.1 On-load Tap Changers

Transformers with variable tap ratios are widely used in distribution networks. These transformers rely on tap changers to adjust the tap ratio, which can be changed while the transformer is deenergised or when it is carrying load. Tap changers that require the transformer to be deenergised before functioning are suitable for uniform loads but impractical for frequently changing voltages, caused by time-varying loads. In practice, such transformers are

found in MV/LV networks, where the voltage is mainly regulated upstream. HV and MV systems make use of tap changers, which can change the tap ratio without interrupting the load current. These are known as OLTCs. When a transformer is equipped with an OLTC there is flexibility in how voltage is regulated. The OLTC is controlled manually or automatically, depending on the prevalence of voltage variations.

OLTCs consist of the following constituent parts [9]:

1. Selector – completes the connection of the selected tap.

2. Change-over switch – inverts the polarity of the tapped winding to adjust the regulating range of the tapped winding.

3. Transition mechanism – equipped with a diverter switch, which allows for smooth transitions between adjacent taps.

4. Drive system – to drive the operating sequence when a tap change signal is received.

Location of the OLTC is one of the important considerations at the design stage; the OLTC can be placed on either the primary side or secondary side of a transformer. For distribution networks, the primary side is where the HV winding is connected. This is the side with more turns and lower current values compared to the secondary side where the LV winding lies. If the OLTC is placed on the primary side, the rated current of the winding will be low but the core size, no-load losses, audible noise and fluctuating voltage steps are of concern. Also, in three winding transformers the third winding will experience voltage variations that are caused by the tap position changes. Placing the OLTC on the secondary side may be desirable because that is where the voltage is regulated. However, the fact that the winding should be able to handle high currents raises costs. On the other hand, the low number of turns on the LV side could simply make this connection impractical [9]. Either of these two connection schemes can be used in practice, where the design trade-offs are considered per application.

To maintain an acceptable voltage profile without human intervention, distributors make use of automatic voltage control systems, also referred to in this work as automatic voltage regulation (AVR). AVR works to keep the voltage around a predetermined value with a certain

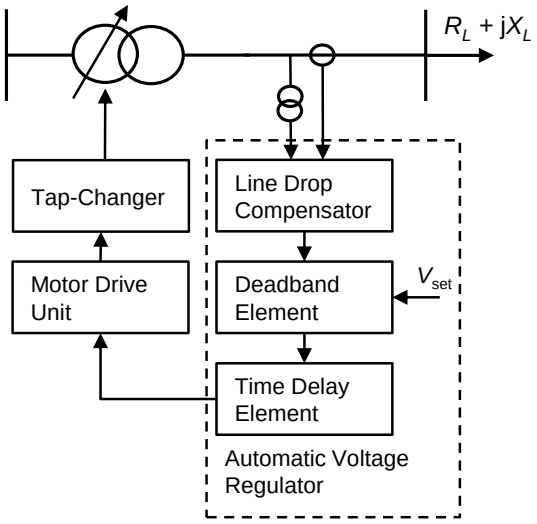

Figure 2.1: Conceptual model of an OLTC control system.

amount of tolerance as the load fluctuates. In general a tap position change is triggered when the measured voltage falls outside this permissible range. The control system requires measurement of voltage at the regulating point. Current measurements may also need to be provided depending on the control method adopted. A typical AVR system is displayed in Figure 2.1. A description of the control system is presented below [10].

Deadband Element – The deadband is the allowed margin/tolerance within which no tap changes are initiated; the controller activates a time delay function whenever the voltage falls outside the deadband. For stable operation of the control system it is important that the selected deadband be higher than the tap-change increment. Whenever this minimum requirement is not met, the tap-change operations are likely to move the voltage beyond the tolerance band every time the controller attempts to reduce the voltage deviation. With each raise or lower signal the voltage falls outside the tolerance band, causing the OLTC to operate unnecessarily. This phenomenon is commonly known as 'hunting'. Obviously a high deadband setting prevents hunting, but it must not be so great that excessive voltage variations are allowed by the AVR system.

The voltage set-point is the desired voltage at the bus controlled by the OLTC. The voltage set-point decision considers feeder losses and voltage regulation. High set-points provide the opportunity to minimize losses depending on the type of load being supplied. This is because

load current drops as the supply voltage is raised [11]. In terms of voltage regulation, a set-point value is desirable if it keeps load bus voltages near nominal values.

Using the set-point V_{set} and the deadband V_{db}, the minimum and maximum voltages that are possible with AVR can be derived. These values must not exceed regulatory voltage limits. The minimum and maximum voltages are expressed as

$$V_A^{\min} = V_{\text{set}} - 0.5\,V_{\text{db}}, \tag{2.1}$$

$$V_A^{\max} = V_{\text{set}} + 0.5\,V_{\text{db}}. \tag{2.2}$$

One way to determine the set-point and the deadband settings is through consideration of extreme loading scenarios. This entails calculating bus voltages under low loading and high loading conditions and selecting settings that ensure compliance with upper and lower voltage limits throughout the network in both scenarios [12].

The deadband element has a hysteresis margin, ε, which gives several output states, h_{db}. These are adjusted according to the magnitude and direction of the voltage error, ΔV^{avr}, which is in turn defined as the difference between the set-point, V_{set}, and the line drop compensator (LDC) voltage, $\bar{V}_s^{sc}$,

$$\Delta V^{\text{avr}} = V_{\text{set}} - \bar{V}_s^{sc}. \tag{2.3}$$

ΔV^{avr} does not change when

$$h_{\text{db}} = 0, \quad \text{if } -0.5\,V_{\text{db}} \leq \Delta V^{\text{avr}} \leq 0.5\,V_{\text{db}}. \tag{2.4}$$

ΔV^{avr} increases when

$$h_{\text{db}} = \begin{cases} 0, & \text{if } \Delta V^{\text{avr}} \leq 0.5\,V_{\text{db}} + \varepsilon; \\ 1, & \text{if } \Delta V^{\text{avr}} > 0.5\,V_{\text{db}} + \varepsilon; \\ -1, & \text{if } \Delta V^{\text{avr}} < -0.5\,V_{\text{db}}. \end{cases} \tag{2.5}$$

ΔV^{avr} decreases when

$$h_{\text{db}} = \begin{cases} 0, & \text{if } \Delta V^{\text{avr}} \geq -0.5\,V_{\text{db}} - \varepsilon; \\ 1, & \text{if } \Delta V^{\text{avr}} > 0.5\,V_{\text{db}}; \\ -1, & \text{if } \Delta V^{\text{avr}} < -0.5\,V_{\text{db}} - \varepsilon. \end{cases} \tag{2.6}$$

Time Delay Element – Introducing time delay lowers the influence of fast voltage variations and avoids unnecessary OLTC operations. The time delay may assume a fixed value, T_0, or

it may be allowed to vary according to the observed voltage deviation. The latter follows an inverse-time curve where small deviations have long time delays before a raise/lower signal is initiated and large deviations trigger faster operation. In this way, transient voltage variations will not cause the OLTC to operate. The characteristic is described by

$$T_{\text{inv}} = \frac{T_0}{|\Delta V^{\text{avr}}/V_{\text{db}}|}, \tag{2.7}$$

in which, T_{inv} denotes the adaptable time delay in seconds (s), and T_0 represents the uniform time delay (s) setting. The output of the time delay varies depending on the value of the time counter t as follows

$$h_{\text{t}} = \begin{cases} 0, & \text{if } t \leq T_{\text{inv}}; \\ 1, & \text{if } t > T_{\text{inv}},\ h_{\text{db}} = 1; \\ -1, & \text{if } t > T_{\text{inv}},\ h_{\text{db}} = -1. \end{cases} \tag{2.8}$$

Application of the time delay concept has been shown to improve the perfomance of cascaded OLTCs. With proper selection of time delays, the OLTC closest to the source of a voltage variation should be the fastest to operate. As a result each OLTC operates only as and when necessary. In this manner the operation of cascaded OLTCs is coordinated, leading to a low number of OLTC operations [13].

Tap-Changing Module – this module is made up of a motor drive and a mechanism to change the physical tap position of the transformer. The process of moving from one tap position to another is incremental, moving one step at a time. In this model each step takes a fixed amount of time as shown in (2.9).

$$\Delta u^i_{\text{TAP}} = \begin{cases} 0, & \text{if } t \leq T_{\text{md}}; \\ 1, & \text{if } t > T_{\text{md}},\ h_{\text{t}} = -1; \\ -1, & \text{if } t > T_{\text{md}},\ h_{\text{t}} = 1; \end{cases} \tag{2.9}$$

after each time instant the tap position is determined by

$$u^i_{\text{TAP}} = u^{i-1}_{\text{TAP}} + \Delta u^i_{\text{TAP}}, \tag{2.10}$$

where

Δu^i_{TAP} is the tap position change at time instant i,

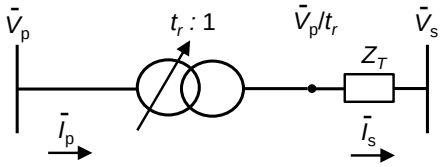

Figure 2.2: Transformer model with off-nominal winding on the primary side and admittance on the secondary side.

T_{md} is the tap change time delay,
u_{TAP}^{i-1} is the tap position at the previous time instant.

The tap position changes are bounded by the highest and lowest tap positions. Therefore tap position updates in excess of this allowable range are clamped to the nearest limit value.

Transformer – The model shown in Figure 2.2 is put to use in order to describe the effect of tap ratio adjustments on a transformer with an off-nominal winding. It is assumed that the impedance of the transformer remains constant for all variations in tap ratio. The relationship between the tap position and the tap ratio is expressed as

$$t_r = 1 - u_{st} u_{\text{TAP}}. \tag{2.11}$$

Voltage on the secondary side of the transformer is impacted by the tap ratio to such an extent that

$$\bar{V}_s = \frac{\bar{V}_p}{t_r} - Z_T \bar{I}_s. \tag{2.12}$$

Since the transformer losses are small in relation to the capacity and load of the transformer, the losses are neglected so that $S_p \approx S_s$. Subsequently, (2.12) can be modified by including the load power $\bar{S}_s = P_s + \mathrm{j}Q_s$ in the following expressions:

$$\bar{I}_s = t_r \frac{\bar{S}_s}{\bar{V}_p^*}, \tag{2.13}$$

$$\bar{V}_s = \frac{\bar{V}_p}{t_r} - (R_T + \mathrm{j}X_T)(t_r \frac{P_s + \mathrm{j}Q_s}{\bar{V}_p^*}) = \frac{\bar{V}_p}{t_r} - t_r \frac{R_T P_s + \mathrm{j}X_T Q_s}{\bar{V}_p^*} - \mathrm{j}t_r \frac{R_T P_s - \mathrm{j}X_T Q_s}{\bar{V}_p^*}, \tag{2.14}$$

where

u_{st} is the size of a single tap increment/decrement step, $\bar{V}_s$ is the transformer secondary side voltage in pu,
$\bar{V}_p$ is the transformer primary side voltage in pu,

t_r is the adjustable tap ratio of the transformer,

$\bar{I}_p$ is the transformer primary side current in pu,

$\bar{I}_s$ is the transformer load/secondary side current,

$\bar{S}_p$ is the complex primary side power in pu,

$\bar{S}_s$ is the complex load/secondary side power in pu,

$Z_T = R_T + \mathrm{j}X_T$ is the transformer leakage impedance in pu.

By inspection of the equations above, it can be seen that besides the tap ratio, the secondary voltage depends on a number of parameters. Because the tap ratio can be controlled, it is used to counter changes in these parameters. Firstly, the presence of the transformer impedance means that there will be voltage drop across the transformer. For operational purposes this parameter is nearly constant, hence it must be considered during the design phase. Secondly, the primary voltage is a function of upstream network control. Good control of the primary network results in small variations in the primary voltage, which leaves local control more capacity to respond to other parameter changes. With no control upstream, the primary voltage will vary with load and larger tap ratio adjustments will be required locally to maintain the secondary voltage within the permissible range. Finally, changes in load definitely need compensation. Like the impedance, load adds to the transformer voltage drop. Also, if the transformer is connected to secondary lines supplying downstream networks, the voltages at remote buses are a major concern.

Measurement Components – Potential and current transformers have the role of reducing the secondary voltage and the secondary current to manageable levels for the OLTC control system. Both transformers are taken as ideal and thus lossless. Under this assumption, the following equations are applied

$$t_{\mathrm{pt}} = \frac{V_s^{\mathrm{pr}}}{V_s^{\mathrm{sr}}}, \tag{2.15}$$

$$\bar{V}_s^{\mathrm{pt}} = \bar{V}_s t_{\mathrm{pt}}, \tag{2.16}$$

$$t_{\mathrm{ct}} = \frac{I_s^{\mathrm{pr}}}{I_s^{\mathrm{sr}}}, \tag{2.17}$$

$$\bar{I}_s^{\mathrm{ct}} = \bar{I}_s t_{\mathrm{ct}}, \tag{2.18}$$

where

t_{pt} is the turns ratio of the potential transformer,

V_s^{pr} is the rated primary voltage of the potential transformer,

V_s^{sr} is the rated secondary voltage of the potential transformer,

$\bar{V}_s^{\text{pt}}$ is the actual secondary voltage of the potential transformer in pu,

t_{ct} is the turns ratio of the current transformer,

I_s^{pr} is the rated primary current of the current transformer,

I_s^{sr} is the rated secondary current of the current transformer,

$\bar{I}_s^{\text{ct}}$ is the actual secondary current of the current transformer in pu.

Line-Drop Compensator – It does not require communication to control voltage remotely. Given the load current, line resistance and reactance, the LDC computes the voltage drop across the line. By compensating for the voltage drop, in this case the product of the current and the impedance, the remote bus voltage can essentially be kept constant. In order to obtain the load current the OLTC control system is extended with an additional input from a current transformer. The voltage adjustment from the LDC is

$$\bar{V}_c = (R_c + \mathrm{j}X_c)\bar{I}_s^{\text{ct}} = \mathrm{m}(R_L + \mathrm{j}X_L)\bar{I}_s, \tag{2.19}$$

$$\bar{V}_s^{sc} = \bar{V}_s^{\text{pt}} - \bar{V}_c. \tag{2.20}$$

Despite the improvements LDC adds to AVR, it is more difficult to obtain suitable control settings when the LDC element is enabled than otherwise. For one, instead of a single feeder, substations may consist of several feeders with different impedance characteristics [14].

2.2.2 Shunt Capacitors

For distribution networks with significant reactive power requirements, capacitors are employed. The application of these devices improves the power factor and raises the voltage at the point of connection in networks with significant reactive power requirements. By reducing the reactive power demand at the application point the voltage drop up to that point is also decreased. Additionally, the load loss is lowered in a similar manner up to the point of application. There are two strategies for connecting capacitors to the power system, namely, fixed connection and switched connection. Fixed capacitors are installed to supply the base reactive power demand. Switched capacitors are then sized to cater for peak load conditions. Since loads vary with time, fixed capacitors are usually inadequate. This is because, in light loading conditions overcompensation may take place, leading to overvoltages in some cases. If overvoltages are avoided it may be likely that compensation is less effective in heavy loading conditions. In such scenarios, it would be beneficial to install switched capacitors.

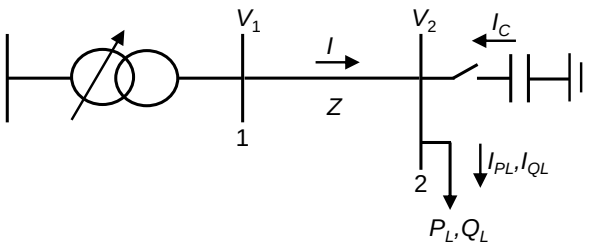

Figure 2.3: Two-bus distribution network with capacitor connected at load bus.

Capacitors provide varying levels of compensation depending on certain characteristics of the network. The ratio between the network reactance and resistance, known as X/R ratio is used to classify how a given network responds to voltage drop. In this respect, capacitors are more effective in networks with X/R ratios of more than 1. In a network with an X/R ratio lower than 1, installation of capacitors will yield relatively low voltage rise even if the power factor is improved greatly. This is because capacitors only compensate the reactive component of the voltage drop while the resistive component remains unchanged. For a line of a given length, the X/R ratio depends on the size of the conductor used; it rises with an increase in the size of the conductor [15].

Consider the network shown in Figure 2.3. When the capacitor at bus 2 is switched off, and is thus out-of-service, the voltage drop is given by

$$\Delta V_{\text{drop}} = IZ = \sqrt{I_{PL}^2 + I_{QL}^2}Z. \tag{2.21}$$

In terms of load power, the voltage drop is expressed as

$$\Delta V_{\text{drop}} = \left|(R + \text{j}X)(\frac{P_L + \text{j}Q_L}{\bar{V}_2^*})\right|. \tag{2.22}$$

With the capacitor connected to bus 2,

$$\Delta V_{\text{drop}} = \sqrt{I_{PL}^2 + (I_{QL}^2 - I_C^2)}Z, \tag{2.23}$$

$$\Delta V_{\text{drop}} = \left|(R + \text{j}X)(\frac{P_L + \text{j}(Q_L - Q_C)}{\bar{V}_2^*})\right|. \tag{2.24}$$

Similarly, the load loss is a function of the active and reactive components of the load current:

$$P_{\text{loss}} = (I_{PL}^2 + I_{QL}^2)R. \tag{2.25}$$

The impact of the capacitor on the load loss is as follows

$$P_{\text{loss}} = [I_{PL}^2 + (I_{QL}^2 - I_C^2)]R, \tag{2.26}$$

where

ΔV_{drop} is the voltage drop between bus 1 and bus 2,

$\bar{V}_2$ is the complex voltage at bus 2,

Z is the magnitude of the line impedance, composed of resistive and reactive parts. $Z = \sqrt{X^2 + R^2}$,

I is the load current,

I_{PL} is the active power component of the load current,

I_{QL} is the reactive power component of the load current,

P_L is the load active power,

Q_L is the load reactive power.

It can be seen from (2.21)–(2.26) that connecting a capacitor reduces reactive power-flow through the substation transformer or the distribution feeder. In this way, the total loss is minimized. The use of capacitors also has the effect of raising voltage in addition to providing reactive power compensation. By reducing the reactive power drawn from an upstream source at the point of connection, capacitors are able to boost the bus voltage. In light loading conditions capacitors may be taken out-of-service to avoid violating upper voltage limits. But, during periods of high loading, capacitors are put in-service to keep the voltage above low voltage limits. With these contrasting loading scenarios there is a need to keep the voltage stable. And responding with capacitor switching actions is one way of doing so. Furthermore, it is possible to minimize losses by switching on and switching off capacitors at appropriate times. One convenient way for controlling switched capacitors is to adopt the automatic on-line control scheme.

Automatic on-line control of capacitors refers to on/off control of capacitors in real-time, based on local measurements. It is based on set-points of the following quantities [1], [16].

Reactive Power – With this control, the capacitor is switched on/off to keep the local reactive power flow low; this is good for loss reduction. Reactive power control requires the installation of a current transformer in addition to a potential transformer for current and

voltage measurements respectively.

Current – Less accurate form of control than reactive power because the total current comprises of active and reactive components. However, only current measurements are needed to achieve control.

Power Factor – This method is effective when the power factor fluctuates with the load demand. It is difficult for this approach to work properly in situations where the load and the power factor are low and also where the load and the power factor are high. Furthermore, there simply may not be sufficient power factor variations to satisfy preset values.

Voltage – Good for keeping the voltage within regulatory limits. The capacitor is switched on in peak loading and switched off in light loading. However, this method does not produce the best results for loss minimization because in some scenarios, the capacitor may remain on even in leading power factor conditions.

Time – Control based on historical behaviour of load. Certain networks experience significant rise or drop in load demand at more or less the same times during the day. This is the least expensive form of control because unlike others, it does not require measurements to implement. However, this mode is the most likely to result in inappropriate switching due to unexpected variations in load.

Temperature – The capacitor on/off switching is reliant on temperature set-points. This method is suitable for loads that vary with weather conditions. More specifically, the reactive power demand must closely follow temperature variations.

The capacitor controls above also have a time-delay feature to manage fast variations. The most conducive way to ensure the voltage change caused by the capacitor does not violate voltage limits is voltage-based control. Other modes of control do not guarantee compliance especially in cases where there are discrepancies between the actual and expected impact of the selected settings on voltage. And they offer advantages which may come secondary to voltage regulation from the perspective of the distributor unless there are other means of regulating voltage, or there is little chance of causing voltage violations.

2.2.3 Other Volt/Var Devices

Another way of regulating voltage is through use of step-voltage regulators. A step-voltage regulator is similar to a transformer with OLTC in that it comprises an autotransformer and a load tap changing system. But, unlike distribution transformers, step-voltage regulators do not alter the operating voltage level. Additionally, step-voltage regulators are predominantly available in single phase arrangements with each unit controlling voltage on one phase [17].

There are other means of providing compensation such as electrical machines and static var compensators. However, these alternatives are more expensive to install and have a high maintenance cost relative to capacitors [2].

2.3 ON-LINE VOLT/VAR CONTROL STRATEGIES

Control of volt and var devices such as on-load tap changers (OLTC) and shunt capacitors affects the voltage profile and the total power loss in distribution networks [1]. Volt/var control (VVC) can be implemented online using real-time measurements and past experience or off-line according to dispatch schedules based on load forecasting. On-line control is either centralized or decentralized. The former depends on network wide measurements while decentralized control only requires local information. Off-line control is described in Section 2.4.

2.3.1 Conventional Control

Because of the complexity of coordinating on-line capacitor and OLTC control, some distributors prefer using AVR and time-based capacitor control to prevent problems, such as unnecessary device operations due to miscoordination.

In this research, a combination of automatic voltage regulation using OLTCs and time-based capacitor control is implemented. This method is referred to as conventional control.

For OLTC control, typical set-point and deadband settings are applied to AVR. These are guided by practical operational objectives. Also, the LDC element is disabled. On the other

hand, capacitor control relies on time settings. These time settings are meant to approximate periods of significant variation in demand. Therefore, the capacitor is switched on during high demand periods and switched off in light loading conditions for a time-varying load.

All the devices are still controlled independently since OLTC control responds to variations on the local bus in real-time, and capacitor control is triggered by time. However, the procedure for determining control settings is simplified and there would be fewer unnecessary operations caused by interaction of the control devices.

2.3.2 Other On-Line Control Approaches

Decentralized on-line control is widespread, however, it can be inadequate for fulfilling certain objectives in networks with varying loading conditions. Various studies propose ways to improve the performance of traditional decentralized control. Automatic control set-points can be selected optimally to minimize network losses and the number of device operations in traditional distribution networks and in networks with distributed generation [18], [19]. These objectives are achieved through a set of rules that aim to coordinate the control devices. In [20], the number of tap movements is reduced through off-line dispatch of capacitors and automatic on-line control of an OLTC.

More sophisticated on-line control provides the capability to respond to dynamic disturbances. For instance, adaptive control of a distribution static compensator reduces the impact of fast-changing loads by minimizing voltage deviation at the point of common coupling [21], [22].

Centralized on-line control deals with operational objectives, constraints and changing network conditions effectively and more explicitly than decentralized control according to formulations in [23–27]. However, centralized control does not include switching constraints which require consideration of large time periods.

2.4 OFF-LINE VOLT/VAR CONTROL STRATEGIES

In comparison to on-line control, off-line control methods also function in a centralized manner. Furthermore, they incorporate more practical constraints although most of them are

based on the premise that the actual load is the same as the forecasted load.

2.4.1 Existing Approaches

Off-line dispatch of distribution control devices in a coordinated manner is performed in a constrained environment to meet specific objectives, usually over a period of one day [5–8,28–34]. This method is suitable for networks with widespread communication coverage. Also, off-line control requires a steady-state model of the whole distribution network and day-ahead prediction of the load behaviour, which is made possible by the existence of load forecasting techniques which provide good accuracy [35], [36]. The complexity of the objective function, constraints, and computation is influenced, by among others: regulatory limits, switching limitations, available devices, topology and size of the network under consideration.

In fact, the proposal in [28] is one of the earliest on the control of voltage/reactive power that is applicable to a practical distribution network. It focuses on an optimal switching schedule for capacitors over a 24-hour period with the objective to minimize line losses. The method incorporates changes in load through load forecasts based on historical load profiles. Also, capacitor switching constraints are introduced in addition to voltage limits. However, bus voltage deviations are not included in the objective function. The same approach is extended to include voltage deviations and then applied to the dispatch of a substation OLTC and capacitors by [7], [31].

Coordinated control of all distribution devices is computationally complex, thus the problem is usually simplified to deal with this difficulty. By modifying some aspects of the problem, the complexity can be greatly reduced. Previous studies solve the problem by simplifying either the problem definition or the solution process. The load levels approach estimates loading behaviour by dividing 24-hour load profiles into intervals of varying lengths thus modifying the original sampling interval [6]. Using load levels has the effect of reducing the number of times the capacitors and OLTCs are required to change states as operations are triggered by load level adjustments. However, this method can lead to suboptimal solutions if the load partitions are inaccurate.

The coordinated VVC problem in distribution has been classified as a mixed integer non-linear programming problem [34]; various optimization techniques including mathematical

programming and stochastic search algorithms have been applied successfully to solve the problem. Dynamic programming, a form of mathematical programming, has been used in the past for scheduling of OLTCs and capacitors in distribution networks. For a network with time-varying loads, the computational demand increases with the number of devices, control interval and the length of the scheduling period. During each time interval there are $(2^n \times N_t)$ states for a network with n capacitors and N_t OLTCs. If the scheduling period is one day then the solution space of dynamic programming would cover $(2^n \times N_t)^{24}$ states in total. Hence some approaches opt to simplify the solution space so as to reduce the computational burden [7], [29], [31]. More specifically, the original number of tap positions is reduced to several possible tap positions that produce the lowest voltage deviation at the substation secondary bus; the rest of the tap positions are ignored. Furthermore, the number of states in all scheduling intervals is restricted to limit the total number of search paths.

A more efficient solver based on the interior-point method is presented in [34]. In [30], a technique combining artificial neural networks (ANN), rule-based method and dynamic programming is introduced. With ANN a much smaller number of possible states is obtained to create a preliminary switching schedule. Then fuzzy variables are incorporated within the schedule to model the operators' decisions. Finally, dynamic programming is used to produce the control settings to be implemented over the next 24-hour period. Use of heuristic rules to sort device operating schedules can also reduce the number of possible device operations, therefore simplifying the optimization model [32].

Another alternative is to divide the scheduling problem into two subproblems: one handling the dispatch of the substation capacitor and OLTC, and the other controlling the feeder capacitors [8]. Dispatch of the substation devices minimizes reactive power-flow and the voltage deviation at the substation bus. Feeder capacitors are then dispatched based on local bus voltage and power factor deviations using a fuzzy control scheme after substation devices have been dispatched. The resulting states of the capacitors are taken as final if they do not violate the bus voltage limits. In [20] the total loss and voltage deviations at load buses are minimized through dispatch of all capacitors. The OLTC is controlled in real-time to keep the substation secondary bus voltage close to the set-point that incorporates the voltage change caused by the capacitors. In these previous approaches, the objectives specified for the substation control problem focus only on the secondary bus at the substation. The rest of the buses are considered in the control schemes for feeder capacitors.

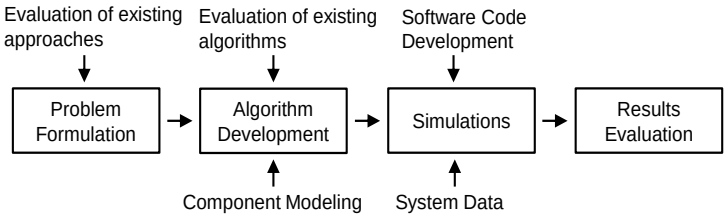

Figure 2.4: Research method.

2.4.2 Proposed Approach

In this research, a two-stage approach to VVC is presented, but the devices are controlled in a different manner. First, a strategy to determine the feeder capacitor dispatch schedule is developed using reactive power set-points. Then, with the feeder capacitor schedule serving as input, coordination of the substation capacitor and OLTC is formulated as an optimization problem. The advantage of this approach is that the voltage deviations can be reduced further by adjusting the transformer tap ratio together with the capacitor on/off statuses. The reason is that transformers have smaller discrete steps than capacitors, therefore the control can achieve better results making use of this. Voltage magnitudes at all load buses are primarily controlled at the substation with the statuses of feeder capacitors taken as input. Since the voltage constraint at each load bus is handled at the substation, the feeder capacitor control problem focuses solely on loss reduction. This strategy facilitates the adoption of a technique relying only on reactive power-flows at the substation to determine the statuses of feeder capacitors. The feeder capacitor control sub-problem minimizes the reactive power-flow through the distribution feeders at the substation bus, while the OLTC and substation capacitor sub-problem minimizes both the total loss and the voltage deviations at all distribution network buses.

2.5 RESEARCH METHOD

The research process followed for this research consists of four main phases: problem formulation, algorithm development, simulations, and results evaluation. The process is illustrated in Figure 2.4 and described below.

An evaluation of existing voltage and reactive power control approaches for distribution

networks is conducted.

Existing algorithms are assessed for application to the optimal VVC problem. Special emphasis is put on the MINLP algorithm due to the nature of the volt/var problem. The existing mixed integer non-linear programming algorithms are evaluated to establish the size, convergence issues, feasibility of results and ease of implementation.

The existing on-line control approaches are suboptimal for time-varying loads and can lead to constraint violations, while optimal off-line VVC solutions show better performance but have increased computational complexity. As a result, the VVC problem is reformulated.

The different power system components that make up typical distribution systems are modeled mathematically, based on the reformulated optimization model, and then an algorithm is developed to solve the proposed optimization model, which is a less computationally complex MINLP problem. The values of control variables are determined with discrete PSO with respect to the non-linear objective and constraints. The power flow problem, which consists of continuous variables uses Newton's method to solve the state variables at each optimization step.

The reformulated VVC model is applied to a distribution network with an OLTC and controllable capacitors. First, the proposed algorithm is translated into software code to be implemented in a mathematical simulation tool. Then, simulations are performed to evaluate the performance of the model. It is shown that added modifications improve the solution of the model.

Furthermore, the proposed method, along with two existing approaches, are simulated for two different reactive power compensation levels and load demand profiles applied to a distribution system. Different scenarios are studied to evaluate the quality and robustness of the solutions. The results are expressed in terms of voltage deviations, network losses, voltage magnitudes and number of operations. And then the results produced are analysed, interpreted and compared with reference to the performance of an uncontrolled system.

2.6 DELIMITATION OF SCOPE AND KEY ASSUMPTIONS

Communication facilities exist between the control centre and the locations of the OLTC and capacitors. The outcome of this is to produce day-ahead control schedules to be used as part of operations planning. With each daily load demand profile comes a daily control schedule, which is convenient to implement with sufficient communication coverage. However, the proposed algorithm is also applicable to systems with limited communication coverage, even though the resulting control schedule would be suboptimal.

The distribution system has adequate generated power and is a three-phase balanced circuit. Thus generator constraints are not taken into account. For unbalanced systems other power flow solutions will have to be used, such as the unbalanced fast decoupled power-flow [37], [38].

Only constant power loads are analyzed. Constant current and constant impedance loads have different loss characteristics compared to constant power loads. Hence the solution will be different for other types of loads. The power-flow routine of the proposed approach should be modified for analysis of constant current and constant impedance loads.

The load remains constant between successive time intervals, and the network configuration does not change throughout the scheduling period. In this study, time-varying load is discretized into a fixed set of time intervals spread across the scheduling period. Therefore, loads whose frequency of change deviates from the expected time intervals are not considered. Furthermore, the proposed technique is not intended to handle changes in network configuration unless the network is reconfigured before the calculation process begins. In this case the power system model can simply be updated to reflect the changes in advance.

The proposed model is an instance of open-loop control and does not incorporate uncertainty in load forecasting and the network model. Unexpected changes are instead introduced as stochastic errors encountered when the control actions are implemented. The extent to which this affects the solution is discussed using a case study.

CHAPTER 3

COORDINATED VOLT/VAR CONTROL

3.1 CHAPTER OVERVIEW

In Chapter 2 the foundation of the proposed VVC approach is explained with reference to existing work. Chapter 3 provides a description of the model of conventional VVC implemented in this study as well as the optimum settings approach. That is followed by detailed modeling of the distribution network components, and the mathematical formulation of the proposed approach, which is a novel algorithm to coordinate the substation OLTC, substation capacitor and feeder capacitors.

3.2 CONVENTIONAL VOLT/VAR CONTROL

3.2.1 Automatic OLTC Control and Time-based Capacitor Control

The automatic OLTC control system represented in Figure 2.1 is simplified here for hourly changes in load. A single tap change cycle lasts several seconds. The total time it takes the tap changer to move from an initial tap position through increments to the one that returns the voltage to within the given limits takes longer and typically depends on the inverse-time relationship; however the time remains in the order of seconds. Considering that the time scale studied here is in the order of hours only the initial and final states are of importance, rather than each tap changing step. Moreover, a model that factors in time delay is not necessary here because delay is not used for coordination of the OLTC and capacitors.

In this formulation, the voltage is decreased by lowering the tap position, u^i_{TAP}, and increased

by raising it. u^i_{TAP} falls between $T^{\min}$ and $T^{\max}$. Thus $T^{\min}$ produces the lowest voltage magnitude and $T^{\max}$ the highest voltage magnitude at the regulated bus. The steady-state tap position at time instant i is determined using

$$u^i_{\text{TAP}} = \begin{cases} u^{i-1}_{\text{TAP}} + \Delta u^i_{\text{TAP}}, & \text{if } V_{\text{set}} - V_i > 0.5\, V_{\text{db}}; \\ u^{i-1}_{\text{TAP}} - \Delta u^i_{\text{TAP}}, & \text{if } V_{\text{set}} - V_i < -0.5\, V_{\text{db}}; \\ u^{i-1}_{\text{TAP}}, & \text{otherwise;} \end{cases} \tag{3.1}$$

where

Δu^i_{TAP} in this case is the number of tap movements required to bring the voltage V_i into the deadband, V_{db}.

In essence the objective of 3.1 is to tap up, tap down, or remain still to minimize the deviation from the set-point.

In most power-flow algorithms there are two main alternatives to treat AVR. The first method handles the tap ratio by making it an independent parameter [39], [40]. Voltage at the controlled bus then becomes a state variable. When the calculated voltage is within the given limits the tap ratio remains unchanged. On the contrary if the voltage is beyond the limits, the tap ratio is adjusted to move the voltage back within limits. This method has good convergence characteristics but depends more on the voltage limits rather than the set-point.

Another way to deal with AVR is to specify the voltage before the power-flow calculation begins [41]. As a result, the voltage is substituted with the tap ratio in the vector of state variables. The disadvantage of specifying the voltage ahead of the calculation is that the algorithm finds it difficult to reach convergence when the tap ratio is in excess of allowable limits.

3.2.2 Optimum Settings Approach

With conventional control voltage regulation is prioritized and loss reduction comes second. The optimum settings approach is an improvement on conventional control suggested in [11], [18]. This approach aims to reduce losses and at the same time keep the voltage within permissible limits. The substation and feeder capacitors are all controlled automatically

based on local bus conditions. The following settings characterize the optimum settings approach.

1. The AVR deadband is twice the voltage change caused by tap increment or a smaller value that keeps the actual voltage close to the voltage set-point. The voltage set-point is set as high as possible taking into account the upper bus voltage limit. This limit must not be exceeded with the pairing of the set-point and deadband.

2. The feeder capacitor switches off when the local bus voltage reaches the maximum allowable value. Using the voltage setting approach eliminates the possibility of an overvoltage.

3. For switching the feeder capacitor on, a lower voltage setting is selected. When the capacitor is switched on at this value the resulting voltage rise must not cause the voltage to go so high that the capacitor is turned off again for exceeding the upper limit. At the same time the setting must be high enough to reduce line losses.

4. Substation capacitor control is triggered by the reactive power drawn or supplied through the transformer. The capacitor is set to switch on as the reactive power demand on the secondary side of the transformer goes beyond the capacitor rating. The substation capacitor is switched off when reactive power is as high as the rating of the capacitor flows in the opposite direction.

5. To minimize the overall number of OLTC and capacitor operations time delay is used. The feeder capacitor has the shortest delay, followed by the substation capacitor, and then the OLTC. As a result operation of the devices is coordinated.

In summary the OLTC is controlled using the AVR scheme, the substation capacitor according to local reactive power set-points and the feeder capacitor according to local voltage set-points. Losses are minimized by making the AVR set-point and feeder capacitor switch-off setting as high as possible. For voltage regulation, the feeder capacitor switch-off setting is restrained to the upper voltage limit. Operating the voltage so close to the upper limit clearly means the lower limit is not an issue for this approach.

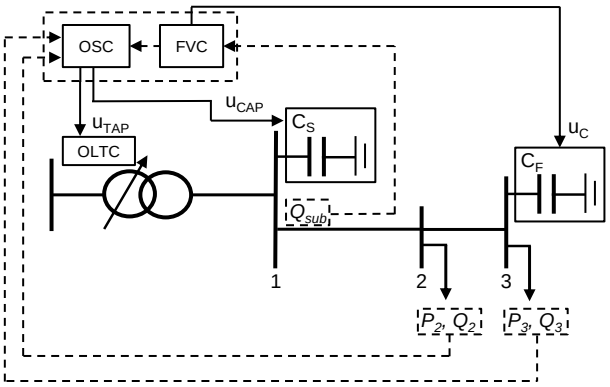

Figure 3.1: Conceptual model of the proposed feeder var control and optimal substation control.

3.3 MODELING OF THE DISTRIBUTION NETWORK

The proposed method minimizes the total loss and voltage deviations in distribution systems. The conceptual model of the method is illustrated in Figure 3.1. It is assumed that the OLTC and all the capacitors are remotely controllable. The solution process comprises two stages: firstly the feeder capacitor schedules are determined, and then the substation capacitor and OLTC are coordinated optimally to complete the dispatch schedules. The feeder capacitors on/off statuses are derived from reactive power variations on the feeder at the substation and the resulting switching sequence, together with the forecasted active power and reactive power profiles of the loads, are supplied to the substation capacitor and OLTC control model. Then, an optimization algorithm is applied in which the switching sequences of the substation capacitor and OLTC are obtained.

Per-phase equivalent models are employed, thus assuming a balanced system. The index i, represented as a superscript indicates the nature of the operating conditions. Variables with this index change with respect to time. Variables without i are constant over all time intervals.

To represent branches i.e. lines and transformers, the two-port model (3.2) depicted in Figure 3.2 is adopted,

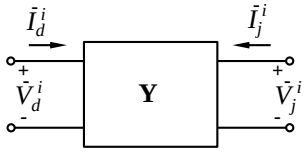

Figure 3.2: Two-port model.

$$\begin{bmatrix} \bar{I}_d^i \\ \bar{I}_j^i \end{bmatrix} = \begin{bmatrix} y_{dd}^i & y_{dj}^i \\ y_{jd}^i & y_{jj}^i \end{bmatrix} \begin{bmatrix} \bar{V}_d^i \\ \bar{V}_j^i \end{bmatrix}, \tag{3.2}$$

$$\boldsymbol{Y} = \begin{bmatrix} y_{dd}^i & y_{dj}^i \\ y_{jd}^i & y_{jj}^i \end{bmatrix}, \tag{3.3}$$

where

$\boldsymbol{Y}$ is the admittance matrix,

subscripts d and j are the buses to which the admittance branch is connected,

$\bar{V}_d^i$ and $\bar{V}_j^i$ are complex bus voltages,

$\bar{I}_d^i$ and $\bar{I}_j^i$ are the complex current injections.

The index i denotes the ith time interval for a sampling period equal to Δt. Also, $[i\Delta t, (i+1)\Delta t)$ denotes one sampling period while N specifies number of sampling periods in the scheduling period, which in this study is 24 because $\Delta t = 1$ h ($N = \frac{24}{\Delta t}$). The time interval and bus indices used in this study satisfy $1 \leq i \leq N$, $1 \leq d \leq D$ and $1 \leq j \leq D$. D is the total number of buses in a given network.

3.3.1 Line Model

Lines with lengths of 80 km or less are considered to be short; and lines longer than 80 km but shorter than 240 km are taken as medium length. Long lines spanning 240 km and longer are predominant in transmission networks. Since the focus of this research is not on transmission networks, only models representing lines of short and medium lengths are discussed.

The admittance model for lines is obtained from the π-circuit representation for lines of medium-length described in [42], [43] and is expressed as

$$\boldsymbol{Y}^l = \begin{bmatrix} y_l + \mathrm{j}\frac{b_{ch}}{2} & -y_l \\ -y_l & y_l + \mathrm{j}\frac{b_{ch}}{2} \end{bmatrix}, \tag{3.4}$$

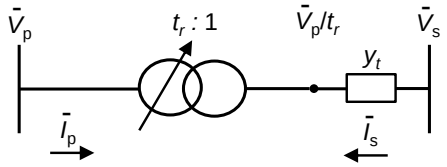

Figure 3.3: Transformer model with off-nominal winding on the primary side and admittance on the secondary side.

where

y_l is the series admittance of the line and b_{ch} is the line charging susceptance.

It follows from (3.3) and (3.4) that

$$y^i_{dd} = y_l + j\frac{b_{ch}}{2},$$

$$y^i_{dj} = -y_l,$$

$$y_{jd} = -y_l,$$

$$y^i_{jj} = y_l + j\frac{b_{ch}}{2}.$$

$\boldsymbol{Y}^l = 0$ if no line exists between bus d and bus j. The short line approximation simply ignores the line charging susceptance. Thus, this model is sufficient for load flow analysis of both short and medium length lines. It is assumed that the line model remains constant throughout the scheduling period.

3.3.2 Transformer Model

A transformer with an off-nominal tap ratio provides regulation in addition to nominal transformation. With such a transformer the voltage and phase angle could be adjusted in response to real and reactive power flows in a network. The phase angle is fixed because this formulation focuses solely on voltage magnitude adjustments. In other words the tap-ratio variable is real and not complex. Transformer models are described in terms of location of the off-nominal winding and the series admittance [44].

Suppose the off-nominal winding is on the primary side and the admittance is represented on the secondary side of the ideal transformer. From Figure 3.3 the following relationship

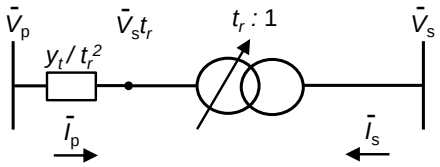

Figure 3.4: Transformer model with both the off-nominal winding and admittance on the primary side.

between the primary current and voltages arises

$$\bar{I}_p t_r = (\bar{V}_p/t_r - \bar{V}_s)y_t, \tag{3.5}$$

rearranging (3.5), the primary current is obtained

$$\bar{I}_p = \frac{\bar{V}_p y_t}{t_r^2} - \frac{\bar{V}_s y_t}{t_r}. \tag{3.6}$$

Similarly the secondary current is

$$\bar{I}_s = -\frac{\bar{V}_p y_t}{t_r} + \bar{V}_s y_t. \tag{3.7}$$

If the admittance is referred to the primary side of the ideal transformer as in Figure 3.4, the nominal admittance is divided by t_r^2 but in the end the current and voltage relations take the same form as equations (3.6) and (3.7).

In some instances the off-nominal winding is represented on the secondary side of the ideal transformer. Using Figure 3.3, this would mean the transformation changes to $1 : t_r$. Re-writing the current and voltage equations yields

$$\bar{I}_p/t_r = (\bar{V}_p t_r - \bar{V}_s)y_t, \tag{3.8}$$

$$\bar{I}_p = \bar{V}_p y_t t_r^2 - \bar{V}_s y_t t_r. \tag{3.9}$$

$$\bar{I}_s = -\bar{V}_p y_t t_r + \bar{V}_s y_t. \tag{3.10}$$

Again, referring the admittance to the primary side gives the same relations as (3.9) and (3.10) provided the admittance is multiplied by t_r^2.

The representation in Figure 3.3 is extended for the formulation of a time-varying transformer model. To fit the two-port model, (3.6) and (3.7) are expressed in matrix form as

$$\boldsymbol{Y}_t^i = \begin{bmatrix} \frac{y_t}{t_r^{i\,2}} & -\frac{y_t}{t_r^i} \\ -\frac{y_t}{t_r^i} & y_t \end{bmatrix},$$

where t_r^i is the tap ratio that varies with interval i.

An OLTC adjusts the transformer tap position in discrete steps, which is related to the tap ratio by

$$t_r^i = 1 - u_{st} u_{\text{TAP}}^i, \tag{3.11}$$

where

u_{st} is the size of a single tap increment/decrement step,

u_{TAP}^i is the integer tap position satisfying

$$u_{\text{TAP}}^i \in \{T^{\min}, \ldots -1, 0, 1, \ldots T^{\max}\} \text{ for all } i = 1, 2, 3 \ldots, N, \tag{3.12}$$

in which, $T^{\min}$ and $T^{\max}$ denote the lowest and highest transformer tap positions, respectively. The transformer model can then be described in terms of the tap position as

$$\boldsymbol{Y}_t^i = \begin{bmatrix} \frac{y_t}{(1-u_{st}u_{\text{TAP}}^i)^2} & -\frac{y_t}{(1-u_{st}u_{\text{TAP}}^i)} \\ -\frac{y_t}{(1-u_{st}u_{\text{TAP}}^i)} & y_t \end{bmatrix},$$

finally, the entries of the admittance matrix (3.3) for a transformer connected between dth bus and the jth bus are written as

$$\begin{aligned} y_{dd}^i &= \frac{y_t}{(1 - u_{st}u_{\text{TAP}}^i)^2}, \\ y_{dj}^i &= -\frac{y_t}{(1 - u_{st}u_{\text{TAP}}^i)}, \\ y_{jd} &= -\frac{y_t}{(1 - u_{st}u_{\text{TAP}}^i)}, \\ y_{jj}^i &= y_t. \end{aligned}$$

$\boldsymbol{Y}_t^i = 0$ if no transformer is connected between bus d and bus j.

3.3.3 Capacitor Model

Capacitors are realized as shunt elements with on/off operations modeled as binary variables. The admittance of the substation capacitor and the control actions have the following

relationship

$$y^i_{dd} = \mathrm{j}B_{dd}u^i_{\mathrm{CAP}}, \tag{3.13}$$

continuing in the same way, on/off control of the feeder capacitor at the dth bus is introduced as

$$y^i_{dd} = \mathrm{j}B_{dd}u^i_{\mathrm{C},d}, \tag{3.14}$$

where u^i_{CAP} and $u^i_{\mathrm{C},d}$ are capacitor switching functions defined as

$$\begin{cases} 1, & \text{when capacitor is switched on at the } i\text{th interval;} \\ 0, & \text{when capacitor is switched off at the } i\text{th interval.} \end{cases} \tag{3.15}$$

The matrix of shunt admittances representing capacitors is denoted by $\boldsymbol{Y}^i_c = diag\{y^i_{11}, y^i_{22}, ...y^i_{dd}, ...y^i_{DD}\}$. $y^i_{dd} = 0$ if bus d is not connected to a capacitor.

Admittances of the different branch and shunt components are combined to form a $D \times D$ bus admittance matrix. Each entry in $\boldsymbol{Y}^i_{bus}$ is the sum of elements with identical bus indices, denoted by subscripts, in $\boldsymbol{Y}_l$, $\boldsymbol{Y}^i_t$ and $\boldsymbol{Y}^i_c$ [42]. $\boldsymbol{Y}^i_{bus}$ entries are zero if the corresponding buses are without any branch or shunt connections. The bus admittance matrix is written as

$$\boldsymbol{Y}^i_{bus} = f(\boldsymbol{Y}_l, \boldsymbol{Y}^i_t, \boldsymbol{Y}^i_c) = \begin{bmatrix} y^i_{11} & y^i_{12} & \cdots & y^i_{1D} \\ y^i_{21} & y^i_{22} & \cdots & y^i_{2D} \\ \vdots & \vdots & \ddots & \vdots \\ y^i_{D1} & y^i_{D2} & \cdots & y^i_{DD} \end{bmatrix},$$

where $y^i_{dj} = G^i_{dj} + \mathrm{j}B^i_{dj}$ is an admittance element of the admittance matrix $\boldsymbol{Y}^i_{bus}$ between buses d and j at the ith interval. G^i_{dj} and B^i_{dj} are the real and imaginary parts of entry (d, j) of the bus admittance matrix; G_{dj} is the conductance and B_{dj} is the susceptance.

3.3.4 Load Forecasting and Load Model Considerations

In addition to the network model, the input for the proposed formulation is completed with load forecast data. For this study they are predicted load demand samples for the next 24 hours, where the time interval between two consecutive demand samples is 1 hour. Generally, load forecasting requires historical data to provide valid future load profiles. Considerations/variables affecting the accuracy of load forecasting include type of customer, and weather conditions. There are many different types of methods for load forecasting; conventional methods focusing mainly on regression analysis and time series analysis [36] or

more advanced techniques such as fuzzy systems, artificial neural networks and expert systems [36], [35]. Since it has been shown in previous studies that these methods provide good accuracy overall, it is reasonable to use day-ahead load predictions for VVC.

Constant current load demand varies with voltage. As voltage rises the demand increases and as voltage drops the demand does the same. In contrast, losses stay almost constant in response. The demand of constant impedance load is affected by voltage in the same manner as that of constant current load. Losses for this load model, however, also change with voltage. Low voltages cause low losses and vice versa. When it comes to constant power load, increasing the voltage decreases the losses and decreasing the voltage increases the losses [11].

Considering that raising voltage with an OLTC would reduce the power loss for constant power load, voltage regulation is expected to be a challenge because capacitors also cause voltage rise along with loss reduction. In other words, operating the network at a high voltage with capacitors in-service would minimise the losses but the voltage may be too close or over the upper limit. In this study both loss reduction and voltage regulation are taken into account and constant power load is assumed for the distribution system.

3.4 FORMULATION OF FEEDER VAR CONTROL AND OPTIMAL SUBSTATION CONTROL

A hybrid coordination mechanism is possible with day-ahead scheduling of distribution devices. In this method the control problem is modeled more explicitly than is the case with conventional control and the optimum settings approach. At the same time there is a need to reduce the computational requirements of this approach, which increase with the number of controlled devices in a given network. This would encourage more practical implementations in view of the fact that coordinated control has been shown to perform well under various operational objectives. For time-varying loads it is advantageous to install switchable feeder capacitors to have adequate reactive power compensation when the network is heavily loaded and avoid overcompensation for light loading.

3.4.1 General Formulation for Optimal Volt/Var Control

The general mathematical formulation of the day-ahead VVC dispatch problem is as follows

$$\min J(\boldsymbol{u}, \boldsymbol{x}) = (J_1(\boldsymbol{u}, \boldsymbol{x}), ..., J_{\mathrm{q}}(\boldsymbol{u}, \boldsymbol{x})), \tag{3.16}$$

subject to

$$g(\boldsymbol{u}, \boldsymbol{x}) = 0, \tag{3.17}$$

$$h(\boldsymbol{u}, \boldsymbol{x}) \leq 0, \tag{3.18}$$

where

J is a multiobjective function composed of objectives, J_1 up to J_{q};

$\boldsymbol{u}$ represents a vector containing control variables that consist of time-varying tap positions and capacitor switching statuses. For a network with one OLTC and one capacitor,

$$\boldsymbol{u} = [u^1_{\mathrm{TAP}}, ...u^{24}_{\mathrm{TAP}}, u^1_{\mathrm{CAP}}, ...u^{24}_{\mathrm{CAP}}]^T.$$

$\boldsymbol{x}$ is a vector containing state variables. These are the voltage magnitudes and angles:

$$\boldsymbol{x} = [V^1_1, ..., V^{24}_D, \delta^1_1, ..., \delta^{24}_D]^T.$$

The equality constraint (3.17) refers to the power balance equations, which must be satisfied with every selected control variable set. The inequality constraints are made up of control variable limits and voltage limits, within which the network is operated at every time instant. Additionally, the number of switching actions by the OLTC and capacitors must not exceed the maximum allowable number at the end of the scheduling period.

3.4.2 Feeder Capacitor Control

A heuristic scheduling technique based on the substation feeder reactive power profiles is proposed for feeder capacitors. The aim of this method is to minimize reactive power-flow through the transformer, with no substation capacitor and OLTC control. The feeder capacitors are only switched on/off if the resulting status decreases the reactive power flowing into or out of the substation from the distribution feeders. Furthermore, the total number of operations for the feeder capacitors during the scheduling period must not exceed the permissible quantity.

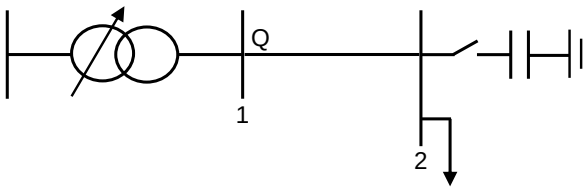

Figure 3.5: Two-bus network with a capacitor connected at the load bus.

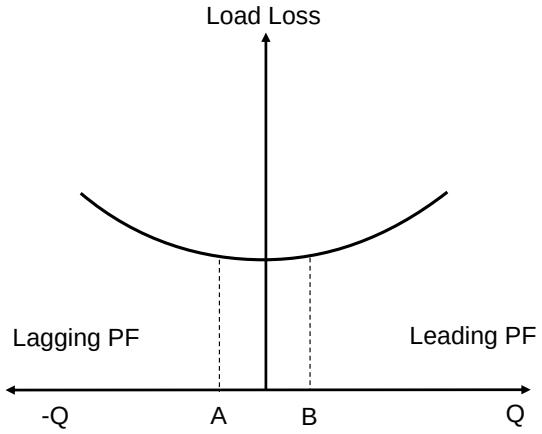

Figure 3.6: Relationship between load loss and reactive power.

Consider the case in Figure 3.5. The capacitor could be controlled based on Figure 3.6 for periodical variations in load. Reactive power flows out of the transformer and into the line supplying the load for a lagging power factor. In the case of a leading power factor, the direction of reactive power flows will be from the line into the transformer. It is noticed that as reactive power diverges beyond levels marked by A and B, the total load loss increases. Therefore, the capacitor could be switched on or off with the purpose of maintaining the reactive power in the region between A and B. Consequently, the load loss will remain low because of the minimized reactive power flow.

When the capacitor is out of service and the reactive power flow remains between A and B, no switching action takes place. The same applies for when the capacitor is in service and the reactive power flow stays within the region between A and B. As soon as the reactive power moves to the left of A the capacitor must be put in service. When the reactive power shifts to the right of B at a leading power factor, the capacitor supplies more reactive power than is required by the line and load. As a result the capacitor is switched off. The procedure for scheduling the feeder capacitors begins with power-flow computation at the ith switching

Table 3.1: Bus Definitions

Bus Type	Parameters
PV	Active Power (MW), Voltage (pu)
PQ	Active Power (MW), Reactive Power (Mvar)
Slack	Voltage (pu), Angle (degrees)

interval:

$$P^i_{\mathrm{G},d} - P^i_{\mathrm{L},d} = V^i_d \sum_{j=1}^{D} V^i_j [G^0_{dj} \cos(\delta^i_d - \delta^i_j) + B^0_{dj} \sin(\delta^i_d - \delta^i_j)], \tag{3.19}$$

$$Q^i_{\mathrm{G},d} - Q^i_{\mathrm{L},d} = V^i_d \sum_{j=1}^{D} V^i_j [G^0_{dj} \sin(\delta^i_d - \delta^i_j) - B^0_{dj} \cos(\delta^i_d - \delta^i_j)], \tag{3.20}$$

where

δ^i_d is the voltage angle at bus d,

δ^i_j is the voltage angle at bus j,

$P^i_{\mathrm{G},d}$ is the generated active power at bus d,

$Q^i_{\mathrm{G},d}$ is the generated reactive power at bus d,

$P^i_{\mathrm{L},d}$ is the active power consumed at the dth bus,

$Q^i_{\mathrm{L},d}$ is the reactive power consumed at the dth bus,

G^0_{dj} is conductance of the admittance element y^0_{dj} in the admittance matrix when the status of the substation capacitor is off and the transformer tap position is at nominal tap,

B^0_{dj} is the susceptance value of the admittance element y^0_{dj} in the admittance matrix when the status of the substation capacitor is off and the transformer tap position is at nominal tap.

The data input for power-flow dynamics to solve (3.19) and (3.20) consists of branch and shunt element data from which $\boldsymbol{Y}^i_{bus}$ is derived, bus data as well as the voltage magnitude and angle of the slack bus. Bus data specify bus types to be used in the calculation. The different bus types are defined in Table 3.1. The unknown variables are V^i_d and δ^i_d at the load (PQ) bus. At the slack bus, $P^i_{\mathrm{G},d}$ and $Q^i_{\mathrm{G},d}$ are unknown. The power-flow equations can be solved iteratively with standard techniques such as Gauss-Seidel and Newton's method for

every switching interval.

$$\bar{S}^i_{d,n} = \bar{V}^i_d \bar{I}^i_d = P^i_{d,n} + \mathrm{j}Q^i_{d,n}, \tag{3.21}$$

$$\text{for all } i = 1, 2, 3, ..., N;\ d = 1, 2, 3, ..., D.$$

Using the π-model, the current flowing through feeder from the bus d towards bus j is calculated as

$$\bar{I}^i_d = V^i_d e^{\mathrm{j}\delta^i_d} y^0_{dd} + V^i_j e^{\mathrm{j}\delta^i_j} y^0_{dj}, \tag{3.22}$$

$$\text{for all } i = 1, 2, 3, ..., N;\ d = 1, 2, 3, ..., D.$$

Therefore the reactive power injected through feeder n at the dth bus towards bus j is

$$Q^i_{d,n} = \mathrm{Im}\{V^i_d e^{\mathrm{j}\delta^i_d}(V^i_d e^{\mathrm{j}\delta^i_d} y^0_{dd} + V^i_j e^{\mathrm{j}\delta^i_j} y^0_{dj})^*\}; \tag{3.23}$$

$$\text{for all } i = 1, 2, 3, ..., N.$$

If d is the substation bus and $d = 1$, to determine the reactive power through one feeder, say feeder 2, which connects bus 1 to bus 3, (3.23) becomes

$$Q^i_{\mathrm{sub},2} = Q^i_{1,2} = \mathrm{Im}\{V^i_1 e^{\mathrm{j}\delta^i_1}(V^i_1 e^{\mathrm{j}\delta^i_1} y^0_{11} + V^i_3 e^{\mathrm{j}\delta^i_3} y^0_{13})^*\};$$

$$\text{for all } i = 1, 2, 3, ..., N.$$

Once the feeder reactive power injections become available, the statuses of the feeder capacitors at interval i are determined using

$$u^i_{\mathrm{C},d} = \begin{cases} 1, & \text{if } Q^i_{\mathrm{sub},n} \geq z_1 Q^{\mathrm{F}}_d; \\ 0, & \text{if } Q^i_{\mathrm{sub},n} \leq z_2 Q^{\mathrm{F}}_d; \\ u^{i-1}_{\mathrm{C},d}, & \text{if } z_2 Q^{\mathrm{F}}_d < Q^i_{\mathrm{sub},n} < z_1 Q^{\mathrm{F}}_d. \end{cases} \tag{3.24}$$

The switching sequence above must satisfy

$$\sum_{i=1}^{N} \left| u^i_{\mathrm{C},d} - u^{i-1}_{\mathrm{C},d} \right| \leq C^{\max}_{\mathrm{C}}, \tag{3.25}$$

where $u^i_{\mathrm{C},d}$ is the feeder capacitor status at bus d during the ith interval, $Q^i_{\mathrm{sub},n}$ is the reactive power through the distribution feeder n at the substation. Q^{F}_d is the reactive power rating of the capacitor. z_1 and z_2 are the switching parameters selected; based on the feeder reactive power-flows at the substation. z_2 is always smaller than z_1 and the two parameters satisfy $0 < z_1 \leq 1$ and $-1 \leq z_2 < 0$. $C^{\max}_{\mathrm{C}}$ denotes the allowed maximum number of daily switching operations for the feeder capacitors.

At each time interval i, power-flow calculations are executed and the status of each feeder capacitor is determined according to the criteria defined above. In order to deal with different network topologies when the switching criteria are met, the capacitors are switched on starting with the furthest one and ending with the closest from the substation. The switch-off procedure starts with the capacitor closest to the substation and ends with the capacitor furthest down the feeder. This method is applicable to most topologies because according to [15] capacitors are seldom installed on laterals. The reasons for avoiding such installations are detailed below.

- Load demand on laterals is usually lower than the minimum size of a capacitor.
- Lateral networks are mostly single-phase while capacitors are cheaper as three-phase units connected to three-phase networks. Furthermore, voltage unbalance is easier to manage in a system with three-phase units.
- Laterals are hard to reach and as a result it would be difficult to conduct maintenance on capacitors in theses locations.
- The impact of reactive power-flows is minimal on laterals compared to other parts of feeder networks, thus making capacitor installations uneconomical.

The feeder capacitor statuses affect the bus voltage magnitudes, but it is not necessary to consider voltage regulation in (3.24) because the bus voltages are kept within the upper and lower limits by the substation capacitor and OLTC control described in Section 3.4.3.

3.4.3 Substation Capacitor and OLTC Control

Generally, day-ahead VVC consists of a load-forecasting step, a power-flow module for evaluating the impact of different control states, and a module to optimally select and dispatch control settings. The VVC problem has mostly been modeled as minimization of losses, voltage deviations and reactive power-flow through the substation transformer subject to various constraints. The losses are directly proportional to the square of the current. The voltage deviation is a measure of how close the actual voltage is to the desired voltage. The reactive power-flow is influenced by capacitor on/off statuses as the load varies over the studied time interval. The constraints include bus voltage limits and equipment limitations, while

the control variables consist of the transformer tap positions and capacitor on/off commands. The equipment limitations are expressed in terms of the number of switching operations of the capacitors and OLTCs respectively. To preserve the life expectancy and meet the rapid voltage change requirements, the number of capacitor switching commands must be limited over the dispatch period. In a similar manner, the wear rate of OLTCs can be minimized by limiting the number of tap movements.

The voltage deviation index (VDI) indicates how close the actual voltage is to the desired voltage at a given bus. The model considers the contribution of each distribution bus to the total voltage deviation over the whole scheduling interval.

The total transformer loss is composed of two components, namely, the no-load loss and load loss [1], [17]. When a transformer is energized and there is no load connected to the secondary windings, currents known as eddy currents flow around the core. The currents are induced by the magnetic field as voltage is applied to the primary terminals. Because of the parasitic behaviour of these currents there is loss of power in the core. Concurrently, while the core undergoes magnetization, a process called hysteresis occurs, causing additional power loss in the core. These losses jointly cause energy dissipation in the core without the transformer supplying any load and are thus referred to as no-load losses. In the course of operation in normal conditions, the contribution of no-load losses is fixed irrespective of the load demand.

It is possible to reduce the magnitude of no-load losses during the design stage and while the transformer is in operation. For example, eddy currents can be minimized by decreasing the thickness of core laminations [1], [17].

On the other hand the load loss is a function of load and varies with load current over time. For this reason the proposed formulation incorporates the reduction of the load loss for time-varying load demand.

The real power loss is generally calculated as I^2R. With voltage magnitudes and angles from the power-flow model, the power loss at the ith time interval can be calculated as shown below.

Line loss:

$$\sum_{d=1}^{D}\sum_{j=1}^{D}\mathrm{Re}\left\{(|V_d^i e^{\mathrm{j}\delta_d^i} - V_j^i e^{\mathrm{j}\delta_j^i}|)^2 y_{dj}^b\right\} = P_{\mathrm{l}}^i. \tag{3.26}$$

Transformer loss:

$$\sum_{d=1}^{D}\sum_{j=1}^{D}\mathrm{Re}\left\{\left(\left|\frac{V_d^i e^{\mathrm{j}\delta_d^i}}{t_r^i} - V_j^i e^{\mathrm{j}\delta_j^i}\right|\right)^2 y_{dj}^b\right\} = P_{\mathrm{t}}^i. \tag{3.27}$$

Total loss:

$$P_{\mathrm{loss}}^i = P_{\mathrm{l}}^i + P_{\mathrm{t}}^i = \sum_{d=1}^{D}\sum_{j=1}^{D}\mathrm{Re}\left\{(|kV_d^i e^{\mathrm{j}\delta_d^i} - V_j^i e^{\mathrm{j}\delta_j^i}|)^2 y_{dj}^b\right\}, \tag{3.28}$$

where

$k = 1/t_r^i$ if a transformer is connected between buses d and j, and $k = 1$ if a line connects the dth bus to the jth bus;

y_{dj}^b is the series admittance i.e. $y_{dj}^b = y_l$ for a line and $y_{dj}^b = y_t$ for a transformer;

G_{dj}^b is the real part of y_{dj}^b.

The objectives of the FVC-OSC problem are formulated as:

minimize the total daily VDI,

$$\sum_{i=1}^{N}\sum_{d=1}^{D}(V_d^{\mathrm{T}} - V_d^i)^2, \tag{3.29}$$

and minimize the total daily energy loss,

$$\sum_{i=1}^{N} P_{\mathrm{loss}}^i \Delta t. \tag{3.30}$$

In this formulation the reference voltage at the substation secondary bus is changed from fixed to adaptive. That is, the objective function (3.29) changes to

$$\lambda_1 \sum_{i=1}^{N}\left((V_R - V_1^i)^2 + \sum_{d=2}^{D}(V_d^{\mathrm{T}} - V_d^i)^2\right), \tag{3.31}$$

where

V_1^i is voltage magnitude at the substation secondary bus,

V_R is the reference voltage at the substation secondary bus.

The idea behind the reference voltage adaptation is illustrated in Figure 3.7. Suppose the voltage deviation at the substation secondary bus is the same for the three reference voltages, V_{R1}, V_{R2} and V_{R3} and the target voltage at load buses is V^{T}. At t_i, the voltage deviations at

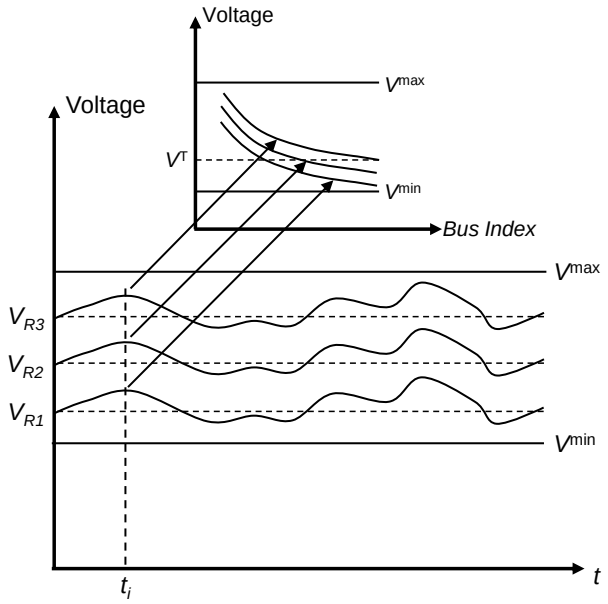

Figure 3.7: Voltage plots at the substation secondary bus (bottom) and the load buses (top).

load buses are lower for V_{R2} as opposed to V_{R1} and V_{R3}. Assuming constant power loads, it can be said that regulating the voltage close to V_{R3} produces the lowest total loss, followed by V_{R2} and then V_{R1}. In this case V_{R2} is optimal since it allows both voltage deviations and the total loss to be minimized. In short, the optimal value of V_R is dependent on the network loading levels and only changes when the load profile changes.

Constraints of the substation capacitor and OLTC control are discussed in Section 3.4.4 to Section 3.4.8.

3.4.4 Adaptive Tap Range

It has been shown in Section 2.2.1 that the secondary transformer voltage depends on the impedance, tap ratio, primary voltage and load. If the secondary voltage is to be kept constant as the load varies, the tap ratio could be adjusted accordingly. This is indeed similar to how AVR operates.

Staying with this principle, consider a case where the transformer is feeding one load directly from the secondary substation bus. An analytical expression can be derived which gives the ideal tap position based on the desired voltage at the secondary bus. In this way the voltage

deviation is minimised. However, realistic distribution networks consist of more than one bus on the secondary side of the transformer. Also, in this work, a reduction of the power loss is expected in addition to the voltage deviation. In other words, both the desired voltage and tap position become difficult to define for the whole network.

This motivates the extension from the ideal tap position for the one secondary bus to a set of tap positions to cater for more buses and operational objectives. The extension is realised by introducing an integer to create new bounds for the tap position. The ideal tap position is taken as the midpoint between the modified lower and upper tap position limits. Depending on the calculated value, some tap positions will be more feasible than others with regard to the deviation from the desired voltage. The furthest tap positions may even give infeasible voltages that are beyond permissible values. By limiting this extension from the ideal tap position, the furthest tap positions can be eliminated, thus reducing the original range to mostly feasible entries. The tap positions in this range are then evaluated according to operational objectives.

The selection of the integer number, u_a, is influenced by variations in primary voltage and load demand over the scheduling period.

It is noticed that not all available tap positions produce feasible bus voltages under time-varying load conditions. Therefore, the search space is reduced by further limiting the tap range, (3.12) to probable tap positions that lead to the lowest voltage deviations. Using the same expression as in [7], the ideal tap ratio is first approximated as

$$t_{\mathrm{id}}^{i} = \left\{ \frac{|Z_{\mathrm{T}}|^2}{\left|V_{\mathrm{p}}^{i}\right|^2 |V_{\mathrm{s}}^{i}|^2} \left[\left(Q_{\mathrm{L}}^{i} + \frac{|V_{\mathrm{s}}^{i}|^2}{|Z_{\mathrm{T}}|} \right)^2 + {P_{\mathrm{L}}^{i}}^2 \right] \right\}^{\frac{1}{2}}, \tag{3.32}$$

$$\text{for all } i = 1, 2, 3, ..., N;$$

and then the tap position range is modified as follows:

$$\frac{t_{\mathrm{id}}^{i} - 1}{u_{st}} - u_a \leq u_{\mathrm{TAP}}^{i} \leq \frac{t_{\mathrm{id}}^{i} - 1}{u_{st}} + u_a, \tag{3.33}$$

$$\text{for all } i = 1, 2, 3, ..., N;\ d = 1, 2, 3, ..., D;$$

where

V_{p}^{i} is the substation primary bus voltage,

V_{s}^{i} is the substation secondary bus voltage,

Z_{T} is the impedance of the transformer related to the admittance by $Z_T = 1/y_t$,
P_{L}^i and Q_{L}^i denote the active and reactive power demand at the substation secondary bus respectively,
u_a is a positive integer.

3.4.5 Voltage Regulation

The bus voltage magnitude must be limited to ensure that end-user equipment operates according to design specifications. Failure to adhere to the voltage limits leads to under-voltages and overvoltages. Undervoltages can cause current flow beyond ratings of constant power loads such as motors. Overvoltages may give rise to failure of motor insulation.

For MV feeders supplying LV networks, voltage drop and voltage rise from the substation bus to the LV connection points must be considered. The MV/LV transformer tap position can only be changed when the transformer is out of service i.e. when it is de-energised. If the voltage drop or voltage rise at MV level is allowed to be high, the voltage at service level will be near or even exceed the permissible LV limits. And operation of load equipment will be affected in response. Keeping the MV network voltages close to desired value will result in better voltage regulation at LV service level and will allow load equipment to operate at full capacity.

MV/LV transformer tap positions are selected according to the voltage variations at the MV supply points [45]. For any given MV feeder with LV points, MV/LV transformers in different supply areas may require distinct tap position settings to satisfy the LV voltage limits. The process of selecting and implementing these tap position settings can be tedious if the MV feeder has large periodical voltage variations. The ideal case is when the MV voltage is regulated within a small band because the MV/LV transformers at different points of the feeder could have the same tap setting and still produce voltages that are within the limits.

Furthermore, voltage limits influence the investment decisions made by distributors regarding upgrades to distribution networks. Advanced control strategies can help delay the investment in the short term or improve operational conditions during the period between planning and

construction of new plant. The bus voltage limits in FVC-OSC are imposed using (3.34)

$$V^{\min} \leq V_d^i \leq V^{\max}, \tag{3.34}$$

$$\text{for all } i = 1, 2, 3, ..., N;\ d = 1, 2, 3, ..., D.$$

At the substation secondary bus, the reference voltage must satisfy the following constraint.

$$V_R^{\min} \leq V_R \leq V_R^{\max}, \tag{3.35}$$

where

$V^{\min}$ is the permissible minimum voltage,

$V^{\max}$ is the permissible maximum voltage,

$V_R^{\min}$ is the lower reference voltage limit,

$V_R^{\max}$ is the upper reference voltage limit.

3.4.6 Power-Flow

The non-linear power-flow equations for substation control are expressed as

$$P_{\mathrm{G},d}^i - P_{\mathrm{L},d}^i = V_d^i \sum_{j=1}^{D} V_j^i [G_{dj}^i \cos(\delta_d^i - \delta_j^i) + B_{dj}^i \sin(\delta_d^i - \delta_j^i)], \tag{3.36}$$

$$\text{for all } i = 1, 2, 3, ..., N;\ d = 1, 2, 3, ..., D;$$

$$Q_{\mathrm{G},d}^i - Q_{\mathrm{L},d}^i = V_d^i \sum_{j=1}^{D} V_j^i [G_{dj}^i \sin(\delta_d^i - \delta_j^i) - B_{dj}^i \cos(\delta_d^i - \delta_j^i)], \tag{3.37}$$

$$\text{for all } i = 1, 2, 3, ..., N;\ d = 1, 2, 3, ..., D.$$

3.4.7 OLTC Switching Movements

Tap changers are responsible for over 30% of transformer failures [46]. One of the causes of these failures is contact wear, which is a function of current, the number of operations and time in service [47], [48]. When the tap position is changed, arcing takes place, producing gases and forming carbon particles. Meanwhile, the contacts are eroded and in the process the dielectric strength of the oil is compromised [9]. OLTCs are designed to endure at least 50 000 operations at rated current before the contacts are to be replaced [49]. Thus,

reducing the rate at which this maximum number of operations is reached extends the OLTC maintenance interval. To inspect and replace contacts, the transformer must be de-energised so deferring maintenance in this way reduces the number of planned outages taking place to execute maintenance work on OLTCs, and decreases the associated expenditure. Also, the overall asset maintenance plan will have relaxed personnel requirements since less time would be allocated to OLTC maintenance. The benefits are even greater for planned outages that cause supply interruptions; customers will benefit from having continuous power supply for longer periods.

The rate of contact wear is introduced into the optimization model as a limitation on the number of operations over a 24-hour period, as seen below:

$$\sum_{i=2}^{N} \left| u_{\text{TAP}}^{i} - u_{\text{TAP}}^{i-1} \right| \leq u_{T}^{\max}. \tag{3.38}$$

3.4.8 Capacitor Switching Operations

The action of energizing and de-energizing capacitors tends to cause transient overvoltages and high inrush currents. First, switching capacitor into service when the system voltage is at or close to peak leads to overvoltages that can reach as much as 2 pu theoretically. Second, when capacitors located next to each other are switched in rapid succession, the resulting inrush current is higher than when one capacitor is switched in isolation [2], [16], [50]. Other known instances which cause overvoltages include reclosing of breakers and restriking [50]. These switching phenomena have implications for capacitors and the power system.

Regarding the impact of switching, capacitors downstream from the capacitor being energised may experience voltage magnification, in which case the voltage exceeds 2 pu. By design, capacitors can tolerate different levels of transient overvoltages per year without shortening their lifespan. Switching of capacitors exposed to overvoltages as high as 3.6 pu should be limited to 40 times yearly. This number increases to about 4 000 times per year for overvoltages reaching 2.05 pu [16].

Since capacitors are also subjected to transient overcurrents during switching, it is important that the magnitudes and operations numbers specified in [16] are followed. The trends show that, for currents below 12 kA, the number of operations over time is inversely proportional

to the peak current capability of the capacitor.

Power electronic equipment is especially sensitive to capacitor switching. Motor drives with power converters are prone to tripping when an overvoltage is detected at the drive terminals. The occurrences of these trips can be high because voltages as low as 1.17 pu are known to trip motor drives. Gating of thyristors and electronic devices whose operation is based on the zero-crossings of the voltage waveform are also affected by capacitor switching. This is due to the distortions in the system voltage waveform [2], [16].

The number of capacitor switching operations are also guided by regulatory requirements. Installations that cause rapid voltage change, such as capacitors, should be restricted in terms of switching actions [51].

Due to the reasons provided above, it is desirable to control the transient levels during capacitor switching and to manage the number of switching events. The transient levels can be reduced via synchronous closing of breakers and using pre-insertion resistors, among other means of control. The method of controlling switched capacitors influences the number of times they are switched. Hence, this should be considered when switched capacitor control is implemented. The FVC-OSC algorithm also offers flexibility in respect of the capacitor control effort. The total number of capacitor operations are adjusted according to

$$\sum_{i=2}^{N} \left| u_{\text{CAP}}^{i} - u_{\text{CAP}}^{i-1} \right| \leq C^{\max}. \tag{3.39}$$

3.5 VALIDATION OF FVC-OSC

The algorithm is applied to a distribution system case study. The code of the algorithm is developed in MATLAB®. Two other approaches, namely, conventional VVC and the optimum settings approach are applied to the same system, but are implemented in DIgSILENT PowerFactory®, a commercial power system simulation package [52]. The results of the algorithms are presented in Chapter 5. It is shown that the proposed algorithm satisfies the constraints and performs better than the other two algorithms in terms of loss and voltage deviation reduction.

FVC-OSC is computationally efficient, considering the number of devices in distribution systems. Consider a system with four feeder capacitors, one substation capacitor and one

OLTC. The scheduling period is 24 h and the sampling period is 1 h. A heuristic technique is used to schedule feeder capacitors, leaving the dispatch schedule of the substation capacitor and OLTC to be solved mathematically. The variables that are determined with optimization are the substation capacitor on/off statuses, transformer tap positions and the reference voltage at the substation secondary bus. Thus, the total number of variables is $(1 + 1 \times 24 + 1 \times 24) = 49$. If the problem covered the substation capacitor and OLTC as well as the feeder capacitors, like in [31], for example, the number of variables would be $(5 \times 24 + 1 \times 24) = 144$. Thus it can be said FVC-OSC problem is simpler to solve because of the reduced dimensions of the optimization model. In terms of computational times, FVC-OSC takes 34.12 minutes to find an optimum solution while full optimization requires 87.97 minutes, on a Dell Inspiron-3542 with quad core 1.7 GHz Intel i5-4210U processors and 8 GB of RAM running Microsoft Windows 8.1. The VVC problem is solved using the particle swarm optimization algorithm, which is described in Chapter 4.

CHAPTER 4

APPLICATION OF FVC-OSC TO CASE STUDIES

4.1 CHAPTER OVERVIEW

The main objective of Chapter 4 is to develop the algorithm to solve the proposed FVC-OSC model. The optimization model is solved with discrete PSO, which calls power-flow routines in each iteration. This chapter also provides the specifications of the distribution network that is used for VVC simulations followed by the details of control implementation in the practical distribution network.

4.2 PARTICLE SWARM OPTIMIZATION

PSO is a stochastic optimization method created to mimic the social behaviour of flocks of birds. The search process follows a population of individuals known as particles. The particles form a swarm in which each one represents a possible solution of an optimization problem. Interaction within the swarm allows the particles to move through the search space using the best individual positions as well as the best position in the neighbourhood [53].

The PSO algorithm compares favourably with conventional optimization techniques for various reasons [54]. Firstly it does not impose restrictions such as the requirement for the objective function to be continuous, differentiable or convex. Secondly, PSO is initialized from a population of candidate solutions. Therefore the algorithm is less dependent on a decent initial solution. Thirdly, it is simpler to combine PSO with other optimization techniques to create hybrid algorithms. Finally, the stochastic nature of PSO enables the algorithm

to transition out of local optimum solutions. When compared with other evolutionary algorithms, PSO is simpler to code and is easily adaptable, has less demanding computational requirements, has fewer parameters to adjust and requires no conversion between different numbering systems [54].

4.2.1 Basic Particle Swarm Optimization

PSO has been successfully applied to other power systems problems. For example, in [55], it is demonstrated that PSO achieves better solutions faster than genetic algorithms for some cases of the optimal power flow problem. The basic PSO algorithm can be implemented in two ways, i.e. the global best PSO in which particles reference the entire particle population and local best PSO, where particles interact locally in smaller regions within the global neighbourhood [53]. The main differences are that global best converges fast while local best PSO provides more diversity during the search process. In this study the approach of the global best PSO is adopted.

Suppose a particle, p, moves from its current position $\boldsymbol{x}_p^k$ to the next position at a certain velocity as it searches multidimensional space using (4.1).

$$\boldsymbol{x}_p^{k+1} = \boldsymbol{x}_p^k + \boldsymbol{v}_p^{k+1}. \tag{4.1}$$

The velocity component, $\boldsymbol{v}_p^k$, adds knowledge of the social interactions in the particle's neighbourhood. In this regard, the knowledge is the past movement of the particle, the particle's best position yet and the current best position of the group as found by any of the particles. The velocity calculation is given in full in (4.2).

$$\boldsymbol{v}_p^{k+1} = w\boldsymbol{v}_p^k + c_1 rand_1(\boldsymbol{y}_p^k - \boldsymbol{x}_p^k) + c_2 rand_2(\boldsymbol{y}_g^k - \boldsymbol{x}_p^k), \tag{4.2}$$

where

$\boldsymbol{y}_p^k$ is the best position of particle p,

$\boldsymbol{y}_g^k$ is the best position of the whole particle group,

c_1 and c_2 are acceleration constants,

$rand_1$ and $rand_2$ are random numbers between 0 and 1.

The acceleration constants are made up of the cognitive parameter c_1 and the social parameter c_2. In [56], it is shown that these parameters can share the following relationship, $c_1 + c_2 \geq 4$.

But it is not the only option; another study uses $c_1 + c_2 \leq 4$ instead [57]. In fact, the default values, $c_1 = c_2 = 2$ were proposed in [58].

Let $f(\boldsymbol{x}_p^k)$ denote the fitness function to be used to quantify the solution of particle p. For problems concerning minimization, the best position of each particle is updated to $\boldsymbol{x}_p^{k+1}$ at step $k+1$ if $f(\boldsymbol{x}_p^{k+1}) < f(\boldsymbol{y}_p^k)$. If $f(\boldsymbol{x}_p^{k+1}) \geq f(\boldsymbol{y}_p^k)$, the particle's best position remains $\boldsymbol{y}_p^k$. From all the best particle positions, the global best position can be found, i.e. when $f(\boldsymbol{y}_g^k) = \min\{f(\boldsymbol{y}_1^k), ..., f(\boldsymbol{y}_{N_p}^k)\}$.

The number of particles that form the swarm affects swarm diversity during initialization, and the search coverage at each iteration. These two aspects improve as the number of particles increases, but computational time increases in response. The maximum iteration number is a function of solution quality and computational time. A sufficient number of iterations allows for good solutions to be obtained. In contrast, good solutions may not be reached if the search is terminated too early [53]. In this study the two parameters are obtained by trial and error.

4.2.2 Multi-Objective Discrete PSO

The FVC-OSC problem is composed of a non-linear fitness function and constraints. The control variables consist of capacitor switch statuses and tap positions. The capacitor switch statuses are binary variables and tap positions are integers. The state variables in this problem are complex voltages and power flows, which are continuous. Therefore, this problem is classified as an MINLP problem.

PSO is capable of solving discrete problems in areas where other techniques like branch and bound are unsuccessful [59]. Several PSO variants are proposed to solve the VVC problem in [60]. However, these approaches are applied to the single-period VVC, which does not consider the time-varying nature of load and the operating effort of the control devices.

Also, FVC-OSC aims to achieve loss reduction and minimize voltage deviations at the same time. Because of these two objectives, substation control in FVC-OSC needs to be treated as a multi-objective optimization problem. For this study, the sum of weighted functions method is adopted, but alternative methods that enable optimization algorithms to handle

problems with more than one objective can be used, as presented in [61].

The PSO algorithm presented here is similar to that of [62]. It can handle discrete variables with simple modifications. In this formulation, the binary and integer variables are solved simultaneously.

The particle p position vector is represented by $\boldsymbol{x}_p = \left[x_p^1, x_p^2, ..., x_p^U\right]^T$, where U is the particle dimension. The velocity vector is $\boldsymbol{v}_p = \left[v_p^1, v_p^2, ..., v_p^U\right]^T$. The position and velocity for particle p in the next iteration $k+1$ are updated as follows

$$\boldsymbol{v}_p^{k+1} = round(w\boldsymbol{v}_p^k + c_1 rand_1(\boldsymbol{y}_p^k - \boldsymbol{x}_p^k) + c_2 rand_1(\boldsymbol{y}_g^k - \boldsymbol{x}_p^k)), \tag{4.3}$$

where $round()$ is a function that rounds off to the nearest discrete value,

It is desirable for the algorithm to be able to explore and exploit the search space during the optimization process. Exploring different parts of the search space enables the algorithm to find optimal values. In contrast, the exploitation ability allows the algorithm to focus on promising regions to further improve existing solutions [63]. In order to achieve a balance between these two aspects, the velocity component is modified using (4.4). The velocity $\boldsymbol{v}_p^k$ is restricted to fall within the range $[v^{\min}, v^{\max}]$. When $\boldsymbol{v}_p^k < v^{\min}$, the velocity is reset to $\boldsymbol{v}_p^k = v^{\min}$ in all iterations. For cases where $\boldsymbol{v}_p^k > v^{\max}$, the velocity is redefined to $\boldsymbol{v}_p^k = v^{\max}$.

$$\boldsymbol{v}_p^k = \begin{cases} v^{\max}, & \text{if } \boldsymbol{v}_p^k > v^{\max}; \\ \boldsymbol{v}_p^k, & \text{if } v^{\max} \leq \boldsymbol{v}_p^k \leq v^{\max}; \\ v^{\min}, & \text{if } \boldsymbol{v}_p^k < v^{\min}. \end{cases} \tag{4.4}$$

As is the case with velocities, the particle position $\boldsymbol{x}_p^k$ is limited by $x^{\min}$ and $x^{\max}$ in (4.5). It is important to restrict the range of possible particle positions because the VVC problem consists of control variables with practical limitations.

$$\boldsymbol{x}_p^k = \begin{cases} x^{\max}, & \text{if } \boldsymbol{x}_p^k > x^{\max}; \\ \boldsymbol{x}_p^k, & \text{if } x^{\min} \leq \boldsymbol{x}_p^k \leq x^{\max}; \\ x^{\min}, & \text{if } \boldsymbol{x}_p^k < x^{\min}. \end{cases} \tag{4.5}$$

The particles are initialized with the calculation in (4.6). This way the initial particle values

will also fall within $x^{\min}$ and $x^{\max}$.

$$\boldsymbol{x}_p^0 = round(x^{\min} + \boldsymbol{rand}_p(x^{\min} - x^{\max})) \tag{4.6}$$

where

$\boldsymbol{rand}_p$ denotes a vector of random numbers between 0 and 1.

The multi-objective function, J is treated as a weighted sum of the total power loss and the VDI. The function does not have a physical unit because the constituent parts are of different classifications,

$$J = \lambda_1 J_1 + \lambda_2 J_2, \tag{4.7}$$

where

$$J_1 = \sum_{i=1}^{N} \left((V_R - V_1^i)^2 + \sum_{d=2}^{D} (V_d^{\mathrm{T}} - V_d^i)^2 \right), \tag{4.8}$$

$$J_2 = \sum_{i=1}^{N} P_{\mathrm{loss}}^i \Delta t, \tag{4.9}$$

λ_1 and λ_2 are positive tuning weights.

To deal with the constraints (3.34)–(3.39), the penalty approach is adopted. Thus the fitness function for PSO with a constraint penalty introduced, is given as follows [64]

$$J + p \sum_{u=1}^{M} \max(0, h_u), \tag{4.10}$$

where

p is the penalty coefficient,

h_u is an expression representing each of the constraints,

M is the total number of constraints.

The value of the second term in (4.10) rises as the search moves into infeasible space and decreases as the search is directed towards feasible regions until it is zero for no constraint violations. The penalty term essentially turns the constrained optimization problem into an unconstrained problem. The selection of the penalty coefficient takes into account the fact that the algorithm must generate feasible solutions and still be able to escape the local solution space. Low penalty factors mostly lead to infeasible solutions whereas high values of the penalty coefficient mean that the algorithm is likely to converge to a local optimum.

The penalty coefficient used in this study lies between the two extremes and is found by trial and error.

The following PSO parameter settings are employed:

- Particle population size of 100;
- The number of iterations, $N_{\text{it}} = 200$, for 20 runs of the algorithm;
- Acceleration constants are set as $c_1 = c_2 = 2$ to satisfy $c_1 + c_2 = 4$;
- The inertia term, $w = 0.5 + \frac{1}{2(\ln k+1)}$, in which k is the iterations count;
- $v^{\max}$ is set to about 25% of the variable range; $v^{\min} = -v^{\max}$.
- The penalty coefficient p is assigned a value of 150.

The steps that are followed to implement the discrete PSO algorithm are described below.

Step 1: Generate a population group of N_p random particles.

Step 2: Evaluate fitness function (4.10) for each particle.

Step 3: Find particle with best solution in the group. $\boldsymbol{y}_p^0 = \boldsymbol{x}_p$.
$\boldsymbol{y}_g^0 = \boldsymbol{y}_p^0$ if $f(\boldsymbol{y}_p^0) = \min\{f(\boldsymbol{y}_1^0), ..., f(\boldsymbol{y}_{N_p}^0)\}$.

Step 4: Iterate through the following steps as long as the predefined maximum iteration number is not reached:

- For each particle $p = 1, ..., N_p$: evaluate the fitness function (4.10), and assign particle best position, *pbest*, i.e. set $\boldsymbol{y}_p^{k+1} = \boldsymbol{x}_p^{k+1}$ if $f(\boldsymbol{x}_p^{k+1}) < f(\boldsymbol{y}_p^k)$; evaluate the fitness function (4.10), and assign global best position, *gbest*, i.e. set $\boldsymbol{y}_g^{k+1} = \boldsymbol{y}_p^{k+1}$ if $f(\boldsymbol{y}_p^{k+1}) < f(\boldsymbol{y}_g^k)$.
- For each particle $p = 1, ..., N_p$: adjust the particle velocity using (4.2), and adjust the particle position using (4.1).

Step 5: Stop the algorithm if the number of iterations, *iter*, has reached the predefined maximum number.

The procedure that is followed to solve the VVC problem is summarised in Figure 4.1 and also presented below.

Step 1: Define a model of the power system network and specify the multi-period load demand data in terms of $P^i_{\mathrm{L},d}$ and $Q^i_{\mathrm{L},d}$.

Step 2: Transfer the model data, load demand samples and initial control actions for each time interval i to the power-flow module. Solve the power-flow problem for all $i = 1, 2, 3, ..., N$ and from the resulting reactive power flows, determine a set of control actions $u^i_{\mathrm{C},d}$, which satisfy (3.24) and (3.25) during the 24-h scheduling period.

Step 3: Determine the applicable transformer tap range for each interval i. Here the original tap position limits change from fixed to interval-specific.

Step 4: Initialise all variables (u^i_{CAP}, u^i_{TAP} and V_R) for all $i = 1, 2, 3, ..., N$.

Step 5: Transfer the model data, load demand samples and control actions for each time interval i to the power-flow module. Solve the power-flow equations to determine the bus voltages and power losses for a given population of particles. At the end of the ith power-flow computation, the vector $[V^i_1, ..., V^i_d]^T$ and P^i_{loss} are stored until the end of the scheduling period and then transferred to the next step where the optimization model is evaluated.

Step 6: Apply discrete PSO.

Step 7: Stop the algorithm if it has reached the predefined maximum number of iterations. Otherwise return to step 5.

4.3 DISTRIBUTION TEST NETWORK

To define a network model, data for the lines, transformers, loads and generators need to be defined. The network topology is created by defining the connections of these components through buses.

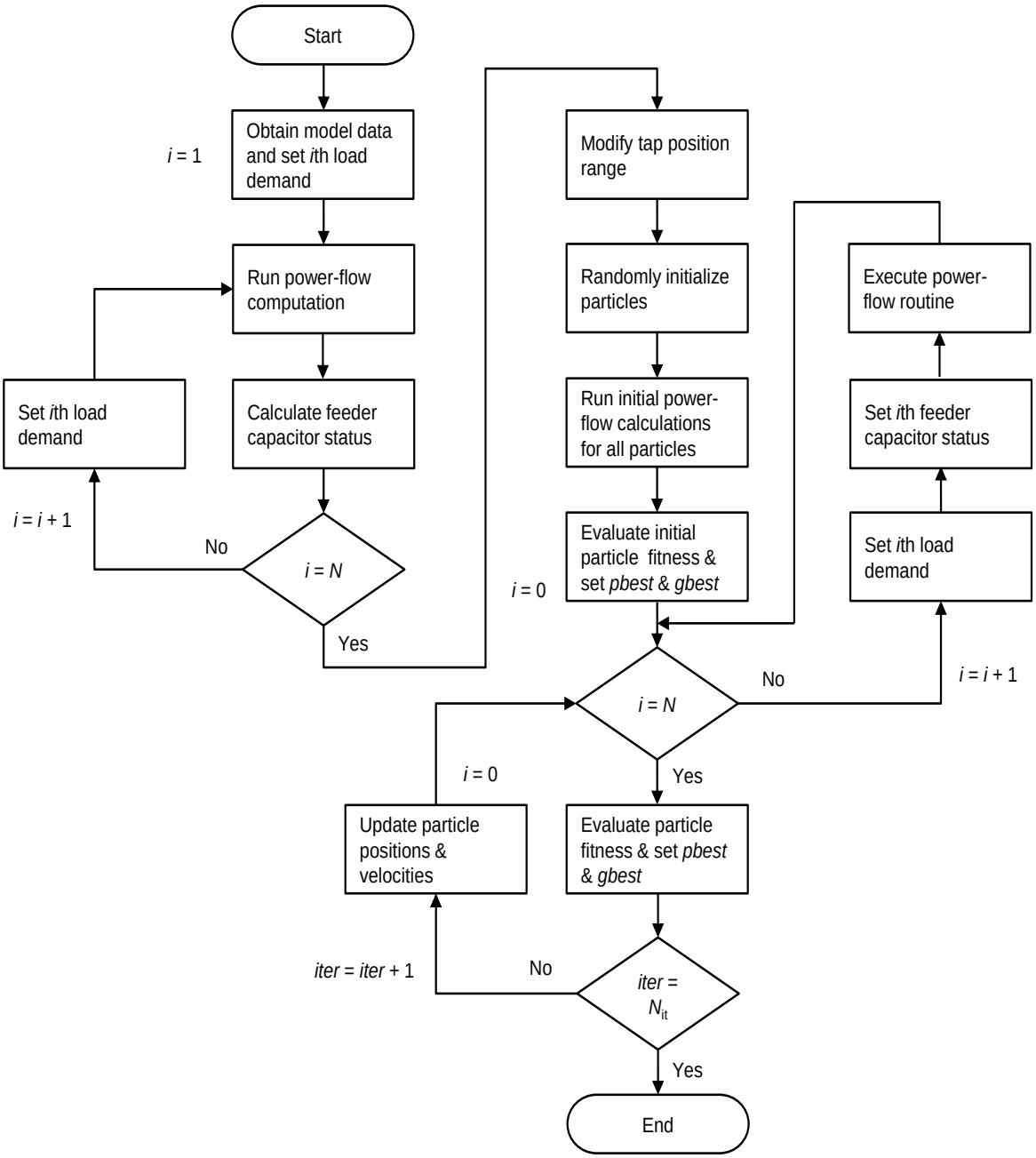

Figure 4.1: Overview of FVC-OSC algorithm.

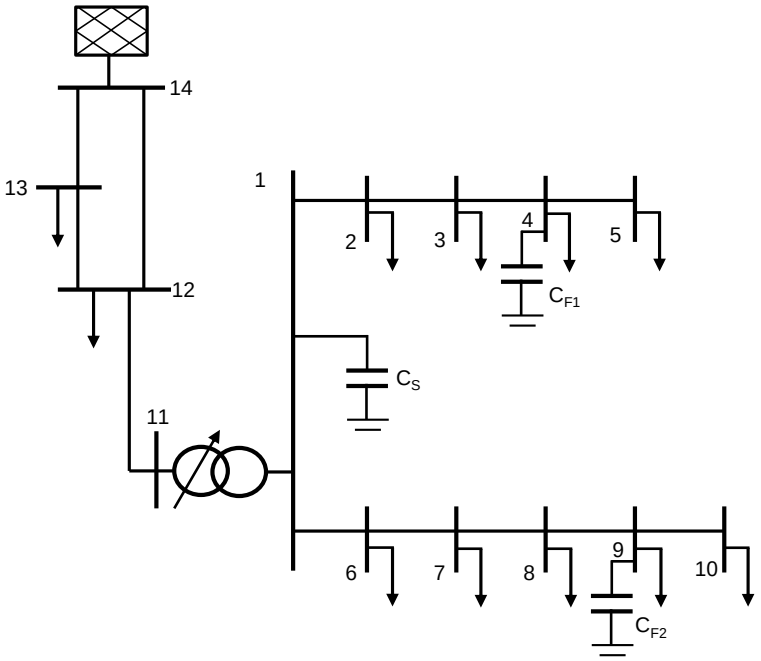

Figure 4.2: Typical distribution network with an OLTC and capacitors (adapted from [18] © 2007 IEEE).

The distribution network depicted in Figure 4.2 is used for performance evaluation of conventional control, the optimum settings approach and the proposed approach.

The system is a modified version of the one described in [18], [19]. Feeder capacitors are reduced to two, one 1.4 Mvar capacitor at bus 4 and another one of the same size at bus 9. One substation capacitor is removed but the remaining 2 Mvar capacitor is switchable. When the network is operated using the conventional method, the feeder capacitors are fixed and remain on throughout the scheduling period. This minimizes cost of maintenance for feeder capacitors for the network distributor. With this approach the distributor would typically attempt to select suitable AVR settings to accommodate the feeder capacitors. FVC-OSC is applied to the same network and its performance evaluated against that of the conventional method. All the loads are constant power loads and each is expressed as a proportion of the base apparent power. The base demand 1.4 MVA. Each load has the $P^i_{\mathrm{L},d}$ and $Q^i_{\mathrm{L},d}$ profiles shown in Figure 4.3 for which $\Delta t = 1$ h. Other variations in load are discussed in Chapter 5. It is assumed that the studied system has adequate generated power at all times. The minimum and maximum allowed voltages are 0.95 pu and 1.05 pu, respectively. The target voltage is $V_d^{\mathrm{T}} = 1$ pu for all load buses. The transformer provides ±10% regulation with

Table 4.1: Bus Data

Bus Number	Bus Type	Load	Capacitor (Mvar)
1-10	PQ	1.4 MVA (Base)	Bus 1: 2 Bus 4: 1.4 Bus 9: 1.4
12	PQ	22 MW, 0.95 pf	-
13	PQ	18 MW, 0.95 pf	-
14	Slack	-	-

Table 4.2: Branch Data (Lines)

Bus (From)	Bus (To)	x (Ω/km)	r (Ω/km)	Length (km)
1	2	0.35	0.12	1.2
2	3	0.35	0.12	1.2
3	4	0.35	0.12	1.2
4	5	0.35	0.12	1.2
1	6	0.35	0.12	1
6	7	0.35	0.12	1
7	8	0.35	0.12	1
8	9	0.35	0.12	1
9	10	0.35	0.12	1
14	12	0.5	0.15	16
14	13	0.5	0.15	9
13	12	0.5	0.15	8
12	11	0.5	0.15	10

Table 4.3: Branch Data (Transformer)

Bus (From)	Bus (To)	Voltage Levels (kV)	Capacity (MVA)	x (pu)	r (pu)	OLTC
11	1	70/10	18	0.12	0.012	-10% to 10% (16 Steps)

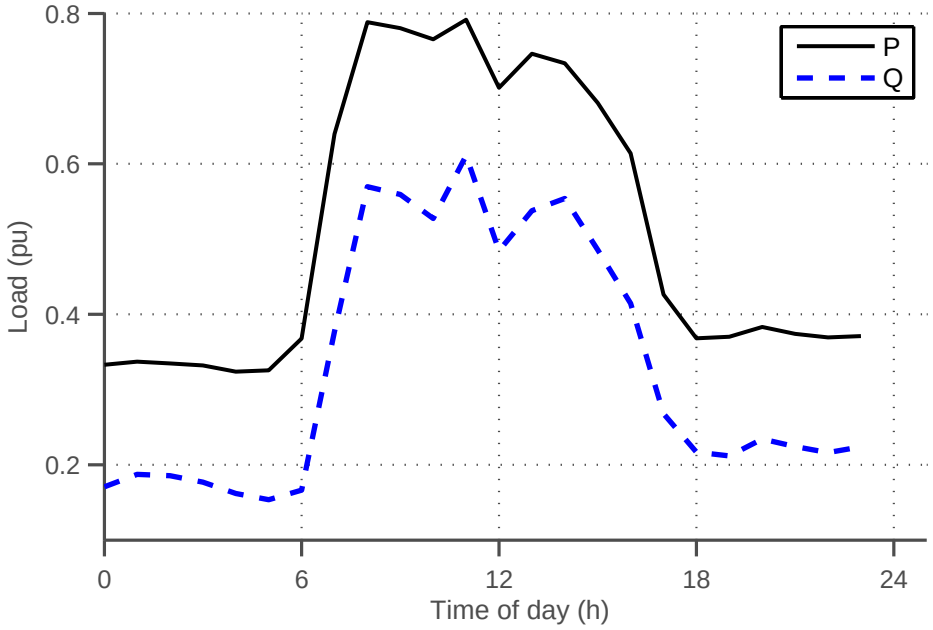

Figure 4.3: Daily load curves.

8 tap steps above and below nominal tap; $T^{\min} = -8$ and $T^{\max} = 8$. Each step gives an increment/decrement of ± 0.0125 pu. The maximum allowable number of tap operations per day is 30. All capacitors can only be operated 8 times a day at the most. The motivation behind studying scenarios with increased reactive power compensation levels is that such measures are taken in practice in response to increased loading or in an effort to reduce losses. For this case study, the distributor installs two more feeder capacitors at bus 4 and bus 9. In the process the conventional method is extended to include the two additional capacitors and the optimum settings approach is adopted due to the increase in installed capacitors and the related risk of violating permissible voltage limits. Again FVC-OSC is tested on this system for comparison with the more sophisticated optimum settings approach.

The performance of the algorithms is evaluated according to:

- Reduction of losses over the scheduling period.
- Voltage deviation reduction i.e. how close the actual voltage is to the desired voltage.
- The control effort, demonstrated by the number of device operations within the scheduling period.

- Voltage limits compliance over the scheduling period.

4.4 MATPOWER IMPLEMENTATION

MATPOWER is an open-source tool for power system simulations in the MATLAB environment [65], [66]. The tool has been designed to solve the single-period power-flow and optimal power-flow problems. Unlike commercial power system simulation tools, MATPOWER does not have a graphical user interface. Instead, a case file needs to be created in which the parameters of the power system components are defined. The file includes bus data, branch data and generator data. On the other hand, the advantage of MATPOWER is that it can be easily extended to deal with a broad range of power-flow and optimal power-flow problems. MATPOWER follows an index structure to build networks. For branch data, two connection points are required; the bus where the branch connection starts and the bus where the connection ends. The impedance between these buses is specified in pu.

The admittance matrix is built from the conductance and susceptance found in the bus data matrix, and the resistance, reactance and the line-charging susceptance obtained from the branch data matrix. For a typical power system, a capacitor is represented as susceptance, in Mvar, in the bus data matrix. Transformers and lines are realized through the resistance, reactance and charging susceptance, all in pu, in the branch data matrix. The load is specified in terms of active and reactive power demand in the bus data matrix; these parameters are in MW and Mvar, respectively.

Bus data include the bus index, bus type and power values. The bus data matrix also requires specification of generator parameters. First, the bus type is defined, then the corresponding parameters can be specified according to Table 3.1.

4.4.1 Power Flow Calculation

In MATPOWER the tap position and range cannot be specified, however, the regulating function of transformers is incorporated through the tap ratio parameter. This parameter does not change during the power-flow computation; it remains fixed and can only be changed before the solution process begins. The same applies to the capacitor switch status. It is specified as a reactive power injection in advance.

For the implementation of FVC-OSC, the tap position and capacitor switch status are treated as variables whose values are calculated iteratively with PSO. At each iteration step the possible tap positions and capacitor switch statuses are converted to tap ratios and reactive power injections respectively, and then passed to MATPOWER, where the power-flow solution is obtained. The algorithm is executed for every set of the control actions i.e. the transformer tap positions and the capacitor statuses.

4.4.2 Input-Output Functions

MATPOWER functions are called during computation of the FVC-OSC solution, mainly to execute the power-flow routine and provide the bus and branch results. In order to run a power-flow routine the user must first load the data of the power system network under study. This step requires the MATPOWER command, `mpc = loadcase('ND')` to obtain the system data from the file denoted by `ND`. Within `ND`, `mpc.branch(r,c)` refers to an entry in the branch data matrix accessed through `r` and `c`, which are row and column indices. Similarly `mpc.bus(r,c)` represents an entry in the bus data matrix.

Prior to starting the power-flow calculation, MATPOWER can be given preferences specific to the solution algorithm and results output. The command, `opt = mpoption('OP', VAL)` allows the user to modify the default options, where `OP` and `VAL` are the option name and value.

The command, `results = runpf(mpc,opt)` executes a power-flow calculation routine and saves the results to a structure. Bus and branch results are then accessed using the commands `results.bus(r,c)` and `results.branch(r,c)`.

4.5 IMPLEMENTATION OF CONTROL ACTIONS

The proposed control sequences can be implemented in two ways; as a form of time control, or remotely via communication links. The former gives a control action corresponding to each interval over the scheduling period, in this case according to time-of-day. These settings are applied at the location of the OLTC or capacitor through a device with characteristics of local controllers [67]. The disadvantage of this strategy is that the settings would be applied over a long period i.e. seasonally rather than daily because implementation would

involve traveling to the control sites every time switching sequences need to be changed. As a result this approach is suboptimal for load profiles that vary depending on the day of the week.

Remote control is more convenient. The control settings are issued from a central point such as the control centre, to the OLTC and capacitor. The advantage of this form of control is that control settings can be applied daily. In this regard, variations taking place over successive days are predicted with daily load forecasts. Another benefit is that the operator at the control centre would be able to intervene in response to real-time operating conditions, such as contingencies affecting network configuration, with a fully integrated communication system. However, remote control requires the network to have communication links to the control devices, thus making it more expensive than 'time-of-day' control.

In fact, the proposed control strategy is flexible in terms of implementation. For example, a network with limited remote control capability (i.e. communication coverage up to the substation) could combine the two forms of control. In this case, the feeder capacitors control schedule would be based on a static load forecast to be repeated over a long period. The substation control schedule would depend on the load forecast that is supplied one day ahead of implementation and the static feeder capacitor control schedule.

CHAPTER 5

VOLT/VAR CONTROL SIMULATION RESULTS

5.1 CHAPTER OVERVIEW

The simulation results of the FVC-OSC approach, formulated in Chapter 3 and Chapter 4, are presented and compared to those of conventional methods. Several simulation scenarios are studied. The first scenario presents the results of the adaptive reference voltage and tap range on the optimal substation control model. Next, the results of the comparison between FVC-OSC and conventional control are given, followed by the impact of disturbances and comparison of FVC-OSC and the optimum settings approach. Lastly, conventional control, the optimum settings approach and FVC-OSC are simulated with the period changed from 24 hours to 48 hours.

5.2 EFFECT OF ADAPTIVE REFERENCE VOLTAGE AND TAP RANGE

Two cases consisting of 30 trials each are studied. The relationship between the solution obtained by PSO and the number of iterations is illustrated in Table 5.1. It is observed that the solution does not improve beyond 200 iterations even though the share of feasible solutions rises to over 83%. Therefore the algorithm is terminated after 200 iterations in each trial. In the first of the studied cases, the reference voltage is fixed at 1 pu and the tap range is limited according to the lowest and highest transformer tap positions, $T^{\min}$ and $T^{\max}$ respectively. In the second case, the tap range and reference voltage are adjusted as

Table 5.1: Effect of iterations number on PSO algorithm

Iterations	Best solution	Feasible solutions (%)
60	2.4284	20.00
80	2.421	23.33
100	2.3884	26.67
120	2.4185	43.33
140	2.3964	60.00
160	2.397	60.00
180	2.3886	60.00
200	2.3612	70.00
1000	2.3641	83.33

defined in Section 3.4.3.

The best solution to the function in (4.10), obtained with a fixed referenced voltage and the full tap range, is a minimum of 2.3853. As mentioned previously, not all tap positions yield bus voltages between $V^{\min}$ and $V^{\max}$. As a result, the search space explored has a number of infeasible solutions. By comparison, the modifications improve the quality of solutions, with the best solution dropping to 2.3612. Similarly, the mean, among others, is lowered to 2.4056 from 2.4225. The solutions are improved in this case because the algorithm explores a narrower search path and is directed towards solutions which minimize both voltage deviations and losses. Details of the statistical results reached by the two cases are shown in Table 5.2.

5.3 COMPARISON OF FVC-OSC AND CONVENTIONAL CONTROL

Performance of conventional on-line control can vary, depending on specified settings. In previous studies the relevant settings adopted for conventional control are not clearly stated, making it difficult to assess the overall improvement brought by the proposed methods.

Table 5.2: Statistical results of FVC-OSC

	FVC-OSC (Fixed)	FVC-OSC (Adaptive)
Worst	2.5407	2.4633
Best	2.3853	2.3612
Mean	2.4225	2.4056
Std	0.0367	0.0249

Table 5.3: Conventional Method Settings

	OLTC		Capacitor	
Scenario	V_{set} (pu)	V_{db} (pu)	t_{on}	t_{off}
CC-A	1.00	0.03	07:00	16:00
CC-B	1.02	0.03	07:00	16:00

Performance under various settings and loading conditions that change hourly is evaluated to illustrate the advantages of the proposed approach.

Three scenarios are studied and compared with reference to a base case in which the transformer tap position is fixed at nominal tap and the substation capacitor status is off. Two cases of conventional control, CC-A and CC-B, which refer to AVR combined with time-based capacitor control at different set-points (V_{set}) are investigated for comparison purposes. The settings used for conventional control are shown in Table 5.3. Results of the CC-A and CC-B show that the substation capacitor is switched on as the load rises towards peak demand and switched off as the load approaches minimum demand. In both cases the substation capacitor is switched on at 07:00 and switched off at 16:00. The feeder capacitors are switched on and remain so throughout the 24-h scheduling period. Regarding the proposed FVC-OSC approach, $z_1 = 0.5$ and $z_2 = -z_1$ are used for feeder capacitor control. The substation OLTC and capacitor control optimization problem is solved with PSO, and the power-flow solutions are computed using Newton's method provided in [65].

Table 5.4: Summary of Results For The System Under Study

Scenario	VDI	Total Loss (MWh)	Number of Operations	
			OLTC	Capacitor
Base Case	1.2778	15.2520	-	-
CC-A	0.1340	14.3422	14	2
CC-B	0.0436	14.1888	14	2
FVC-OSC	0.0375	13.9798	21	5

Table 5.4 shows the summarised results for the base case, Conventional Control and FVC-OSC. In conventional control, only the substation secondary bus voltage i.e. bus 1 in Figure 4.2 is monitored and controlled. As the load changes according to the trend in Figure 4.3, the voltage is kept within the specified deadband margins at bus 1 as illustrated in Figure 5.1. On the contrary, the bus voltages at other buses fluctuate with load. Hence the lower voltage limit is violated at bus 9 and at bus 10 during the day for CC-A. The voltage profiles for bus 9 are shown in Figure 5.2. The voltage remains within the allowable range throughout the day and the total daily loss is reduced in CC-B. This is due to the higher voltage set-point in this scenario. The total VDI decreases by 67.46% and the total loss by 1.07% from 0.1340 and 14.3422 MWh produced by CC-A respectively. It should be noted that raising the voltage set-point does not always improve the solution. For example, changing the set-point from 1.02 pu to 1.03 pu lowers the total loss to 14.0946 MWh but increases VDI to 0.0628. In FVC-OSC, the feeder capacitors are switched on and never switched off because the reactive power-flow at either of the substation feeders does not exceed $-0.5Q_d^{\mathrm{F}}$ at any instant during the 24-h period. The resulting bus voltages are kept even closer to the desired values while there is also an improvement in the total loss reduction recorded in CC-B. Compared to CC-B, VDI and total loss are reduced by an additional 13.99% and 1.47% respectively. FVC-OSC results correspond to a calculated reference voltage of 1.02 pu. For high load (07:00–18:00), FVC-OSC regulates the voltage higher than conventional control. The rest of the time, the voltage is maintained closer to CC-A or CC-B. This adaptive ability allows FVC-OSC to maintain a steadier voltage profile downstream in both high and light loading conditions as seen in Figure 5.2. Also, the network experiences higher loss reduction due to FVC-OSC as

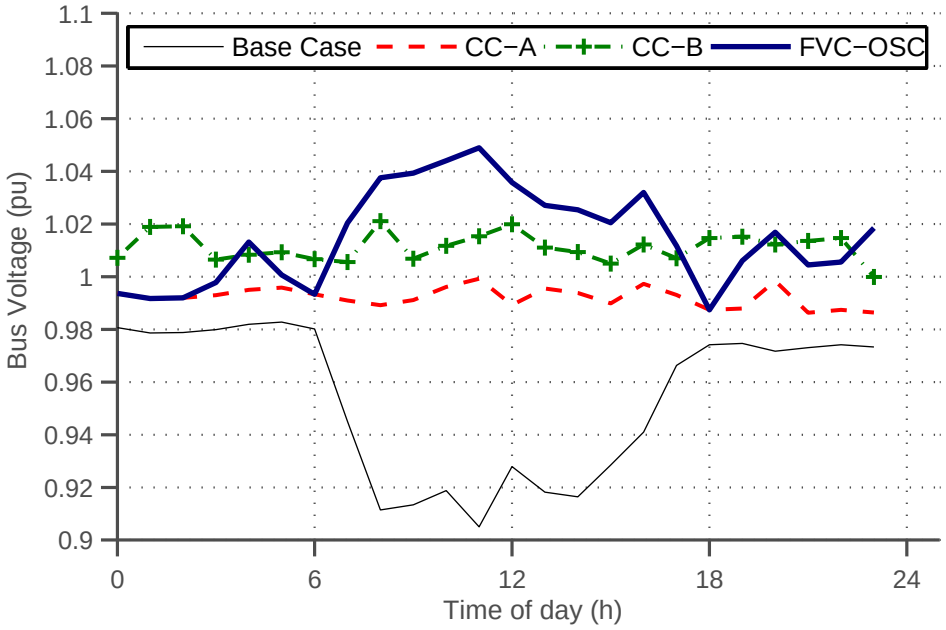

Figure 5.1: Bus 1 voltage profiles.

compared to conventional control during the same period.

The tap movements and capacitor control actions resulting from the cases under study are displayed in Figure 5.3 and Figure 5.4. In general, the transformer tap position is raised as load rises and lowered as the load drops. But compared with conventional control, FVC-OSC further ensures that the voltages at all the load buses are kept close to a reference value of 1 pu. The substation capacitor also responds better to load variations under FVC-OSC. Consider the state of the capacitor towards the end of the peak period; it is switched out at a later time than in CC-A and CC-B, which maximizes loss reduction. In all scenarios, the number of device operations remained below the specified limits although FVC-OSC resulted in the highest of all four. It can be observed that in FVC-OSC, the OLTC raises the transformer tap position higher than in CC-A and CC-B, most notably at peak load. It is, however, during this period that FVC-OSC produces the highest loss reduction. The voltage at bus 1 is higher thereby causing the current to decrease because the current is inversely proportional to the bus voltage.

It is noticed that the relative additional performance improvement brought by FVC-OSC relative to conventional control depends on the selected settings of conventional control to

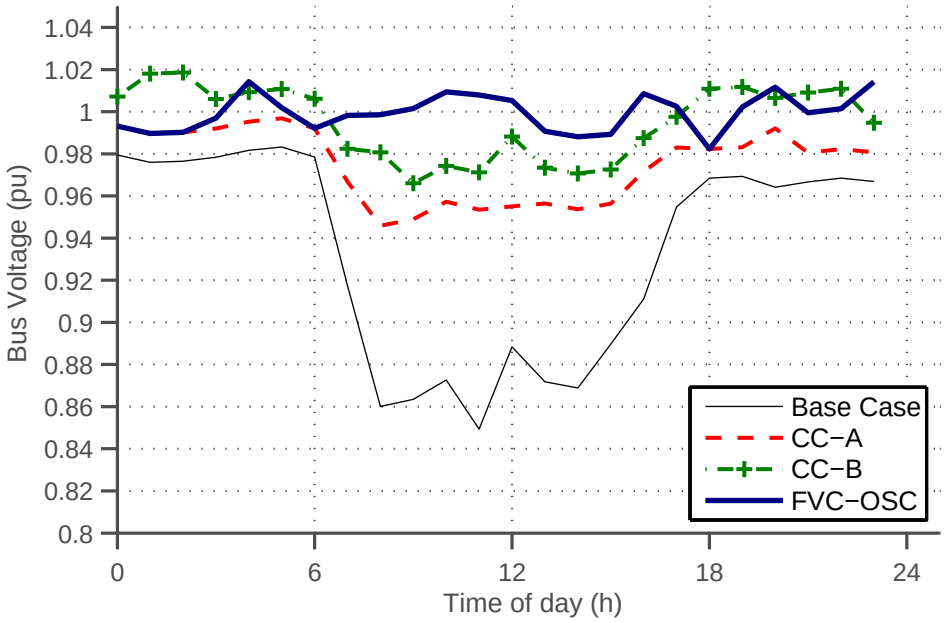

Figure 5.2: Bus 9 voltage profiles.

an extent. However, this only relates to the minimum and maximum levels of improvement as FVC-OSC performs better for all variations in conventional control settings. The only factor is that the improvement level is influenced by the settings group decision. Compared with the base case, conventional control brings loss reduction improvement of between 5.97% and 7.59% while the voltage deviation drops by 89.51%–96.59% from the base case values. On the other hand, FVC-OSC decreases the loss and voltage deviation by 8.34% and 97.07% respectively.

Bus voltages along the network from bus 1 to bus 10 are displayed in Figure 5.5. These voltages are produced by conventional control and FVC-OSC when the load peaks at 11:00. It can be seen that the voltage is closer to 1 pu and more uniform for FVC-OSC than for CC-A and CC-B.

The impact of the adaptive tap range is shown in Figure 5.6. 'Ideal Tap' is the tap position at the ith hour, derived from the tap ratio in (3.32). 'Min Tap' and 'Max Tap' represent the minimum and maximum allowable tap positions, respectively, calculated from (3.33). 'Optimal Tap' is the final tap position produced by FVC-OSC. Note that the values of the actual tap position upper limit, $T^{\max}$, and lower limit, $T^{\min}$, are 8 and -8 respectively.

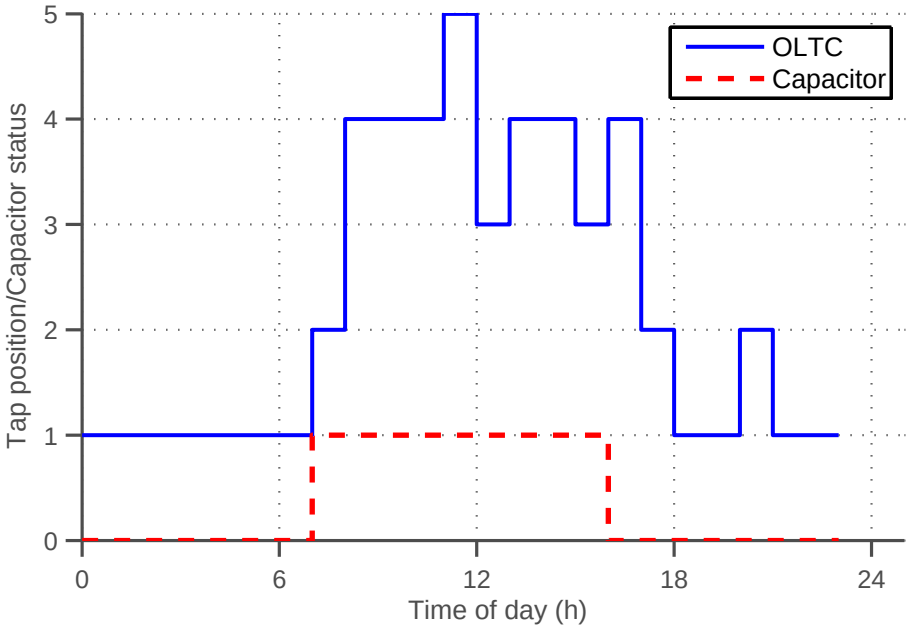

(a) CC-A

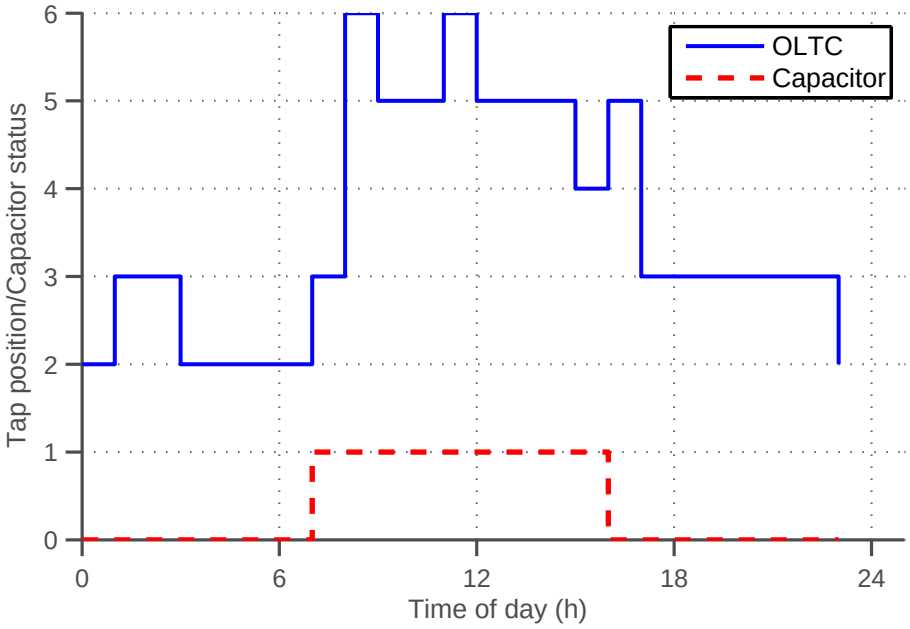

(b) CC-B

Figure 5.3: Simulated switching sequences of the substation devices under conventional control.

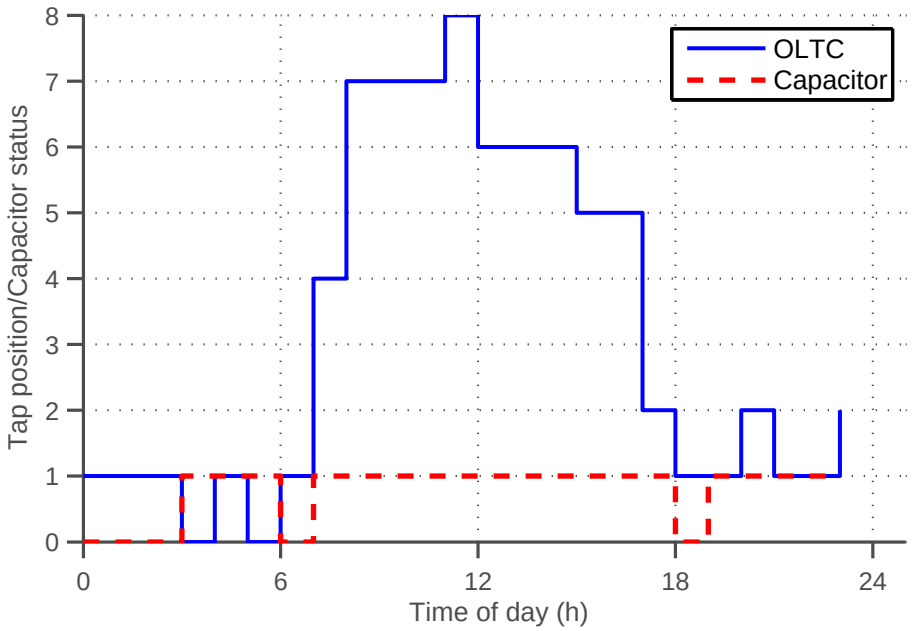

Figure 5.4: Simulated switching sequences of the substation devices under FVC-OSC.

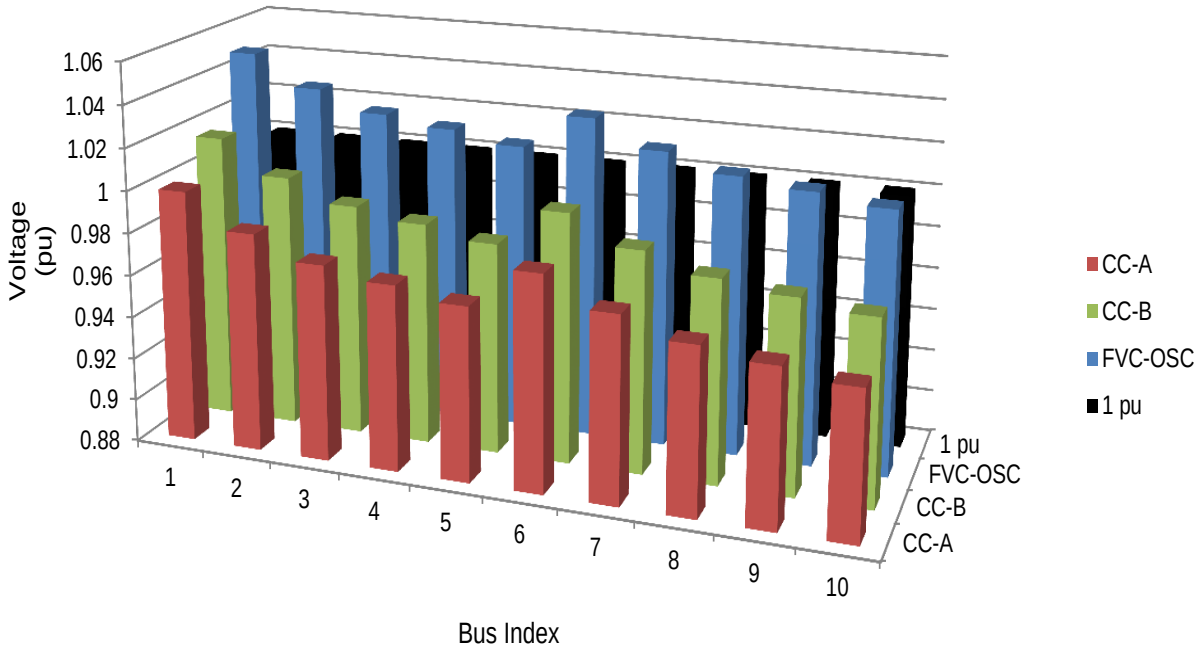

Figure 5.5: Bus voltages at 11:00.

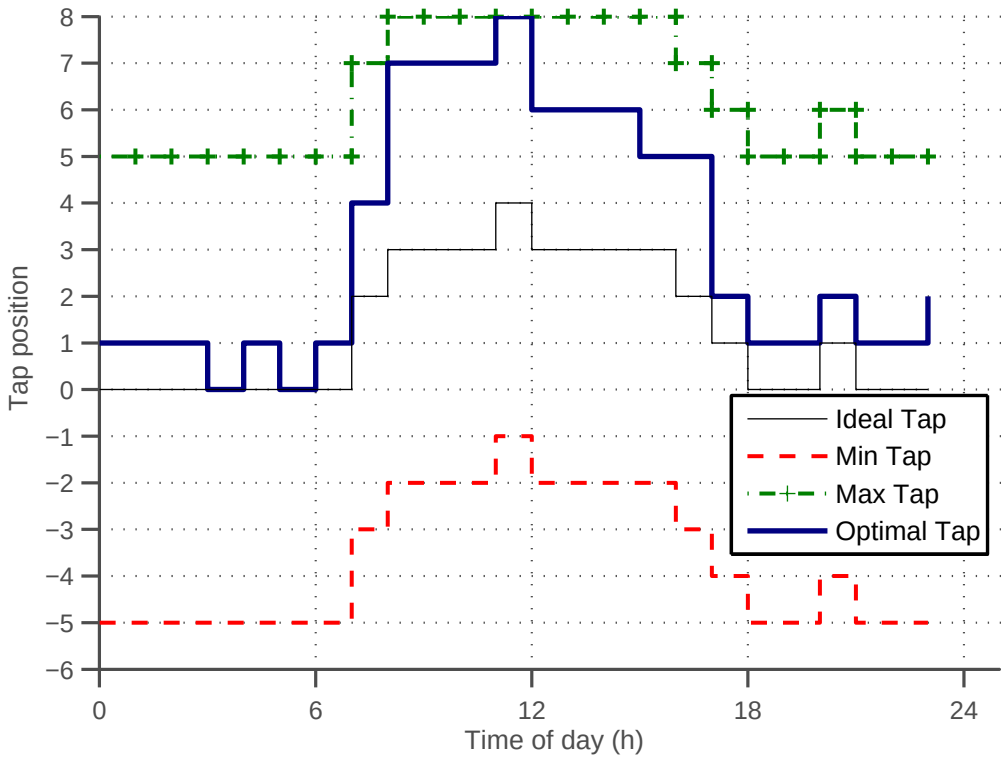

Figure 5.6: Adaptive tap range adjustments.

It can be seen that the adaptive tap position limit, 'Max Tap', increases towards the actual allowable upper value of 8 during high demand hours and then drops below this limit in low demand hours. 'Optimal Tap' lies inside the modified range and not at the limit values most of the time during the 24 hours. At times, during low demand periods, 'Optimal Tap' is the same as 'Ideal Tap'. The one time that 'Optimal Tap' has the same value as 'Max Tap' is quite appropriately, when the actual upper limit of the OLTC is reached. At the same time, the load is equal to the day's peak demand. Hence it can be deduced that there were no other higher tap positions left unexplored because of this adaptive limitation. This point illustrates the suitability of the dynamic tapping range. The original range of the tap position variable was modified but in this case did not compromise the solution.

5.4 EFFECT OF LIMITING OLTC AND CAPACITOR OPERATIONS

As previously mentioned, the total number of operations produced by FVC-OSC optimal solution is higher than that of conventional control. It is desirable to determine how the optimal solution is affected by the number of capacitor and OLTC operations. The relationship between the maximum allowed number of operations, VDI and the total daily loss is shown in Table 5.5 and Table 5.6. For OLTC switching limits over 25, the number of feasible solutions increases together with the OLTC switching operations, but the best solution is not improved. The same pattern is displayed for capacitor control action limits over 6. For OLTC movements under 20 and capacitor control actions below 6, VDI and the total loss increase as the number of operations drops. It is difficult for FVC-OSC to provide feasible solutions as the switching requirements become more stringent. In this case study, the algorithm cannot provide solutions which satisfy (3.38) and (3.39) when the limits on OLTC movements and capacitor operations are lower than nine and two respectively.

5.5 IMPACT OF LOAD FORECAST ERROR

To simulate the impact of load demand prediction disturbances during implementation of FVC-OSC and CC-B, an error is introduced to the trends in Figure 4.3 at each hour i such that

$$w_i = (1 + \varepsilon_i^{lb}) + (\varepsilon_i^{ub} - \varepsilon_i^{lb}) rand_i, \tag{5.1}$$

$$P_{d,i}^{\varepsilon} = P_{d,i} w_i,$$

Table 5.5: Effect of Limiting OLTC Operations

Operations Limit	VDI	Total Loss (MWh)	Actual Number of Operations	
			OLTC	Capacitor
30	0.0485	13.9927	29	7
25	0.0375	13.9798	21	5
20	0.0385	14.116	18	4
15	0.0367	14.1402	14	4
10	0.0469	14.1558	9	4

Table 5.6: Effect of Limiting Capacitor Switching Operations

Operations Limit	VDI	Total Loss (MWh)	Actual Number of Operations	
			OLTC	Capacitor
10	0.0378	14.034	29	9
8	0.0485	13.9927	29	7
6	0.0375	13.9798	21	5
4	0.0389	14.0773	26	4
2	0.0405	14.1038	20	2

Table 5.7: $w_i \in [0.991, 1.183]$

	CC-B	FVC-OSC
Average VDI	0.05258	0.04274
Average Loss	15.1878	15.0204
Min Voltage	0.9479	0.9519
Max Voltage	1.0219	1.0487

$$Q^{\varepsilon}_{d,i} = Q_{d,i} w_i.$$

where ε_i^{lb} and ε_i^{ub} are the lower and upper error bounds respectively. In brief, ε_i^{lb} is the value that is obtained when the load magnitude is decreased gradually from $P_{d,i}$ and $Q_{d,i}$ until the power-flow solution violates (3.34). In the same way, ε_i^{ub} is obtained when the load is increased. For this case, it is noticed that errors ranging from $\varepsilon_i^{lb} = -0.9\%$ to $\varepsilon_i^{ub} = 18.3\%$ do not cause violation of the voltage constraint when FVC-OSC is employed. Hence these are selected as error bounds to prevent infeasibility. $rand_i$ is a random number between 0 and 1. $P^{\varepsilon}_{d,i}$ and $Q^{\varepsilon}_{d,i}$ designate the new active power and reactive power consumption at bus d. AVR, the OLTC control mechanism in CC-B, is a form of closed-loop control. Therefore CC-B can respond to sudden changes which affect the voltage at bus 1 by adjusting the transformer tap position. FVC-OSC cannot detect unexpected variations which deviate from the predicted load profiles. Thus the proposed schedule displayed in Figure 5.4 remains the same throughout the dispatch interval of one day. Table 5.7 details results of CC-B and FVC-OSC when ten error samples are applied to the load data. Even though the FVC-OSC solution is no longer optimal, it still produces lower VDI and total loss in comparison with CC-B for errors ranging from -0.9% to 18.3%. Also, the CC-B solution fails to satisfy the voltage constraint with a minimum of 0.9479 pu out of the ten solutions. For errors lower than -0.9% FVC-OSC produces infeasible solutions. On the other hand, CC-B can only tolerate load increases of up to 16.8% but produces feasible solutions for loads as low as zero.

5.6 IMPACT OF INACCURATE MODEL DATA

In the same manner as in Section 5.5, errors in model data can be simulated. Instead of load demand, the impedance parameters of the transformer and all the lines in Figure 4.2 are

Table 5.8: $w_i \in [0.989, 1.246]$

	CC-B	FVC-OSC
Average VDI	0.05091	0.04027
Average Loss	15.35023	15.16828
Min Voltage	0.9495	0.9538
Max Voltage	1.0244	1.0496

made to deviate from the values specified in Table 4.2 and Table 4.3. The disturbance factor, w, is again derived using (5.1) and applied to the resistance, r, and reactance, x, based on the expressions below.

$$r^{\varepsilon} = rw,$$

$$x^{\varepsilon} = xw.$$

FVC-OSC produces feasible solutions when $\varepsilon^{lb} = -1.1\%$ and $\varepsilon^{ub} = 24.6\%$. It is thus observed from this range that FVC-OSC can handle positive model errors better than negative errors.

The results of the simulations are provided in Table 5.8. FVC-OSC has lower average VDI and average loss compared to CC-B. The minimum voltage of 0.9495 pu demonstrates that the closed-loop nature of CC-B does not guarantee compliance with the voltage limits.

5.7 COMPARISON OF FVC-OSC AND OPTIMUM SETTINGS APPROACH

The optimal set-points for AVR, substation capacitor and feeder capacitors can be determined as an improvement to conventional control. As described in Section 3.2.2, losses in a traditional distribution network can be minimized by making V_{set} for AVR high but below $V^{\max}$ and selecting V_{db} in a way that keeps the actual voltage close to V_{set} but does not cause too many tap movements. The substation capacitor set-points, Q_{on} and Q_{off}, are based on the reactive power-flow through the substation transformer. The feeder capacitor set-points denoted by V_{on} and V_{off} depend on the bus voltage thresholds at the point of connection. Here, the V_{db} is selected such that the number of tap movements does not exceed $u_T^{\max}$. To compare the combined substation and feeder control using optimum settings approach and

Table 5.9: Optimum settings

OLTC		Substation Capacitor		Feeder Capacitors	
V_{set} (pu)	V_{db} (pu)	Q_{on} (Mvar)	Q_{off} (Mvar)	V_{on} (pu)	V_{off} (pu)
1.035	0.03	-2	2	0.99	1.05

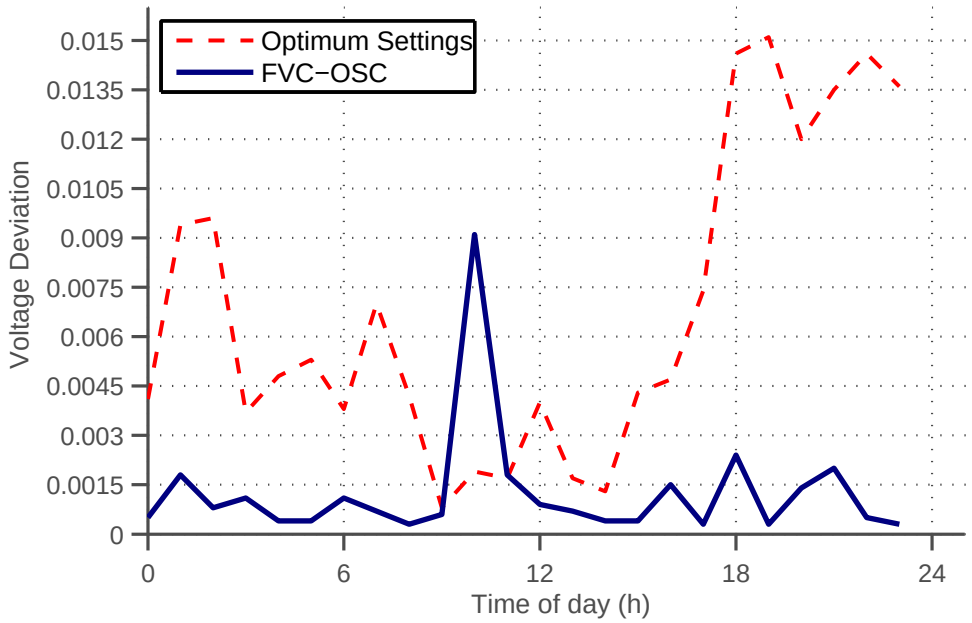

Figure 5.7: 24-h voltage deviation trends of FVC-OSC and optimum settings method.

FVC-OSC, the number of feeder capacitors at bus 4 and bus 9 in Figure 4.2 is changed to two. There are now four 1.4 Mvar feeder capacitors connected along the two distribution lines. The same settings as in [18] are used in this case study as shown in Table 5.9.

The voltage deviation trends for optimum settings and FVC-OSC are shown in Figure 5.7. VDI is 0.0296 for FVC-OSC and 0.163 for the optimum settings method. Both methods keep the voltage within upper and lower limits. Optimum settings maintain bus 1 voltage close to a predetermined set-point which, in this case, is largely in favour of loss reduction. In this case study, VDI is low for high loading but high for low loading. In contrast, FVC-OSC allows bus 1 voltage variations that are suitable for low losses and voltage deviations considering all the distribution buses.

One capacitor at bus 4 and one at bus 9 are in service for 24 hours for both methods. For

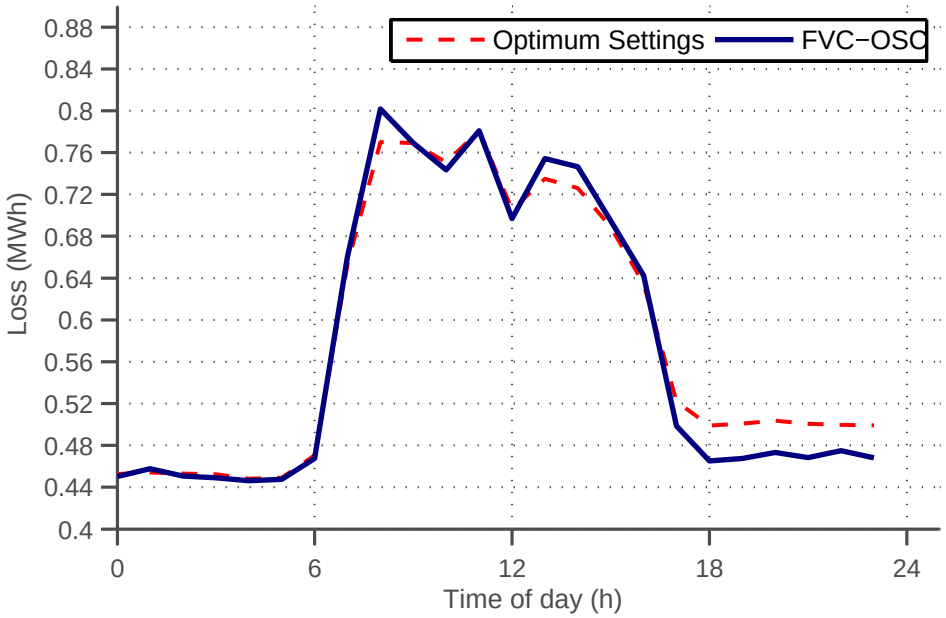

Figure 5.8: 24-h loss trends of FVC-OSC and optimum settings method.

FVC-OSC, the other two feeder capacitors are out of service from the start of the scheduling period until the feeder load starts rising above $0.5\,Q_d^{\mathrm{F}}$. They are both switched off at 18:00 when the feeder load drops below $-0.5\,Q_d^{\mathrm{F}}$. The optimum settings approach also allows the feeder capacitors to switch on at the same time as in FVC-OSC, but as the load decreases towards the end of the scheduling period, the feeder capacitors remain switched on. The impact of the two different philosophies on losses is illustrated in Figure 5.8. FVC-OSC produces losses equal to 13.7749 MWh for the whole system and 2.4595 MWh for the distribution network. On the other hand, the optimum settings method gives values of 13.9183 MWh for the whole system and 2.6357 MWh for the distribution network. The lower loss magnitudes shows the effectiveness of controlling the feeder capacitors based on reactive power set-points and incorporating the resulting switching sequences into the optimal substation control model.

5.8 VVC SIMULATION OVER 48 HOURS

Some networks exhibit different loading levels depending on the day in any given period. From one day to the next, the load demand magnitude can go up or down, reflecting the behaviour of the consumer. Examples of these include industrial loads that curtail process operations

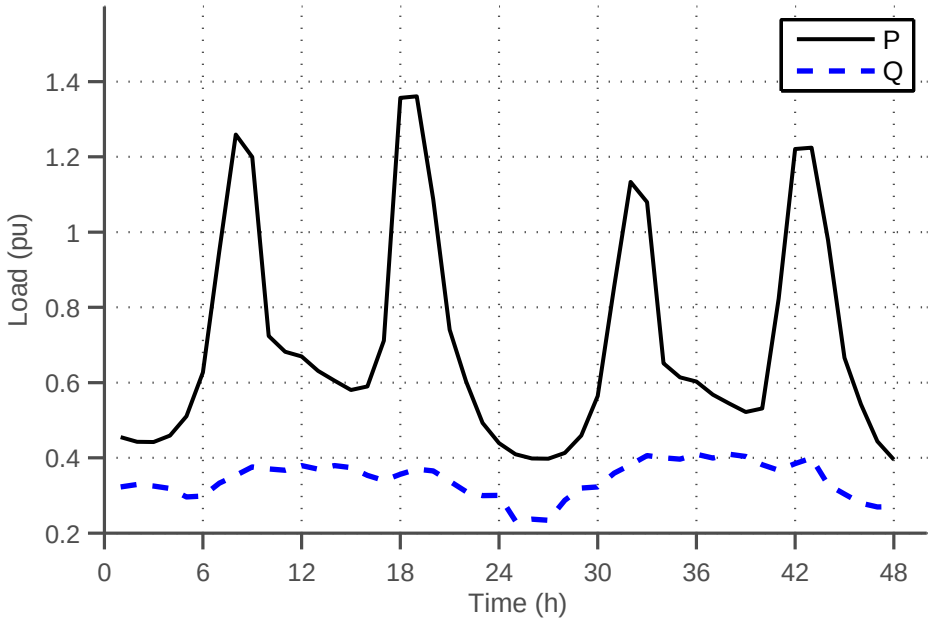

Figure 5.9: Load curves for a scheduling period of 48 hours.

during weekends or holidays as well as loads that vary with temperature or environmental conditions [35]. A typical load trend of day to day variations is illustrated in Figure 5.9. This load demand profile is applied to the system in Figure 4.2, but again with two additional capacitors at bus 4 and bus 9. The first 24-hour period makes up day 1 and the second, day 2. For the whole period of 48 hours, the three VVC approaches are evaluated against an uncontrolled system and then compared with one another.

In the uncontrolled system, two additional feeder capacitors, one at bus 4 and the other at bus 9 along with the substation capacitor are all out-of-service throughout the scheduling period. The remaining ones are switched on the whole time. The uncontrolled system is referred to as the base case. For conventional control i.e. CC-A and CC-B, two capacitors at bus 4 and bus 9 are switched on for the whole scheduling period. The remaining capacitors at bus 4, bus 9 and the substation are time-controlled according to the settings in Figure 5.10. The optimum settings approach and FVC-OSC remain unchanged. Hourly bus voltages, VDIs and losses for all VVC approaches are detailed in Appendix A.

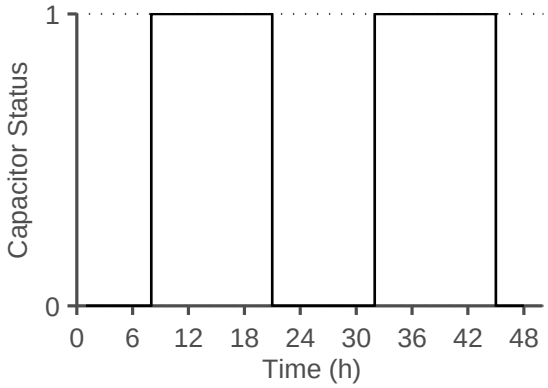

Figure 5.10: Switching sequence for capacitors on time-control.

5.8.1 Conventional Control

The OLTC dispatch sequence is displayed in Figure 5.11 and the voltage profiles at selected buses, namely bus 5 and bus 9 are presented in Figure 5.12 and Figure 5.13. On day 1 the voltage at bus 5 remains below 1 pu in the case of CCA. The bus voltage then picks up on the second day because the load demand is lower than on day 1. CCB displays better voltage regulation on day 1 due to the higher voltage set-point. However, this works against CCB on day 2 because the network experiences lower voltage drop than on day 1. Overall CCA and CCB end up with VDIs of 0.17 and 0.1037 respectively. The system loss for CCA is 36.0026 MWh, which is an improvement from the base case value of 38.9009 MWh. By comparison, CC-B further reduces the loss to 35.5186 MWh since the bus voltages across the network are higher.

Because the control effort of AVR in conventional control is in response to voltage variations at the secondary substation bus, variations at other buses do not cause tap position movements unless the voltage at bus 1 falls outside the deadband. The total number of OLTC operations is 22 for CC-A and 20 for CC-B. Due to time-control the substation and feeder capacitor operations are limited to two a day.

5.8.2 Optimum Settings

Figure 5.14 presents switching sequences of the controlled devices when the optimum settings approach is employed. The substation capacitor does not switch on at any time during the

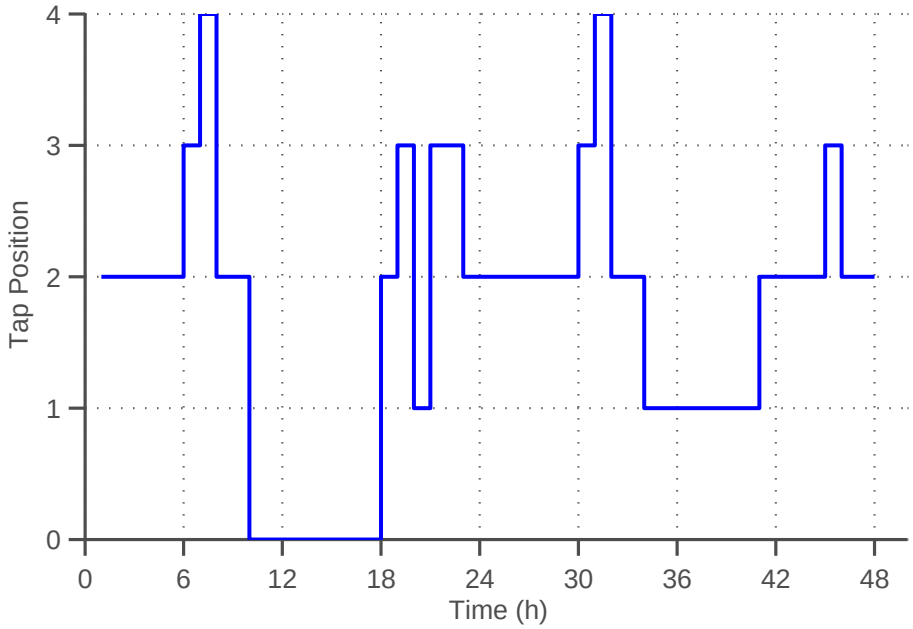

(a) CCA tap position sequence.

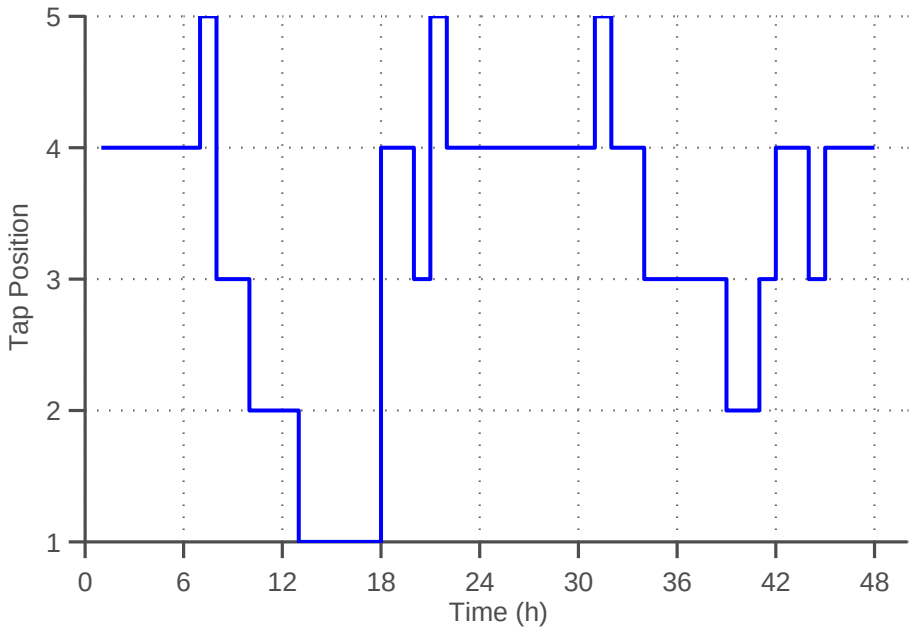

(b) CCB tap position sequence.

Figure 5.11: Dispatch sequences for conventional control.

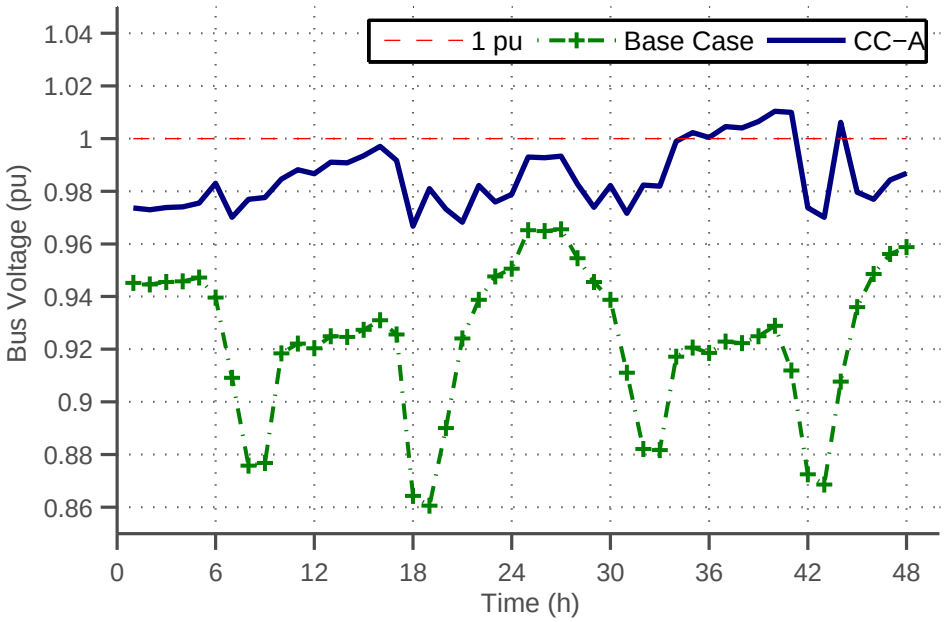

(a) Bus 5 voltage profiles for an uncontrolled system and CCA.

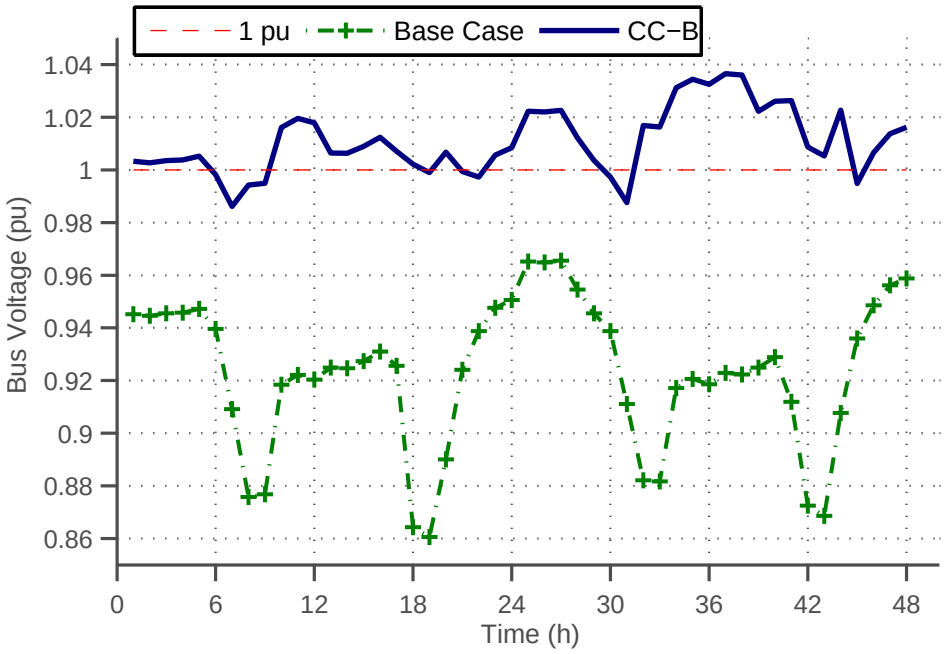

(b) Bus 5 voltage profiles for an uncontrolled system and CCB.

Figure 5.12: Voltage profiles for conventional control at Bus 5.

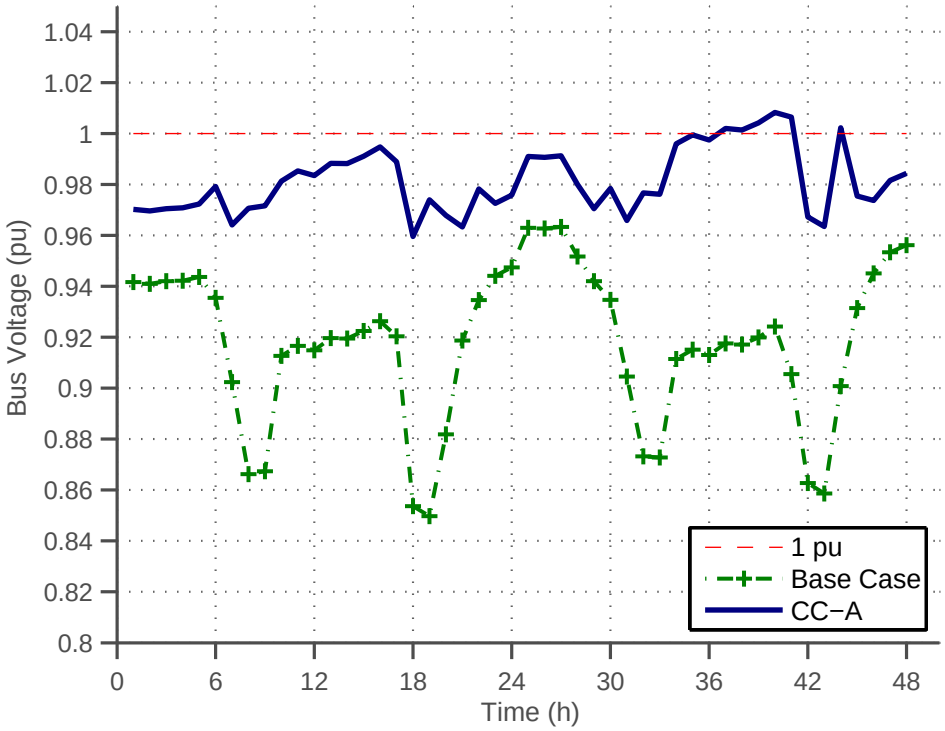

(a) Bus 9 voltage profiles for an uncontrolled system and CCA.

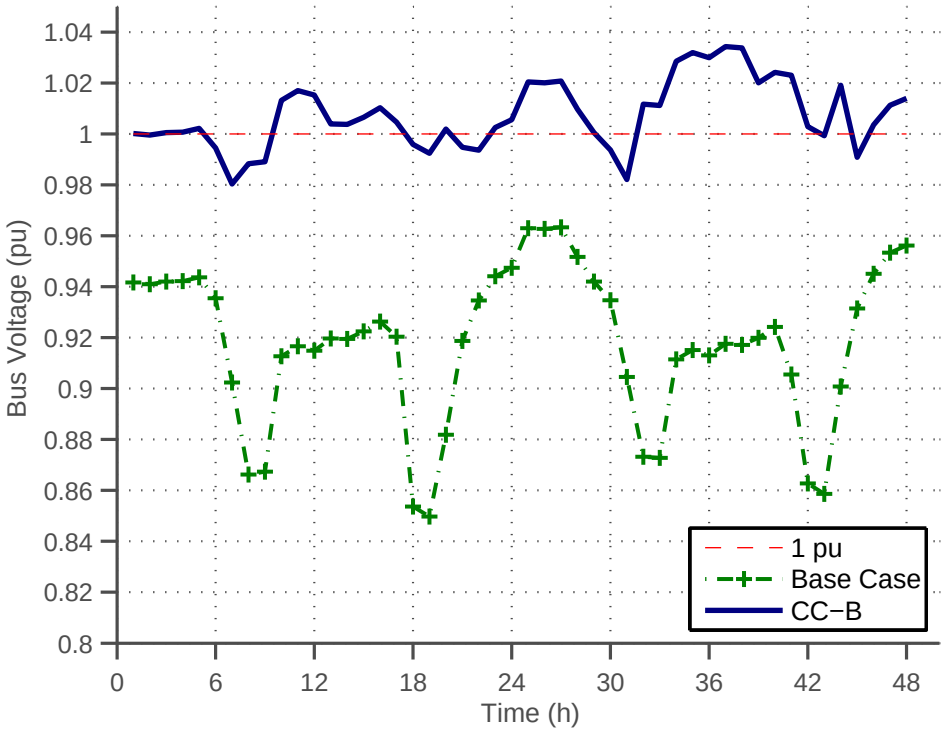

(b) Bus 9 voltage profiles for an uncontrolled system and CCB.

Figure 5.13: Voltage profiles for conventional control at Bus 9.

two-day period because the total reactive power demand of the two secondary distribution feeders does not reach 2 Mvar over the same period.

As seen in Figure 5.15, the voltage at bus 5 rises as high as 1.0469 pu and mostly stays over 1 pu for the whole scheduling period. It drops closer to 1 pu during peak loading periods; the opposite is true in light loading periods as the voltage drop across the network is lower. This is in line with the optimum settings philosophy of keeping the voltage as high as possible to minimise losses. Still, voltage regulation is taken into account by keeping the bus voltages between $V^{\min}$ and $V^{\max}$ using the AVR settings and switch-off settings of feeder capacitors. Consequently this philosophy produces a VDI of 0.3164 by the end of the 48-hour period.

5.8.3 FVC-OSC

FVC-OSC performance with respect to the two-day period can be observed in Figure 5.16 and Figure 5.17. At bus 1, the reference voltage is calculated at 1.01 pu. The total loss when FVC-OSC is implemented is 35.3126 MW compared with 38.9009 MW for an uncontrolled system. This is a loss reduction of 9.22%. What stands out is that FVC-OSC minimizes the total system loss throughout the scheduling period, even more so during peak periods. The highest loss reduction is 17.7% at the 19th hour. VDI produced by FVC-OSC is 0.081. The highest voltage deviation for both days takes place at the 20th hour. This is because the previous device statuses from hour 18 and hour 19 are maintained even though the load demand decreases between hour 19 and hour 20. During this period the highest percentage loss reduction for the whole 48-hour period is achieved. However, it can be said that at the 20th hour the loss reduction objective dominates the FVC-OSC solution.

Since the $u_T^{\max}$ and $C^{\max}$ are 30 and 8 per day respectively, FVC-OSC distributes the OLTC and substation capacitor effort considering the available capacity to reduce the loss and voltage deviation. The permissible number can be adjusted as desired as illustrated in Section 5.4. Feeder capacitor operations are dependent on the values of parameters, z_1 and z_2. Figure 5.16b displays the effort of the two additional capacitors at bus 4 and bus 9. Given that the feeder supplying bus 9 is drawing more active and reactive power from the substation, the capacitor at bus 9 operates less than the one at bus 4. Despite that, the total number of operations for each complies with the allowable maximum number.

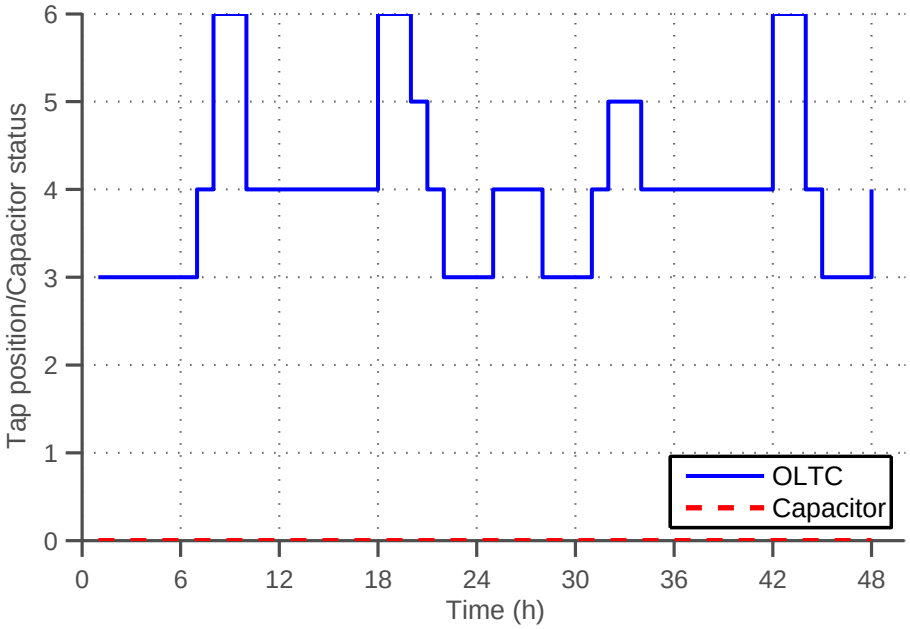

(a) Substation device sequences of the optimum settings approach.

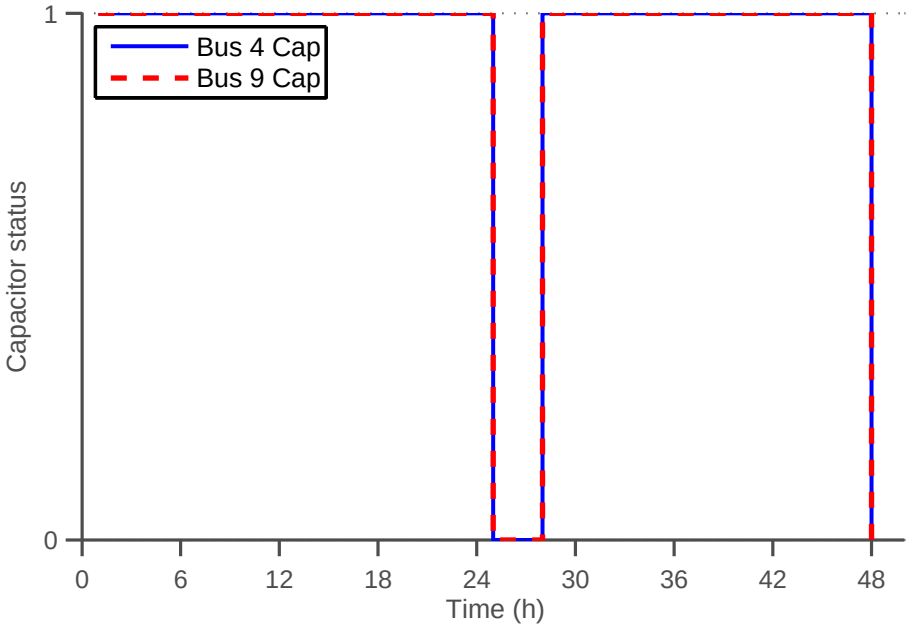

(b) Feeder capacitor operating sequences of the optimum settings approach.

Figure 5.14: Dispatch sequences and voltage profiles for the optimum settings approach.

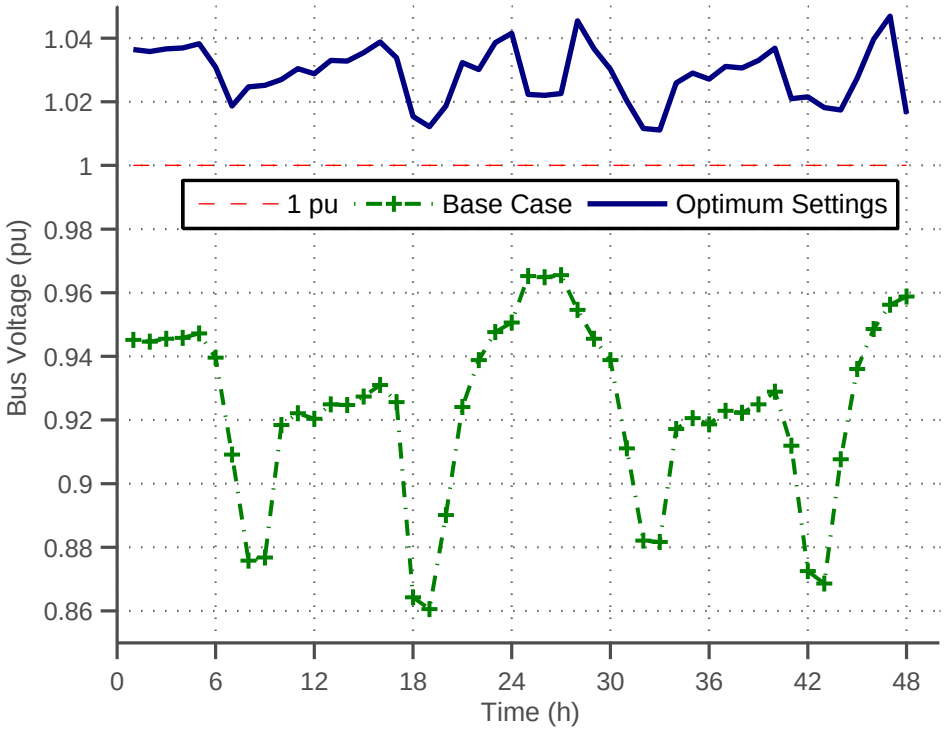

(a) Bus 5 voltage profiles for an uncontrolled system and the optimum settings approach.

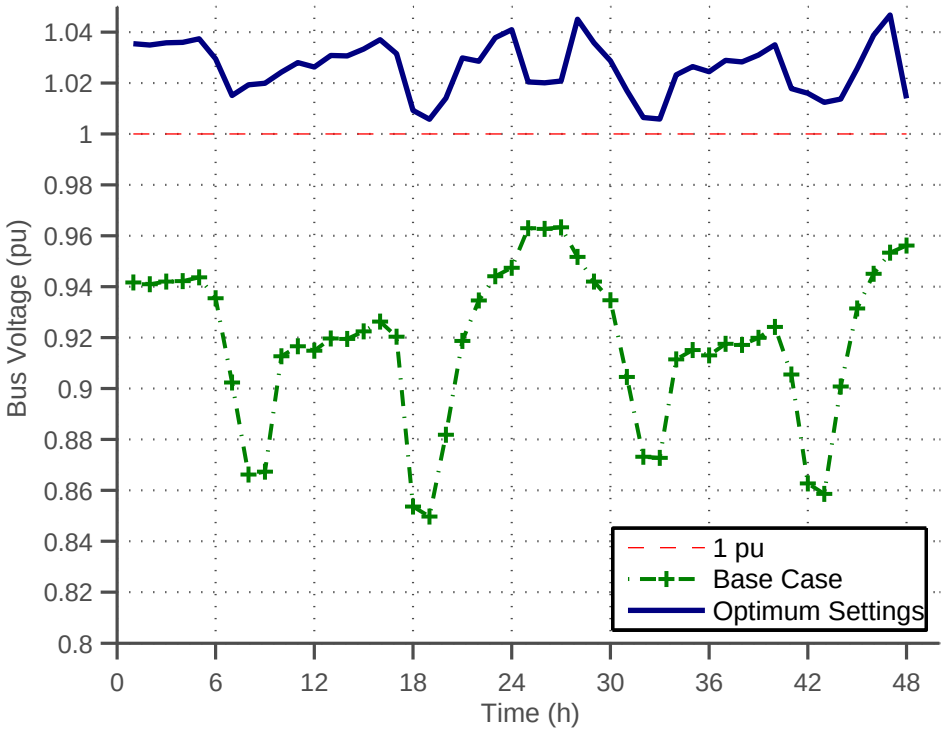

(b) Bus 9 voltage profiles for an uncontrolled system and the optimum settings approach.

Figure 5.15: Dispatch sequences and voltage profiles for the optimum settings approach.

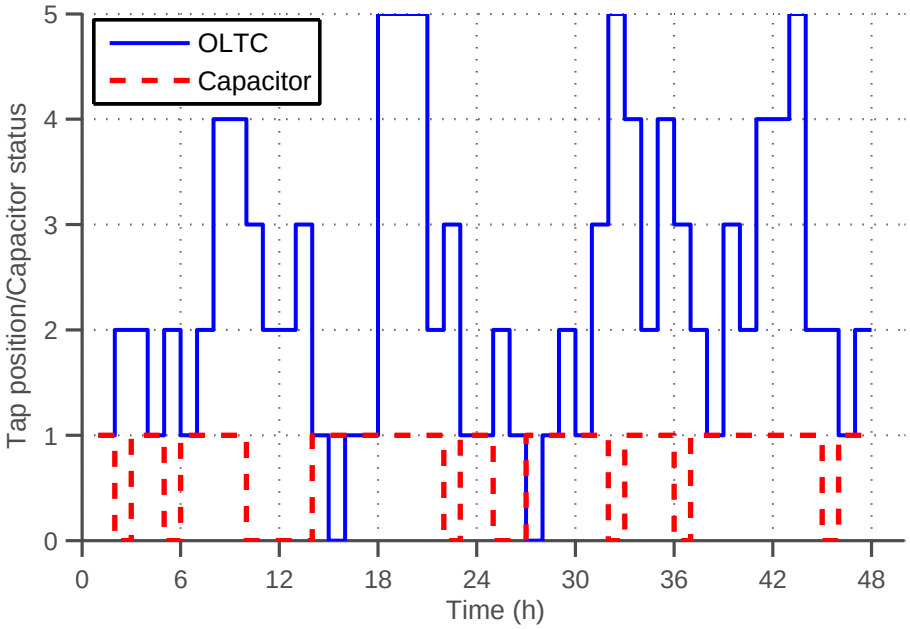

(a) FVC-OSC substation device sequences.

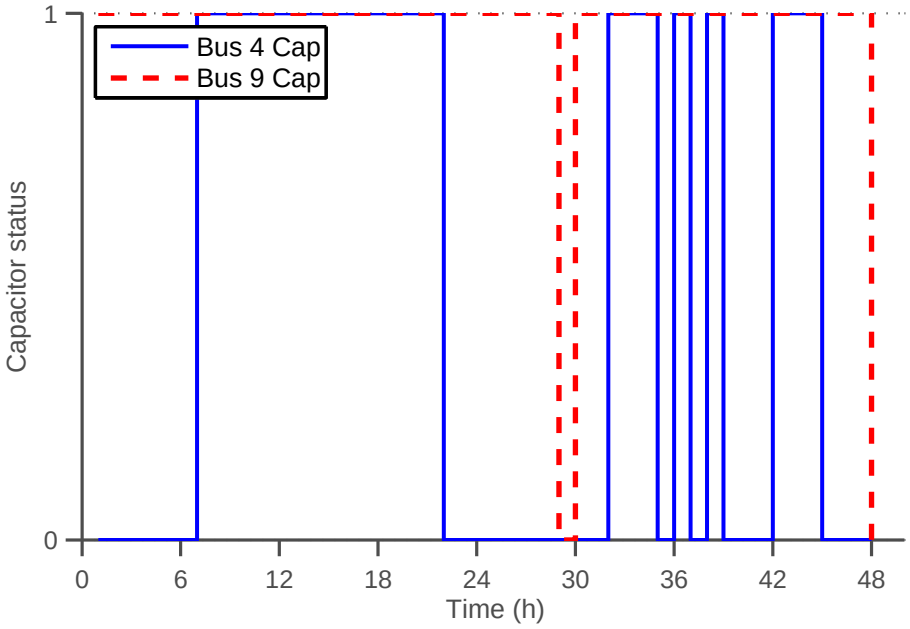

(b) FVC-OSC feeder capacitor operating sequence.

Figure 5.16: Dispatch sequences for FVC-OSC.

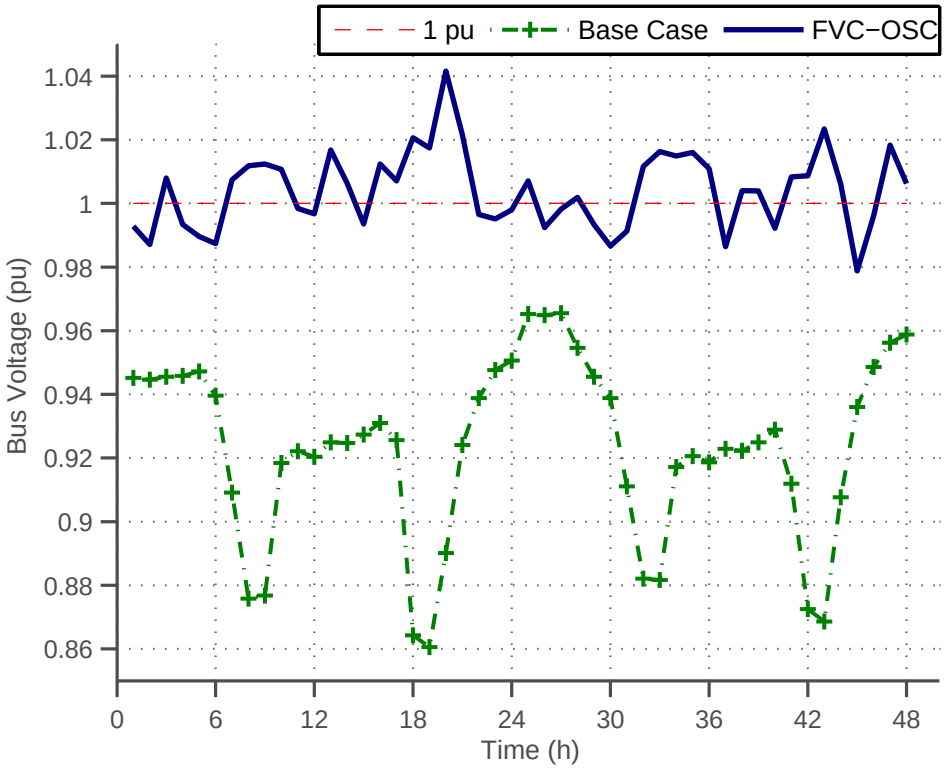

(a) Bus 5 voltage profiles for an uncontrolled system and FVC-OSC.

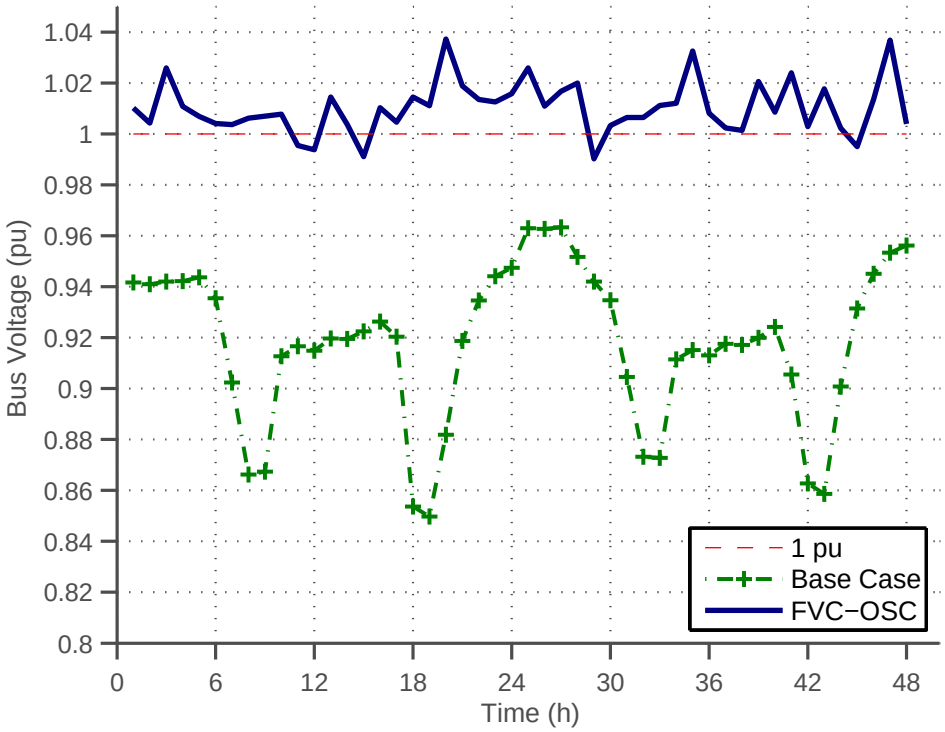

(b) Bus 9 voltage profiles for an uncontrolled system and FVC-OSC.

Figure 5.17: Voltage profiles for FVC-OSC.

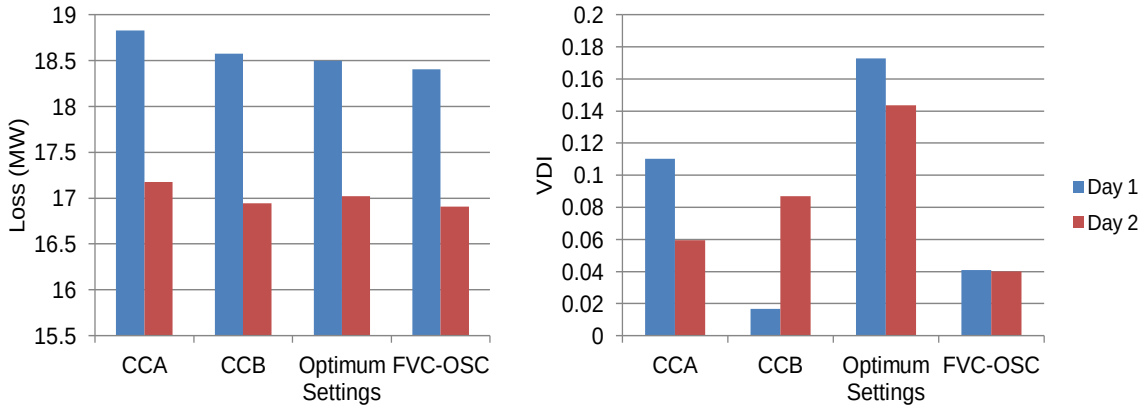

(a) System Loss **(b)** VDI

Figure 5.18: Performance comparison of VVC approaches for day 1 and day 2.

5.8.4 Performance Comparison

The three VVC approaches are compared in Figure 5.18. With conventional control there is a risk of the bus voltage violating the permissible limits when loading levels deviate from those assumed. CCA could be selected on the basis of curbing the risk of exceeding the upper voltage limit because of uncertain time-control of capacitors. On the other hand, CCB could be favoured due to superior performance when it comes to loss reduction since it has a higher voltage set-point. Then again, the performance of conventional control in terms of voltage deviation depends on the dominant profile over time. CCA is suitable to the 'day 2' load profile whereas CCB performs well for the load profile seen in day 1. In essence conventional control cannot minimize both losses and voltage deviations simultaneously over long periods.

The advantage of the optimum settings method is that in addition to minimizing losses, it is capable of switching on/off the feeder capacitors if either switching action causes the bus voltage to exceed permissible limits. Therefore this method ensures that voltage limits are not violated. However, VDI for the optimum settings approach is relatively high. The objective of loss reduction means that the bus voltages are maintained at values close to the upper limit.

FVC-OSC has the highest number of operations out of the three VVC methods. On the other

hand, it produces the highest loss reduction and lowest VDI over the two days. FVC-OSC demonstrates consistent performance regardless of the loading levels. VDI is uniform for the whole scheduling period.

In fact the feeder capacitors do not have to operate at all to further illustrate FVC-OSC advantages over conventional control. The voltage regulation superiority of FVC-OSC remains even when this extreme case is considered. If all four feeder capacitors are switched on the whole day for a 'day 2' load profile, VDI for FVC-OSC becomes 0.0314 and the highest voltage encountered at any bus during the day is 1.0362 pu. In comparison, CC-B, selected on the basis of the higher set-point, provides 0.1743 for VDI and 1.0493 pu for the maximum voltage experienced during the course of the day. It can be observed that CC-B has a greater risk of violating the upper voltage limit. The violation would occur mainly at uncontrolled buses because voltage limits are considered locally, at the controlled bus. For FVC-OSC voltage regulation is not a concern as long as there is capacity for tap position adjustments.

CHAPTER 6

CONCLUSION

6.1 SUMMARY OF FINDINGS

VVC in distribution networks concerns the control of voltage and reactive power resources to fulfill various objectives in constrained operational environments. The main purpose of this study is to formulate a heuristic optimal method called feeder var control and optimal substation control (FVC-OSC) to solve the daily VVC problem. Based on the results from case study scenarios, the performance of FVC-OSC and two other VVC approaches is summarized below.

FVC-OSC:

- Minimizes the total system loss.
- Minimizes the total voltage deviation.
- Ensures compliance with voltage limits.
- Substation capacitor and OLTC operations can be controlled to comply with device switching limitations.
- Feeder capacitor operations depend on z_1 and z_2 parameters.

Optimum Settings Approach:

- Minimizes the total system loss. Ranks lower than FVC-OSC but higher than conven-

tional control.

- Ranks lowest in terms of voltage deviation reduction.
- Ensures compliance with voltage limits.
- OLTC and capacitor operations depend on AVR and automatic capacitor control settings.

Conventional Control:

- Ranks behind FVC-OSC and the optimum settings approach with regard to total system loss reduction.
- Ranks lower than FVC-OSC and higher than the optimum settings approach in terms of voltage deviation reduction.
- Associated with a risk of violating voltage limits.
- OLTC operations depend on AVR settings.
- Feeder capacitor operations are fixed based on time settings.

6.2 CONCLUSIONS

FVC-OSC has been presented with the purpose of dealing with the computationally complex problem of VVC control. The feeder capacitors are controlled according to reactive power-flows on the secondary feeders at the substation while the on-load tap changer and substation capacitor problem is formulated with respect to operational constraints and then solved with discrete particle swarm optimization. It is shown that the proposed method determines the most suitable substation secondary bus reference voltage and dispatch sequences to minimize daily voltage deviations and total loss over 24 hours.

FVC-OSC reduces the number of variables required to solve the VVC problem, thus simplifying the solution process. Despite this simplification, FVC-OSC shows good performance. Using a case study, it is shown that FVC-OSC achieves better performance compared to

conventional control in terms of losses and voltage deviations. To achieve loss and voltage deviation reduction, conventional control requires proper tuning, which can be difficult since there is no coordination between the OLTC and capacitor switching schedules. Even with good settings, on-line control can only minimize one out of the two objectives. Additionally, suboptimal settings of conventional control can lead to violation of voltage constraints because the approach only incorporates local voltage measurements while violations can occur at any of the buses in the network. These problems are avoided by FVC-OSC. With FVC-OSC, the network model and load demand data are considered in addition to an explicit formulation of the objective functions and constraints.

Parameter adjustments affect the FVC-OSC solution. Firstly, FVC-OSC is sensitive to the allowable maximum number of control movements. As this number decreases, the losses and voltage deviations increase. Secondly, the influence of inaccurate load forecast data on FVC-OSC and conventional control is shown by applying disturbances to the predicted load profiles. In the same manner, model data inaccuracies are also taken into account. For disturbances where FVC-OSC yields feasible solutions, there are instances in which conventional control violates the voltage limits because it solely responds to local bus voltage changes. Considering the applied disturbances, FVC-OSC again performs better in terms of loss and voltage deviation reduction.

6.3 RECOMMENDATIONS FOR FURTHER STUDY

Closed-loop methods should be investigated with the purpose of improving the performance of FVC-OSC when the data given are inaccurate. The quality of data is compromised by factors such as load prediction errors and system data inaccuracies. Because of the reduced problem size, closed-loop control can be applied particularly to substation control. Consequently the voltages across the network can be kept within permissible levels in response to disturbances.

It would be desirable to test FVC-OSC in distribution systems that differ in topology, size and characteristics to the one studied in this work. Some practical distribution systems are integrated with distributed generation. In this case FVC-OSC can be coordinated with distributed generators to further reduce losses and voltage deviations while spreading the operating effort between the traditional control devices and the distributed generators.

REFERENCES

[1] T. A. Short, *Electric Power Distribution Handbook*. Boca Raton, FL: CRC, 2004.

[2] R. C. Dugan and M. F. McGranaghan, *Electrical Power Systems Quality*. New York: McGraw-Hill, 2002.

[3] "NRS 048-2 Electricity Supply - Quality of Supply Part 2: Voltage Characteristics, Compatibility Levels, Limits and Assessment Methods," Standards South Africa, South Africa, 2007.

[4] M. M. Aman, G. B. Jasmon, A. H. A. Bakar, H. Mokhlis, and M. Karimi, "Optimum Shunt Capacitor Placement in Distribution System - A Review and Comparitive Study," *Renewable Sustainable Energy Rev.*, vol. 30, pp. 429–439, 2014.

[5] T. Senjyu, Y. Miyazato, A. Yona, N. Urasaki, and T. Funabashi, "Optimal Distribution Voltage Control and Coordination With Distributed Generation," *IEEE Trans. Power Del.*, vol. 23, no. 2, pp. 1236–1242, Apr. 2008.

[6] Z. Hu, X. Wang, H. Chen, and G. A. Taylor, "Volt/Var Control in Distribution Systems Using a Time-Interval based Approach," *Proc. Inst. Elect. Eng.*, vol. 150, no. 5, pp. 548–554, Sept. 2003.

[7] F.-C. Lu and Y.-Y. Hsu, "Reactive Power/Voltage Control in a Distribution Substation Using Dynamic Programming," *Proc. Inst. Elect. Eng.*, vol. 142, no. 6, pp. 639–645, May 1995.

[8] Y. Liu, P. Zhang, and X. Qiu, "Optimal Volt/Var Control in Distribution Systems," *Elect. Power Energy Syst.*, vol. 24, no. 4, pp. 271–276, May 2002.

[9] R. D. Vecchio, B. Poulin, P. Feghali, D. M. Shah, and R. Ahuja, *Transformer Design Principles: With Applications to Core-Form Power Transformers.* New York: Gordon and Breach, 2001.

[10] M. S. Calovic, "Modeling and Analysis of Under-Load Tap-Changing Transformer Control Systems," *IEEE Trans. Power App. Syst.*, vol. PAS-103, no. 7, pp. 1909–1915, Jul. 1984.

[11] F. A. Viawan, "Voltage Control and Voltage Stability of Power Distribution Systems in the Presence of Distributed Generation," Ph.D. dissertation, Chalmers University of Technology, 2008.

[12] T. Gönen, *Electrical Power Distribution System Engineering.* New York: McGraw-Hill, 1986.

[13] M. Larsson and D. Karlsson, "Coordinated Control of Cascaded Tap Changers in a Radial Distribution Network," in *Proc. IEEE/KTH Stockholm Power Tech*, 1995.

[14] F. A. Viawan, A. Sannino, and J. Daalder, "Voltage Control With On-Load Tap Changers in Medium Voltage Feeders in Presence of Distributed Generation," *Electr. Power Syst. Res.*, vol. 77, pp. 1314–1322, 2007.

[15] H. L. Willis, *Power Distribution Planning Reference Book.* New York: Marcel Dekker, 1997.

[16] *IEEE Guide for Application of Shunt Power Capacitors*, IEEE Std. 1036-2010.

[17] J. H. Harlow, *Electric Power Transformer Engineering.* Boca Raton, FL: CRC, 2004.

[18] F. A. Viawan and D. Karlsson, "Combined Local and Remote Voltage and Reactive Power Control in the Presence of Induction Machine Distributed Generation," *IEEE Trans. Power Syst.*, vol. 22, no. 4, pp. 2003–2012, Nov. 2007.

[19] ——, "Voltage and Reactive Power Control in Systems With Synchronous Machine-based Distributed Generation," *IEEE Trans. Power Del.*, vol. 23, no. 2, pp. 1079–1087, Apr. 2008.

[20] J.-Y. Park, S.-R. Nam, and J.-K. Park, "Control of a ULTC Considering the Dispatch Schedule of Capacitors in a Distribution System," *IEEE Trans. Power Syst.*, vol. 22, no. 2, pp. 755–761, May 2007.

[21] P. Mitra and G. K. Venayagamoorthy, "An Adaptive Control Strategy for Dstatcom Applications in an Electric Ship Power System," *IEEE Trans. Power Electron.*, vol. 25, no. 1, pp. 95–104, Jan. 2010.

[22] M. Falahi, K. L. Butler-Purry, and M. Ehsani, "Reactive Power Coordination of Shipboard Power Systems in Presence of Pulsed Loads," *IEEE Trans. Power Syst.*, vol. 28, no. 4, pp. 3675–3682, Nov. 2013.

[23] J. J. Grainger and S. Civanlar, "Volt/Var Control on Distribution Systems With Lateral Branchces Using Shunt Capacitors and Voltage Regulators: parts I-III," *IEEE Trans. Power App. Syst.*, vol. PAS-104, no. 11, pp. 3278–3297, Nov. 1985.

[24] R. Baldic and F. F. Wu, "Efficient Integer Optimization Algorithm for Optimal Coordination of Capacitors and Regulators," *IEEE Trans. Power Del.*, vol. 5, no. 3, pp. 805–812, Aug. 1990.

[25] I. Roytelman, B. K. Wee, and R.-L. Lugtu, "Volt/Var Control Algorithm for Modern Distribution Management System," *IEEE Trans. Power Syst.*, vol. 10, no. 3, pp. 1454–1460, Aug. 1995.

[26] Z. Gu and D. Rizy, "Neural Networks for Combined Control of Capacitor Banks and Voltage Regulators in Distribution Systems," *IEEE Trans. Power Del.*, vol. 11, no. 4, pp. 1921–1928, Oct. 1996.

[27] J.-C. Wang, H.-D. Chiang, K. N. Miu, and G. R. Darling, "Capacitor Placement and Real Time Control in Large-Scale Unbalanced Distribution Systems: Loss Reduction Formula, Problem Formulation, Solution Methodology and Mathematical Justification," *IEEE Trans. Power Del.*, vol. 12, no. 2, pp. 953–958, Apr. 1997.

[28] Y.-Y. Hsu and H.-C. Kuo, "Dispatch of Capacitors on Distribution System Using Dynamic Programming," *Proc. Inst. Elect. Eng., Gen., Transm., Distrib.*, vol. 140, no. 6, pp. 433–438, Nov. 1993.

[29] F.-C. Lu and Y.-Y. Hsu, "Fuzzy Dynamic Programming Approach to Reactive Power/Voltage Control in a Distribution Substation," *IEEE Trans. Power Syst.*, vol. 12, no. 2, pp. 681–688, May 1997.

[30] Y.-Y. Hsu and F.-C. Lu, "A Combined Artificial Neural Network-fuzzy Dynamic Programming Approach to Reactive Power/Voltage Control in a Distribution Substation," *IEEE Trans. Power Syst.*, vol. 13, no. 4, pp. 1265–1271, Nov. 1998.

[31] R.-H. Liang and C.-K. Cheng, "Dispatch of Main Transformer ULTC and Capacitor in a Distribution System," *IEEE Trans. Power Del.*, vol. 16, no. 4, pp. 625–630, Oct. 2001.

[32] D. Youman, R. Xiaojuan, Z. Changcheng, and Z. Dapu, "A Heuristic and Algorithmic Combined Approach for Reactive Power optimization With Time-Varying Load Demand in Distribution Systems," *IEEE Trans. Power Syst.*, vol. 17, no. 4, pp. 1068–1072, Nov. 2002.

[33] R.-H. Liang and Y.-S. Wang, "Fuzzy-Based Reactive Power and Voltage Control in a Distribution System," *IEEE Trans. Power Del.*, vol. 18, no. 2, pp. 610–618, Apr. 2003.

[34] M. B. Liu, C. A. Cañizares, and W. Huang, "Reactive Power and Voltage Control in Distribution Systems With Limited Switching Operations," *IEEE Trans. Power Syst.*, vol. 24, no. 2, pp. 889–899, May 2009.

[35] T. Senjyu, P. Mandal, K. Uezato, and T. Funabashi, "Next Day Load Curve Forecasting Using Hybrid Correction Method," *IEEE Trans. Power Syst.*, vol. 20, no. 1, pp. 102–109, Feb. 2005.

[36] H. Kebriaei, B. Araabi, and A. Rahimi-Kian, "Short-Term Load Forecasting With a New Nonsymmetric Penalty Function," *IEEE Trans. Power Syst.*, vol. 26, no. 4, pp. 1817–1825, Nov. 2011.

[37] R. D. Zimmerman and H. D. Chiang, "Fast Decoupled Power Flow for Unbalanced Radial Distribution Systems," *IEEE Trans. Power Syst.*, vol. 10, no. 4, pp. 2045–2052, Nov. 1995.

[38] W. Kersting, *Distribution System Modeling and Analysis.* Boca Raton, FL: CRC, 2002.

[39] S.-K. Chang and V. Brandwajn, "Adjusted Solutions in Fast Decoupled Load Flow," *IEEE Trans. Power Syst.*, vol. 3, no. 2, pp. 726–733, May 1988.

[40] N. M. Peterson and W. S. Meyer, "Automatic Adjustment of Transformer and Phase-Shifter Taps in the Newton Power Flow," *IEEE Trans. Power App. Syst.*, vol. PAS-90, no. 1, pp. 103–108, Jan. 1971.

[41] R. N. Allan and C. Arruda, "Ltc Transformers and MVAR Violations in the Fast Decoupled Load Flow," *IEEE Trans. Power App. Syst.*, vol. PAS-101, no. 9, pp. 3328–3332, Sep. 1982.

[42] J. J. Grainger and W. D. Stevenson, *Power System Analysis*. New York: McGraw-Hill, 1994.

[43] J. D. Glover, M. S. Sarma, and T. J. Overbye, *Power System Analysis and Design*. Toronto, Canada: Thomas Learning, 2008.

[44] L. Z. Barboza, H. H. Zürn, and R. Salgado, "Load Tap Change Transformers: A Modeling Reminder," *IEEE Power Eng. Rev.*, vol. 21, no. 2, pp. 51–52, Feb. 2001.

[45] C. G. Carter-Brown and C. T. Gaunt, "Model for the Apportionment of the Total Voltage Drop in Combined Medium and Low Voltage Distribution Feeders," *SAIEE Trans. Africa Res. Journal*, vol. 97, no. 1, pp. 66–73, Mar. 2006.

[46] J. J. Erbrink, E. Gulski, P. P. Seitz, and R. Leich, "Advanced On-Site Diagnosis of Transformer On-Load Tap Changer," in *Proc. IEEE Int. Symp. Electrical Insulation*, Jun. 2008, pp. 252–256.

[47] M. Redfern and W. Handley, "Duty Based Maintenance for On-Load Transformer Tap Changers," in *Proc. IEEE Power Eng. Soc. Summer Meeting*, vol. 3, Jul. 2001, pp. 1824–1829.

[48] B. Handley, M. Redfern, and S. White, "On Load Tap-Changer Conditioned Based Maintenance," *Proc. Inst. Elect. Eng., Gen., Transm., Distrib.*, vol. 148, no. 4, pp. 296–300, Jul. 2001.

[49] *IEEE Standard Requirements for Load Tap Changers*, IEEE Std. C57.131-1995.

[50] R. Natarajan, *Power System Capacitors.* New York: Taylor & Francis, 2005.

[51] "NRS 048-2 Electricity Supply - Quality of Supply Part 4: Application Practices for Licencees," Standards South Africa, South Africa, 2009.

[52] DIgSILENT PowerFactory. DIgSILENT GmbH. [Online]. Available: http://www.digsilent.de/

[53] A. Engelbrecht, *Computational Intelligence: An Introduction.* England: John Wiley & Sons Ltd, 2007.

[54] M. R. AlRashidi and E. M. El-Hawary, "Hybrid Particle Swarm Optimization Approach for Solving the Discrete OPF Problem Considering the Valve Loading Effects," *IEEE Trans. Power Syst.*, vol. 22, no. 4, pp. 2030–2038, Nov. 2007.

[55] N. Mo, Z. Y. Zou, , K. W. Chan, and T. Y. G. Pong, "Transient Stability Constrained Optimal Power Flow Using Particle Swarm Optimisation," *IET Gen., Transm., Distrib.*, vol. 1, no. 3, pp. 476–483, May 2007.

[56] A. Ratnaweera, S. Halgamuge, and H. Watson, "Self-Organizing Hierarchical Particle Swarm Optimizer With Time Varying Accelerating Coefficients," *IEEE Trans. Evol. Comput.*, vol. 8, no. 3, pp. 240–255, Jun. 2004.

[57] K. Parsopoulos and M. Vrahatis, "Recent Approaches to Global Optimization Problems Through Particle Swarm Optimization," *Natural Computing*, vol. 1, pp. 235–306, May 2002.

[58] R. Eberhart and Y. Shi, "Particle Swarm Optimization: Developments, Applications and Resources," in *Proc. IEEE Congr. Evol. Comput.*, vol. 1, May 2001, pp. 81–86.

[59] E. Laskari, K. Parsopoulos, and M. Vrahatis, "Particle Swarm Optimization for Integer Programming," in *Proc. IEEE Congr. Evol. Comput.*, vol. 2, May 2002, pp. 1582–1587.

[60] J. G. Vlachogiannis and K. Y. Lee, "A Comparative Study on Particle Swarm Optimization for Optimal Steady-State Performance of Power Systems," *IEEE Trans. Power*

Syst., vol. 21, no. 4, pp. 1718–1728, Nov. 2006.

[61] S. Lalwani, S. Singhal, R. Kumar, and N. Gupta, "A Comprehensive Survey: Applications of Multi-Objective Particle Swarm Optimization (MOPSO) Algorithm," *Trans. Combinatorics*, vol. 2, no. 1, pp. 39–101, Mar. 2013.

[62] Y.-X. Jin, H.-Z. Cheng, J. Yan, and L. Zhang, "New Discrete Method for Particle Swarm Optimization and its Application in Transmission Network Expansion Planning," *Elect. Power Syst. Res.*, vol. 77, no. 3-4, pp. 227–233, Nov. 2007.

[63] Y. del Valle, G. K. Venayagamoorthy, S. Mohagheghi, J.-C. Hernandez, and R. G. Harley, "Particle Swarm Optimization: Basic Concepts, Variants and Applications in Power Systems," *IEEE Trans. Evol. Comput.*, vol. 12, no. 2, pp. 171–195, Apr. 2008.

[64] C. A. C. Coello, "Theoretical and Numerical Constraint-Handling Techniques Used With Evolutionary Algorithms: A Survey of the State of the Art," *Comput. Methods Appl. Mech. Eng.*, vol. 191, no. 11-12, pp. 1245–1287, Jan. 2002.

[65] R. D. Zimmerman, C. E. Murillo-Sánchez, and R. J. Thomas, "MATPOWER: Steady-State Operations, Planning and Analysis Tools for Power Systems Research and Education," *IEEE Trans. Power Syst.*, vol. 26, no. 1, pp. 12–19, Feb. 2011.

[66] R. D. Zimmerman and C. E. Murillo-Sánchez, "MATPOWER 4.1 User's Manual," PSERC, 2011.

[67] "Multilin DGCC Capacitor Bank Controller Instruction Manual," GE Digital Energy, Canada, 2013.

APPENDIX A

RESULTS OF 48-H VVC SIMULATIONS

Table A.1: Day 1 hourly bus voltages (pu) for an uncontrolled system.

Hour	Bus 1	Bus 2	Bus 3	Bus 4	Bus 5	Bus 6	Bus 7	Bus 8	Bus 9	Bus 10
1	0.959	0.952	0.949	0.948	0.945	0.951	0.945	0.942	0.942	0.939
2	0.958	0.952	0.948	0.948	0.945	0.950	0.944	0.942	0.941	0.939
3	0.959	0.952	0.949	0.949	0.946	0.951	0.945	0.942	0.942	0.940
4	0.959	0.953	0.949	0.949	0.946	0.951	0.946	0.943	0.942	0.940
5	0.960	0.954	0.951	0.950	0.947	0.952	0.947	0.944	0.944	0.941
6	0.956	0.948	0.944	0.943	0.940	0.946	0.940	0.936	0.936	0.933
7	0.937	0.924	0.917	0.913	0.909	0.922	0.912	0.905	0.902	0.899
8	0.915	0.898	0.887	0.881	0.876	0.895	0.881	0.871	0.866	0.862
9	0.916	0.899	0.888	0.882	0.877	0.896	0.882	0.872	0.867	0.863
10	0.942	0.932	0.925	0.922	0.918	0.930	0.921	0.915	0.913	0.909
11	0.945	0.934	0.928	0.926	0.922	0.933	0.924	0.919	0.917	0.913
12	0.944	0.933	0.927	0.924	0.920	0.931	0.922	0.917	0.915	0.912
13	0.946	0.937	0.931	0.929	0.925	0.935	0.927	0.922	0.920	0.917
14	0.946	0.936	0.931	0.928	0.925	0.935	0.926	0.921	0.920	0.916
15	0.948	0.938	0.933	0.931	0.927	0.937	0.929	0.924	0.923	0.919
16	0.950	0.941	0.936	0.935	0.931	0.940	0.932	0.928	0.926	0.923
17	0.947	0.937	0.931	0.929	0.926	0.935	0.927	0.922	0.920	0.917
18	0.908	0.889	0.876	0.870	0.864	0.886	0.870	0.859	0.854	0.849
19	0.905	0.886	0.873	0.866	0.861	0.883	0.866	0.855	0.850	0.845
20	0.925	0.910	0.900	0.895	0.890	0.907	0.894	0.886	0.882	0.878
21	0.946	0.936	0.930	0.928	0.924	0.934	0.926	0.921	0.919	0.916
22	0.955	0.947	0.943	0.942	0.939	0.946	0.939	0.936	0.935	0.932
23	0.960	0.954	0.951	0.951	0.948	0.952	0.947	0.944	0.944	0.942
24	0.962	0.956	0.953	0.953	0.951	0.955	0.950	0.947	0.947	0.945

Table A.2: Day 2 hourly bus voltages (pu) for an uncontrolled system.

Hour	Bus 1	Bus 2	Bus 3	Bus 4	Bus 5	Bus 6	Bus 7	Bus 8	Bus 9	Bus 10
25	0.971	0.968	0.966	0.968	0.965	0.966	0.963	0.962	0.963	0.961
26	0.971	0.967	0.966	0.967	0.965	0.966	0.963	0.962	0.963	0.961
27	0.971	0.968	0.967	0.968	0.966	0.966	0.963	0.962	0.963	0.961
28	0.964	0.959	0.957	0.957	0.955	0.958	0.954	0.952	0.952	0.950
29	0.959	0.952	0.949	0.949	0.946	0.951	0.945	0.942	0.942	0.940
30	0.955	0.947	0.943	0.942	0.939	0.946	0.939	0.936	0.935	0.932
31	0.938	0.926	0.918	0.915	0.911	0.924	0.914	0.907	0.905	0.901
32	0.920	0.903	0.893	0.887	0.882	0.901	0.887	0.878	0.873	0.869
33	0.919	0.903	0.892	0.887	0.882	0.901	0.887	0.877	0.873	0.868
34	0.942	0.931	0.924	0.921	0.917	0.929	0.920	0.914	0.912	0.908
35	0.944	0.933	0.927	0.925	0.921	0.931	0.923	0.917	0.915	0.912
36	0.942	0.932	0.925	0.923	0.919	0.930	0.921	0.915	0.913	0.910
37	0.945	0.935	0.929	0.927	0.923	0.933	0.925	0.920	0.918	0.915
38	0.944	0.934	0.928	0.926	0.922	0.933	0.924	0.919	0.917	0.914
39	0.946	0.936	0.931	0.929	0.925	0.935	0.927	0.922	0.920	0.917
40	0.949	0.940	0.934	0.933	0.929	0.938	0.930	0.926	0.924	0.921
41	0.939	0.927	0.919	0.916	0.912	0.925	0.915	0.908	0.906	0.902
42	0.913	0.896	0.884	0.878	0.873	0.893	0.878	0.868	0.863	0.858
43	0.911	0.893	0.880	0.874	0.869	0.890	0.874	0.864	0.859	0.854
44	0.936	0.923	0.915	0.912	0.908	0.921	0.911	0.904	0.901	0.897
45	0.954	0.945	0.941	0.939	0.936	0.944	0.937	0.933	0.932	0.929
46	0.961	0.955	0.952	0.952	0.949	0.953	0.948	0.945	0.945	0.943
47	0.966	0.961	0.958	0.959	0.956	0.959	0.955	0.953	0.953	0.951
48	0.967	0.963	0.961	0.961	0.959	0.961	0.957	0.956	0.956	0.954

Table A.3: Day 1 hourly system loss and VDI values for an uncontrolled system.

Hour	Loss (MWh)	VDI
1	0.5472	0.0283
2	0.5406	0.0289
3	0.5391	0.028
4	0.5488	0.0277
5	0.5796	0.0263
6	0.6717	0.034
7	1.027	0.0749
8	1.5199	0.1388
9	1.4287	0.1363
10	0.784	0.0606
11	0.742	0.0555
12	0.7349	0.0578
13	0.6966	0.0517
14	0.6772	0.0519
15	0.6545	0.0484
16	0.656	0.0439
17	0.7608	0.0507
18	1.713	0.1655
19	1.7335	0.1746
20	1.2375	0.1087
21	0.7884	0.0528
22	0.6547	0.0349
23	0.5681	0.026
24	0.5319	0.0233

Table A.4: Day 2 hourly system loss and VDI values for an uncontrolled system.

Hour	Loss (MWh)	VDI
25	0.5031	0.0121
26	0.497	0.0123
27	0.4963	0.0119
28	0.513	0.0199
29	0.5494	0.028
30	0.6264	0.0349
31	0.9217	0.0718
32	1.321	0.125
33	1.2513	0.1256
34	0.7262	0.0623
35	0.691	0.0576
36	0.6864	0.0604
37	0.6535	0.0544
38	0.6384	0.0552
39	0.6188	0.0517
40	0.618	0.0465
41	0.8884	0.0705
42	1.4742	0.146
43	1.4922	0.1547
44	1.0625	0.0773
45	0.7076	0.038
46	0.6	0.025
47	0.5294	0.0185
48	0.4995	0.0166

Table A.5: Day 1 hourly bus voltages (pu) for CC-A.

Hour	Bus 1	Bus 2	Bus 3	Bus 4	Bus 5	Bus 6	Bus 7	Bus 8	Bus 9	Bus 10
1	0.986	0.980	0.977	0.977	0.974	0.978	0.973	0.970	0.970	0.968
2	0.985	0.979	0.976	0.976	0.973	0.978	0.972	0.970	0.970	0.967
3	0.986	0.980	0.977	0.977	0.974	0.978	0.973	0.971	0.971	0.968
4	0.986	0.980	0.977	0.977	0.974	0.978	0.973	0.971	0.971	0.968
5	0.987	0.981	0.978	0.978	0.976	0.980	0.975	0.972	0.972	0.970
6	0.997	0.990	0.987	0.986	0.983	0.988	0.983	0.980	0.979	0.977
7	0.994	0.983	0.976	0.974	0.970	0.981	0.972	0.966	0.964	0.961
8	0.992	0.983	0.980	0.982	0.977	0.980	0.972	0.969	0.971	0.967
9	0.992	0.984	0.981	0.982	0.978	0.980	0.973	0.970	0.972	0.968
10	0.988	0.984	0.984	0.988	0.985	0.981	0.978	0.978	0.981	0.978
11	0.990	0.987	0.987	0.992	0.988	0.984	0.981	0.982	0.985	0.982
12	0.989	0.985	0.986	0.990	0.987	0.983	0.980	0.980	0.984	0.981
13	0.991	0.989	0.990	0.995	0.991	0.986	0.984	0.985	0.988	0.985
14	0.991	0.989	0.990	0.994	0.991	0.986	0.984	0.984	0.988	0.985
15	0.993	0.991	0.992	0.997	0.994	0.988	0.986	0.987	0.991	0.988
16	0.995	0.993	0.995	1.000	0.997	0.991	0.989	0.991	0.995	0.992
17	0.992	0.989	0.991	0.995	0.992	0.987	0.984	0.985	0.989	0.986
18	0.985	0.975	0.971	0.972	0.967	0.971	0.963	0.959	0.960	0.955
19	0.999	0.989	0.985	0.986	0.981	0.985	0.977	0.973	0.974	0.970
20	0.985	0.978	0.975	0.978	0.973	0.974	0.968	0.966	0.968	0.964
21	0.988	0.979	0.973	0.972	0.968	0.977	0.969	0.965	0.963	0.960
22	0.996	0.989	0.986	0.985	0.982	0.988	0.982	0.979	0.978	0.976
23	0.987	0.982	0.979	0.979	0.976	0.980	0.975	0.973	0.973	0.970
24	0.989	0.984	0.981	0.982	0.979	0.982	0.978	0.976	0.976	0.974

Table A.6: Day 2 hourly bus voltages (pu) for CC-A.

Hour	Bus 1	Bus 2	Bus 3	Bus 4	Bus 5	Bus 6	Bus 7	Bus 8	Bus 9	Bus 10
25	0.998	0.995	0.994	0.995	0.993	0.993	0.991	0.990	0.991	0.989
26	0.998	0.994	0.994	0.995	0.993	0.993	0.990	0.990	0.991	0.989
27	0.998	0.995	0.994	0.996	0.993	0.994	0.991	0.990	0.991	0.990
28	0.991	0.987	0.985	0.985	0.983	0.985	0.981	0.980	0.980	0.978
29	0.986	0.980	0.977	0.977	0.974	0.978	0.973	0.971	0.971	0.968
30	0.996	0.989	0.986	0.985	0.982	0.988	0.982	0.979	0.978	0.976
31	0.995	0.984	0.978	0.976	0.972	0.982	0.973	0.968	0.966	0.963
32	0.996	0.988	0.985	0.987	0.982	0.984	0.977	0.975	0.977	0.973
33	0.995	0.987	0.984	0.987	0.982	0.984	0.977	0.975	0.976	0.972
34	1.001	0.998	0.998	1.003	0.999	0.995	0.992	0.993	0.996	0.993
35	1.003	1.000	1.001	1.006	1.002	0.998	0.995	0.996	1.000	0.997
36	1.002	0.999	1.000	1.004	1.000	0.996	0.993	0.994	0.998	0.994
37	1.004	1.002	1.003	1.008	1.005	0.999	0.997	0.998	1.002	0.999
38	1.004	1.002	1.003	1.008	1.004	0.999	0.997	0.998	1.001	0.999
39	1.006	1.003	1.005	1.010	1.007	1.001	0.999	1.000	1.004	1.001
40	1.008	1.007	1.008	1.014	1.010	1.004	1.002	1.004	1.008	1.006
41	1.013	1.009	1.009	1.014	1.010	1.006	1.003	1.003	1.007	1.003
42	0.990	0.981	0.977	0.979	0.974	0.977	0.969	0.966	0.967	0.963
43	0.988	0.978	0.974	0.975	0.970	0.974	0.966	0.963	0.964	0.959
44	1.011	1.006	1.006	1.010	1.006	1.003	0.999	0.999	1.002	0.999
45	0.995	0.987	0.983	0.983	0.980	0.986	0.980	0.976	0.976	0.973
46	0.988	0.982	0.980	0.980	0.977	0.981	0.976	0.974	0.974	0.971
47	0.992	0.988	0.986	0.987	0.984	0.986	0.983	0.981	0.982	0.980
48	0.994	0.990	0.988	0.989	0.987	0.988	0.985	0.984	0.984	0.982

Table A.7: Day 1 hourly system loss and VDI values for CC-A.

Hour	Loss (MWh)	VDI
1	0.5404	0.0065
2	0.5339	0.0067
3	0.5325	0.0063
4	0.542	0.0062
5	0.5721	0.0055
6	0.6555	0.0026
7	0.9742	0.0076
8	1.3331	0.0057
9	1.2502	0.0054
10	0.7277	0.0032
11	0.6918	0.0021
12	0.6813	0.0026
13	0.6505	0.0015
14	0.6301	0.0015
15	0.6118	0.001
16	0.6203	0.0005
17	0.7178	0.0013
18	1.4866	0.0112
19	1.4725	0.004
20	1.112	0.0077
21	0.7643	0.0088
22	0.6392	0.0029
23	0.5609	0.0054
24	0.5259	0.0042

Table A.8: Day 2 hourly system loss and VDI values for CC-A.

Hour	Loss (MWh)	VDI
25	0.4989	0.0006
26	0.4929	0.0006
27	0.4923	0.0005
28	0.5078	0.0029
29	0.5425	0.0063
30	0.6121	0.0029
31	0.8775	0.0068
32	1.1604	0.0036
33	1.0938	0.0037
34	0.6626	0.0002
35	0.6334	0.0001
36	0.6247	0.0002
37	0.5996	0.0001
38	0.5829	0.0001
39	0.5679	0.0002
40	0.5751	0.0006
41	0.8081	0.0007
42	1.2833	0.0072
43	1.2918	0.009
44	0.9681	0.0003
45	0.6892	0.0037
46	0.592	0.005
47	0.5239	0.0024
48	0.4949	0.0018

Table A.9: Day 1 hourly bus voltages (pu) for CC-B.

Hour	Bus 1	Bus 2	Bus 3	Bus 4	Bus 5	Bus 6	Bus 7	Bus 8	Bus 9	Bus 10
1	1.014	1.008	1.006	1.006	1.003	1.007	1.002	1.000	1.000	0.998
2	1.013	1.008	1.005	1.006	1.003	1.006	1.002	0.999	1.000	0.997
3	1.014	1.009	1.006	1.006	1.004	1.007	1.002	1.000	1.001	0.998
4	1.014	1.009	1.006	1.007	1.004	1.007	1.003	1.001	1.001	0.998
5	1.015	1.010	1.008	1.008	1.005	1.009	1.004	1.002	1.002	1.000
6	1.011	1.005	1.001	1.001	0.998	1.003	0.998	0.995	0.995	0.992
7	1.009	0.999	0.992	0.990	0.986	0.997	0.988	0.982	0.980	0.977
8	1.008	0.999	0.997	0.999	0.994	0.996	0.989	0.987	0.988	0.984
9	1.008	1.000	0.997	1.000	0.995	0.997	0.990	0.987	0.989	0.985
10	1.017	1.014	1.015	1.020	1.016	1.011	1.009	1.009	1.013	1.010
11	1.019	1.017	1.018	1.023	1.020	1.014	1.012	1.013	1.017	1.014
12	1.018	1.015	1.017	1.022	1.018	1.013	1.010	1.011	1.015	1.012
13	1.006	1.004	1.005	1.010	1.006	1.001	0.999	1.000	1.004	1.001
14	1.006	1.003	1.005	1.010	1.006	1.001	0.999	1.000	1.004	1.001
15	1.007	1.005	1.007	1.012	1.009	1.003	1.001	1.002	1.007	1.004
16	1.010	1.008	1.010	1.016	1.012	1.005	1.004	1.006	1.010	1.008
17	1.007	1.004	1.006	1.011	1.007	1.001	0.999	1.001	1.005	1.002
18	1.018	1.009	1.005	1.007	1.002	1.005	0.997	0.994	0.996	0.992
19	1.015	1.006	1.002	1.004	0.999	1.002	0.994	0.991	0.992	0.988
20	1.016	1.009	1.008	1.011	1.007	1.006	1.001	0.999	1.002	0.998
21	1.017	1.009	1.004	1.003	0.999	1.007	1.000	0.996	0.995	0.992
22	1.011	1.004	1.001	1.000	0.997	1.002	0.997	0.994	0.994	0.991
23	1.016	1.010	1.008	1.008	1.006	1.009	1.004	1.002	1.003	1.000
24	1.017	1.012	1.010	1.011	1.008	1.011	1.007	1.005	1.006	1.003

Table A.10: Day 2 hourly bus voltages (pu) for CC-B.

Hour	Bus 1	Bus 2	Bus 3	Bus 4	Bus 5	Bus 6	Bus 7	Bus 8	Bus 9	Bus 10
25	1.026	1.023	1.023	1.024	1.022	1.022	1.020	1.019	1.020	1.019
26	1.026	1.023	1.022	1.024	1.022	1.022	1.019	1.019	1.020	1.018
27	1.026	1.023	1.023	1.025	1.023	1.022	1.020	1.019	1.021	1.019
28	1.019	1.015	1.014	1.015	1.012	1.014	1.010	1.009	1.010	1.008
29	1.014	1.009	1.006	1.006	1.004	1.007	1.003	1.000	1.001	0.998
30	1.011	1.004	1.001	1.000	0.997	1.002	0.997	0.994	0.994	0.991
31	1.010	1.000	0.994	0.992	0.988	0.998	0.989	0.984	0.982	0.979
32	1.027	1.020	1.018	1.021	1.017	1.017	1.011	1.009	1.012	1.008
33	1.027	1.020	1.018	1.021	1.016	1.017	1.011	1.009	1.011	1.007
34	1.031	1.029	1.030	1.035	1.031	1.026	1.024	1.025	1.029	1.026
35	1.033	1.031	1.033	1.038	1.034	1.028	1.026	1.028	1.032	1.029
36	1.032	1.029	1.031	1.036	1.033	1.027	1.025	1.026	1.030	1.027
37	1.034	1.033	1.035	1.040	1.037	1.030	1.028	1.030	1.034	1.032
38	1.034	1.032	1.034	1.039	1.036	1.029	1.028	1.029	1.034	1.031
39	1.020	1.019	1.020	1.026	1.022	1.016	1.014	1.016	1.020	1.017
40	1.023	1.022	1.024	1.029	1.026	1.019	1.018	1.020	1.024	1.022
41	1.028	1.025	1.026	1.030	1.026	1.022	1.019	1.019	1.023	1.020
42	1.022	1.014	1.011	1.013	1.009	1.010	1.004	1.001	1.003	0.999
43	1.020	1.011	1.008	1.010	1.005	1.008	1.000	0.998	0.999	0.995
44	1.026	1.022	1.022	1.027	1.023	1.019	1.016	1.016	1.019	1.016
45	1.009	1.002	0.998	0.998	0.995	1.000	0.995	0.991	0.991	0.988
46	1.016	1.011	1.009	1.009	1.007	1.010	1.005	1.003	1.004	1.001
47	1.021	1.017	1.015	1.016	1.014	1.015	1.012	1.011	1.011	1.009
48	1.022	1.018	1.017	1.019	1.016	1.017	1.014	1.013	1.014	1.012

Table A.11: Day 1 hourly system loss and VDI values for CC-B.

Hour	Loss (MWh)	VDI
1	0.5339	0.0002
2	0.5275	0.0002
3	0.5263	0.0003
4	0.5355	0.0003
5	0.565	0.0004
6	0.6504	0.0002
7	0.962	0.0019
8	1.314	0.0009
9	1.2329	0.0008
10	0.719	0.0016
11	0.6847	0.0025
12	0.6743	0.0021
13	0.6476	0.0004
14	0.6275	0.0004
15	0.6096	0.0005
16	0.6183	0.0009
17	0.714	0.0004
18	1.44	0.0003
19	1.449	0.0004
20	1.0858	0.0004
21	0.7492	0.0003
22	0.6342	0.0003
23	0.554	0.0004
24	0.5202	0.0007

Table A.12: Day 2 hourly system loss and VDI values for CC-B.

Hour	Loss (MWh)	VDI
25	0.4949	0.0042
26	0.489	0.0041
27	0.4885	0.0043
28	0.5029	0.0013
29	0.536	0.0003
30	0.6076	0.0003
31	0.8671	0.0015
32	1.1313	0.0022
33	1.0672	0.0021
34	0.6561	0.0073
35	0.6282	0.0089
36	0.6194	0.0079
37	0.5956	0.0101
38	0.5792	0.0098
39	0.5663	0.0033
40	0.5737	0.0047
41	0.8024	0.0051
42	1.2472	0.0007
43	1.2544	0.0004
44	0.9594	0.0037
45	0.6834	0.0005
46	0.5844	0.0005
47	0.5187	0.0016
48	0.4906	0.0022

Table A.13: Day 1 hourly bus voltages (pu) for the optimum settings approach.

Hour	Bus 1	Bus 2	Bus 3	Bus 4	Bus 5	Bus 6	Bus 7	Bus 8	Bus 9	Bus 10
1	1.027	1.028	1.032	1.039	1.036	1.026	1.027	1.030	1.036	1.033
2	1.027	1.028	1.032	1.039	1.036	1.025	1.026	1.029	1.035	1.033
3	1.028	1.029	1.033	1.039	1.037	1.026	1.027	1.030	1.036	1.034
4	1.028	1.029	1.033	1.040	1.037	1.026	1.027	1.030	1.036	1.034
5	1.029	1.030	1.034	1.041	1.038	1.027	1.028	1.032	1.037	1.035
6	1.025	1.025	1.028	1.034	1.031	1.022	1.022	1.024	1.030	1.027
7	1.022	1.018	1.018	1.023	1.019	1.015	1.012	1.012	1.015	1.012
8	1.036	1.028	1.026	1.029	1.025	1.025	1.019	1.017	1.019	1.016
9	1.036	1.029	1.027	1.030	1.025	1.026	1.019	1.018	1.020	1.016
10	1.027	1.024	1.026	1.031	1.027	1.022	1.019	1.020	1.024	1.021
11	1.029	1.027	1.029	1.034	1.030	1.024	1.022	1.024	1.028	1.025
12	1.028	1.026	1.027	1.032	1.029	1.023	1.021	1.022	1.026	1.023
13	1.031	1.029	1.031	1.036	1.033	1.026	1.025	1.026	1.031	1.028
14	1.030	1.029	1.031	1.036	1.033	1.026	1.025	1.026	1.031	1.028
15	1.032	1.031	1.033	1.039	1.035	1.028	1.027	1.029	1.033	1.031
16	1.034	1.033	1.036	1.042	1.039	1.031	1.030	1.032	1.037	1.034
17	1.031	1.030	1.032	1.037	1.034	1.027	1.025	1.027	1.032	1.029
18	1.030	1.021	1.018	1.020	1.015	1.017	1.010	1.008	1.009	1.005
19	1.027	1.018	1.015	1.017	1.012	1.015	1.007	1.004	1.006	1.002
20	1.027	1.021	1.020	1.023	1.019	1.018	1.013	1.011	1.014	1.011
21	1.030	1.029	1.030	1.036	1.032	1.026	1.024	1.026	1.030	1.027
22	1.024	1.024	1.027	1.033	1.030	1.021	1.021	1.024	1.029	1.026
23	1.029	1.030	1.034	1.041	1.039	1.028	1.029	1.032	1.038	1.036
24	1.031	1.032	1.037	1.044	1.042	1.030	1.031	1.035	1.041	1.039

Table A.14: Day 2 hourly bus voltages (pu) for the optimum settings approach.

Hour	Bus 1	Bus 2	Bus 3	Bus 4	Bus 5	Bus 6	Bus 7	Bus 8	Bus 9	Bus 10
25	1.026	1.023	1.023	1.024	1.022	1.022	1.020	1.019	1.020	1.019
26	1.026	1.023	1.022	1.024	1.022	1.022	1.019	1.019	1.020	1.018
27	1.026	1.023	1.023	1.025	1.023	1.022	1.020	1.019	1.021	1.019
28	1.033	1.035	1.040	1.048	1.045	1.033	1.035	1.039	1.045	1.043
29	1.028	1.029	1.033	1.039	1.037	1.026	1.027	1.030	1.036	1.034
30	1.024	1.024	1.027	1.033	1.030	1.021	1.021	1.024	1.029	1.026
31	1.023	1.019	1.020	1.024	1.020	1.016	1.013	1.013	1.017	1.014
32	1.022	1.015	1.013	1.016	1.012	1.012	1.006	1.004	1.007	1.003
33	1.022	1.015	1.013	1.016	1.011	1.012	1.006	1.004	1.006	1.002
34	1.026	1.023	1.025	1.030	1.026	1.021	1.018	1.019	1.023	1.020
35	1.028	1.026	1.027	1.033	1.029	1.023	1.021	1.022	1.027	1.024
36	1.027	1.024	1.026	1.031	1.027	1.022	1.019	1.021	1.025	1.022
37	1.029	1.027	1.029	1.035	1.031	1.025	1.023	1.025	1.029	1.026
38	1.029	1.027	1.029	1.034	1.031	1.024	1.023	1.024	1.028	1.026
39	1.030	1.029	1.031	1.036	1.033	1.026	1.025	1.027	1.031	1.028
40	1.033	1.032	1.034	1.040	1.037	1.029	1.028	1.030	1.035	1.032
41	1.023	1.020	1.020	1.025	1.021	1.017	1.014	1.014	1.018	1.015
42	1.034	1.026	1.024	1.026	1.022	1.023	1.016	1.014	1.016	1.012
43	1.032	1.023	1.021	1.023	1.018	1.020	1.013	1.011	1.012	1.008
44	1.021	1.017	1.017	1.021	1.017	1.014	1.010	1.010	1.014	1.011
45	1.022	1.022	1.025	1.031	1.027	1.019	1.019	1.021	1.026	1.023
46	1.030	1.031	1.035	1.042	1.040	1.029	1.030	1.033	1.039	1.037
47	1.034	1.037	1.042	1.049	1.047	1.034	1.036	1.040	1.047	1.045
48	1.022	1.018	1.017	1.019	1.016	1.017	1.014	1.013	1.014	1.012

Table A.15: Day 1 hourly system loss and VDI values for the optimum settings approach.

Hour	Loss (MWh)	VDI
1	0.5325	0.0094
2	0.5247	0.0091
3	0.5246	0.0095
4	0.535	0.0097
5	0.5686	0.0104
6	0.6489	0.0067
7	0.9365	0.0025
8	1.2945	0.0048
9	1.2168	0.0051
10	0.7208	0.0053
11	0.6862	0.0067
12	0.6765	0.006
13	0.6466	0.008
14	0.6273	0.0079
15	0.6094	0.0092
16	0.6169	0.0111
17	0.7104	0.0083
18	1.4382	0.002
19	1.4479	0.0014
20	1.0865	0.0027
21	0.7345	0.0076
22	0.6305	0.0064
23	0.5574	0.0106
24	0.5253	0.0124

Table A.16: Day 2 hourly system loss and VDI values for the optimum settings approach.

Hour	Loss (MWh)	VDI
25	0.4949	0.0042
26	0.489	0.0041
27	0.4885	0.0043
28	0.5122	0.0149
29	0.5351	0.0095
30	0.6023	0.0064
31	0.8402	0.003
32	1.1471	0.0012
33	1.0834	0.0011
34	0.6628	0.0048
35	0.6339	0.0061
36	0.626	0.0053
37	0.6009	0.007
38	0.5849	0.0068
39	0.5698	0.008
40	0.5758	0.01
41	0.8099	0.0032
42	1.2479	0.0037
43	1.256	0.0027
44	0.9674	0.0022
45	0.6787	0.0053
46	0.5914	0.0112
47	0.5316	0.016
48	0.4906	0.0024

Table A.17: Day 1 hourly bus voltages (pu) for FVC-OSC.

Hour	Bus 1	Bus 2	Bus 3	Bus 4	Bus 5	Bus 6	Bus 7	Bus 8	Bus 9	Bus 10
1	1.004	0.998	0.996	0.996	0.993	1.002	1.002	1.005	1.010	1.008
2	0.999	0.993	0.990	0.990	0.987	0.996	0.997	0.999	1.004	1.002
3	1.018	1.013	1.011	1.011	1.008	1.017	1.017	1.020	1.026	1.024
4	1.004	0.999	0.996	0.996	0.993	1.002	1.003	1.006	1.011	1.008
5	1.001	0.995	0.992	0.993	0.990	0.998	0.999	1.002	1.007	1.005
6	1.001	0.994	0.991	0.990	0.987	0.998	0.997	0.999	1.004	1.002
7	1.012	1.007	1.007	1.011	1.007	1.004	1.001	1.000	1.004	1.001
8	1.024	1.016	1.014	1.016	1.012	1.013	1.006	1.004	1.006	1.002
9	1.024	1.017	1.014	1.017	1.012	1.013	1.007	1.005	1.007	1.003
10	1.012	1.009	1.010	1.014	1.011	1.006	1.003	1.004	1.008	1.005
11	0.999	0.996	0.997	1.002	0.998	0.994	0.991	0.992	0.996	0.993
12	0.998	0.995	0.996	1.000	0.997	0.992	0.990	0.990	0.994	0.991
13	1.016	1.014	1.015	1.020	1.017	1.011	1.009	1.010	1.015	1.012
14	1.006	1.003	1.005	1.010	1.006	1.001	0.999	1.000	1.004	1.001
15	0.993	0.991	0.992	0.997	0.994	0.988	0.986	0.987	0.991	0.988
16	1.010	1.008	1.010	1.016	1.012	1.005	1.004	1.006	1.010	1.008
17	1.007	1.004	1.006	1.011	1.007	1.001	0.999	1.001	1.005	1.002
18	1.034	1.026	1.023	1.025	1.021	1.022	1.015	1.013	1.015	1.011
19	1.032	1.023	1.020	1.022	1.017	1.020	1.012	1.010	1.011	1.007
20	1.048	1.043	1.042	1.046	1.042	1.039	1.035	1.034	1.037	1.034
21	1.020	1.018	1.020	1.025	1.022	1.015	1.014	1.015	1.019	1.016
22	1.010	1.003	1.000	1.000	0.997	1.007	1.006	1.009	1.014	1.011
23	1.006	1.000	0.998	0.998	0.995	1.004	1.004	1.007	1.013	1.010
24	1.007	1.002	1.000	1.001	0.998	1.006	1.007	1.010	1.016	1.014

Table A.18: Day 2 hourly bus voltages (pu) for FVC-OSC.

Hour	Bus 1	Bus 2	Bus 3	Bus 4	Bus 5	Bus 6	Bus 7	Bus 8	Bus 9	Bus 10
25	1.011	1.008	1.008	1.009	1.007	1.012	1.015	1.019	1.026	1.024
26	0.997	0.994	0.993	0.995	0.992	0.998	1.000	1.005	1.011	1.009
27	1.003	1.000	0.999	1.000	0.998	1.003	1.006	1.010	1.017	1.015
28	1.010	1.005	1.004	1.004	1.002	1.009	1.011	1.014	1.020	1.018
29	1.004	0.999	0.996	0.996	0.993	0.997	0.993	0.990	0.990	0.988
30	1.000	0.994	0.990	0.990	0.987	0.997	0.996	0.999	1.003	1.001
31	1.013	1.003	0.997	0.995	0.991	1.006	1.003	1.003	1.007	1.003
32	1.022	1.015	1.013	1.016	1.012	1.012	1.006	1.004	1.007	1.003
33	1.027	1.020	1.018	1.021	1.016	1.017	1.011	1.009	1.011	1.007
34	1.016	1.013	1.014	1.019	1.015	1.010	1.008	1.008	1.012	1.009
35	1.034	1.025	1.021	1.020	1.016	1.029	1.027	1.028	1.033	1.030
36	1.012	1.009	1.010	1.015	1.011	1.006	1.004	1.004	1.008	1.005
37	1.005	0.996	0.991	0.990	0.986	1.000	0.998	0.998	1.002	1.000
38	1.004	1.002	1.003	1.008	1.004	0.999	0.997	0.998	1.001	0.999
39	1.021	1.013	1.008	1.007	1.004	1.016	1.015	1.016	1.021	1.018
40	1.008	1.001	0.996	0.996	0.992	1.004	1.003	1.004	1.009	1.006
41	1.029	1.019	1.014	1.012	1.008	1.023	1.020	1.020	1.024	1.021
42	1.022	1.014	1.011	1.013	1.009	1.010	1.004	1.001	1.003	0.999
43	1.036	1.028	1.026	1.028	1.023	1.025	1.018	1.016	1.018	1.014
44	1.011	1.006	1.006	1.010	1.006	1.003	0.999	0.999	1.002	0.999
45	0.994	0.987	0.983	0.982	0.979	0.990	0.989	0.991	0.995	0.992
46	1.006	1.001	0.999	0.999	0.996	1.005	1.005	1.008	1.014	1.011
47	1.025	1.021	1.020	1.021	1.018	1.025	1.027	1.031	1.037	1.035
48	1.012	1.009	1.007	1.009	1.006	1.007	1.004	1.003	1.004	1.002

Table A.19: Day 1 hourly system loss and VDI values for FVC-OSC.

Hour	Loss (MWh)	VDI
1	0.5232	0.0003
2	0.5243	0.0006
3	0.5139	0.0027
4	0.5256	0.0003
5	0.5657	0.0004
6	0.6419	0.0005
7	0.9369	0.0003
8	1.2958	0.0013
9	1.2165	0.0014
10	0.7257	0.0006
11	0.6947	0.0004
12	0.685	0.0006
13	0.65	0.0018
14	0.6275	0.0002
15	0.6118	0.0012
16	0.6183	0.0008
17	0.714	0.0002
18	1.4184	0.004
19	1.4267	0.003
20	1.0621	0.0153
21	0.7348	0.0032
22	0.6294	0.0005
23	0.5474	0.0004
24	0.5143	0.0006

Table A.20: Day 2 hourly system loss and VDI values for FVC-OSC.

Hour	Loss (MWh)	VDI
25	0.504	0.0023
26	0.4984	0.0006
27	0.4966	0.0007
28	0.5	0.0012
29	0.5231	0.0005
30	0.5954	0.0006
31	0.8357	0.0002
32	1.1471	0.0012
33	1.0672	0.0023
34	0.6592	0.0014
35	0.6238	0.0065
36	0.6295	0.0007
37	0.5982	0.0004
38	0.5829	0.0001
39	0.5632	0.0019
40	0.571	0.0002
41	0.7978	0.0035
42	1.2472	0.0008
43	1.2371	0.0052
44	0.9681	0.0002
45	0.6832	0.0019
46	0.5812	0.0005
47	0.518	0.0067
48	0.481	0.0003